Reactivity of CaO-based sorbent for Calcium Looping Technology in presence of steam

Leonor Amaral Pinheiro da Silva Rosa

Dissertação para obtenção do Grau de Mestre em

Engenharia Química

Júri:

Presidente: Prof. Dr. Maria Filipa Gomes Ribeiro (IST)

Orientador: Prof. Dr. Carla Isabel Costa Pinheiro (IST)

Orientador: Prof. Dr. Paul Fennell (Imperial College London)

Orientador: Prof. Dr. Belen Gonzalez Garcia (Imperial College London)

Vogal: Dr. Edgar Tavares dos Santos (IBB)

Novembro 2012

TÉCNICO LISBOA

Reactivity of CaO-based sorbent for Calcium Looping Technology in presence of steam

Leonor Amaral Pinheiro da Silva Rosa

Thesis to obtain the Master of Science Degree in

Chemical Engineering

Examination Committee:

Chairperson: Prof. Dr. Maria Filipa Gomes Ribeiro (IST)

Supervisor: Prof. Dr. Carla Isabel Costa Pinheiro (IST)

Supervisor: Prof. Dr. Paul Fennell (Imperial College London)

Supervisor: Prof. Dr. Belen Gonzalez Garcia (Imperial College London)

Member of the Committee: Dr. Edgar Tavares dos Santos (IBB)

November 2012

There is no question that climate change is happening,

the only arguable point is what part humans are playing in it.

Sir David Frederick Attenborough

British broadcaster and author (born 8 May 1926)

Abstract

This thesis focuses on a post-combustion CO_2 capture technology known as calcium looping. This technology uses a CaO-based sorbent and takes advantage of the reversible reaction between CaO and CO_2 to form $CaCO_3$. The influence of the presence of steam in the flue gas on the carbonation reaction has been studied. Thirty calcination/carbonation cycles experiments were carried out in a thermogravimetric analyzer (TGA) in the presence of 1.5% steam with Havelock and Purbeck limestones. Particles were also observed using a scanning electron microscope.

Results obtained for Havelock showed a significant increase in conversion as opposed to the case when steam was not present. In the 5^{th} cycle a value of 37% carbonation conversion was obtained and in the last cycle an improvement in conversion of about 91% was achieved in comparison with no steam experiments. The uptake of CO_2 had a smaller degradation with cycles and a value of $0.13 gCO_2/gCaO$ was obtained for the 30^{th} cycle. In total, 49% more CO_2 was absorbed by Havelock in presence of steam than its absence. Steam was found to enhance the diffusion-controlled stage of carbonation, however the enhancement is not the same for all types of limestone. Purbeck limestone showed no significant improvement in carbonation extent, however no negative influence was also found. Reaction rate coefficients for the chemically-controlled stage of carbonation reaction were determined using a random pore model. The mean reaction rate for experiments performed without steam was $(4.33\pm1.50)x10^{-10} m^4.mol^{-1}.s^{-1}$ whereas the steam experiments yielded a value of $(2.47\pm1.01)x10^{-10} m^4.mol^{-1}.s^{-1}$. Particles cycled without steam seemed to be more reactive, however this model has to be repeated using different texture parameters (S,L and ε)

Keywords: CO_2 Capture, CaO looping cycle, Steam, Carbonation, Reaction Rate

Resumo

A presente tese foca um método de pós-combustão utilizado na captura de CO_2 denominado de ciclo do cálcio. Esta tecnologia utiliza um adsorvente constituído por CaO e tira proveito da existência da reação reversível entre CaO e CO_2 para formar $CaCO_3$. Fez-se um estudo sobre a influência que o vapor de água existente nos gases de combustão tem na performance dos adsorventes. Realizaram-se trinta ciclos de calcinação/carbonatação numa termobalança (TGA) na presença de uma concentração de 1.5% de vapor com os calcários *Havelock* e *Purbeck*. A fim de ajudar na análise dos resultados, as partículas foram observadas num microscópio eletrónico de varrimento.

Os resultados obtidos para *Havelock* mostraram um aumento significativo na conversão. No 5º ciclo obteve-se um valor de 37% de conversão e no último ciclo registou-se um aumento na conversão de 91%, comparativamente com os resultados obtidos nas experiências sem vapor. A absorção de CO_2 decaiu com menor intensidade durante a execução dos ciclos e para o ciclo 30 obteve-se cerca de $0.13 gCO_2/gCaO$ de capacidade de absorção. No total dos trinta ciclos, o calcário *Havelock* absorveu cerca de 49% mais CO_2 quando o vapor esteve presente. Nestas experiências comprovou-se que o vapor melhora a fase da carbonatação controlada por processos difusivos.

Contudo, este aumento não acontece na mesma proporção para todos os tipos de calcário. No caso de *Purbeck* não se verificou nenhuma melhoria, porém também não foi encontrada nenhuma influência negativa. Foram determinadas constantes de velocidade de reação para a fase controlada exclusivamente pela cinética, usando um modelo de poro denominado *Random Pore Model.* A constante de velocidade de reação obtida para as experiências realizadas sem vapor apresentou um valor igual a $(4.33 \pm 1.50)\ x10^{-10} m^4.mol^{-1}.s^{-1}$. Por outro lado, para os ciclos realizados na presença de vapor obteve-se um valor de $(2.47 \pm 1.01)\ x10^{-10} m^4.mol^{-1}.s^{-1}$. As partículas calcinadas e carbonatadas sem vapor parecem então ser mais reativas, contudo este modelo deverá ser repetido utilizando-se diferentes parâmetros texturais (S,L and ε).

Palavras-Chave: Captura de CO_2, Ciclo do cálcio, Vapor, Carbonatação, Velocidade de reação

Acknowledgements

First of all, I would like to give my great thanks to my supervisors: Prof. Dr. Carla Pinheiro, Prof. Dr. Paul Fennell and Dr. Belen Gonzalez, for all help and support throughout. Furthermore, I really appreciated the warmly way Prof. Dr. Paul Fennell and all Energy Engineering group welcomed me. I also would like to thank Dr. Nicholas Florin for the initial introduction to the topic and to show me Imperial College London.

I particularly have to thank Dr. Belen Gonzalez and Dr. John Blamey, for their patience and for all their help and support during my stay at Imperial College. I am also very grateful to all of the Energy Engineering group for their kindness and friendship and for all the moments of fun we shared. I am very grateful to Zili, Kelvin, Matt, Thom, Mohammed, Xin, Wenying, Charlie and Danlu. I also would like to thank David and Niall for their thoughtful advices and friendship which was so important to make my stay very pleasant.

I cannot forget the confidence Prof. Dr. Sebastião Alves had in me and I want to thank him and Prof. Dr. Filipa Ribeiro for the opportunity to do my master thesis at Imperial College London. I also thank to the ERASMUS Program for the scholarship.

I have to thank all my friends that were with me through all good and bad moments, specially to Carla, Luísa, João,Lita, João Cabaço, Inês and Tiago. I cannot also forget my “London” family Teresa, Mark and Sophie for all the good moments they shared with me.

Finally, I would like to thank my family, specially my parents and my sister for all the support, for giving me the opportunity to stay in London and for always believe in me.

Thank you all!

Nomenclature

Symbol	SI Units	Description
r_{CO_2}	$mol.kg_{CaO}^{-1}.s^{-1}$	Observed rate of reaction
k_o	$m^3.kg^{-1}.s^{-1}$	Overall rate coefficient
C	$mol.m^{-3}$	Molar concentration
k_g	$m^3.kg^{-1}.s^{-1}$	External mass transfer coefficient
k_r	$m^3.kg^{-1}.s^{-1}$	Rate coefficient for chemical reaction
S_m	$m^2.kg_{CaO}^{-1}$	Specific surface area
η	-	Effectiveness factor
Φ	-	Thiele Modulus
d	m	Diameter
D_{eff}	$m^2.s^{-1}$	Effective Diffusivity
k_v	s^{-1}	Volumetric rate constant
m_v	$kg_{CaO}.m^{-3}$	Mass per unit volume of sorbent
D_k	$m^2.s^{-1}$	Knudsen Diffusivity
D_{AB}	$m^2.s^{-1}$	Molecular Diffusivity
$\overline{r_p}$	m	Porous radius
MM	$kg.mol^{-1}$	Molar mass
T	K	Temperature
F	$mol.s^{-1}$	Molar flow rate
x	-	Molar fraction
ρ	$kg.m^{-3}$	Density
Q_v	$m^3.s^{-1}$	Volumetric flow rate
P	Pa	Pressure
R	$J.K^{-1}.mol^{-1}$	Perfect gas constant
M	kg	Mass
X	kg CO_2.kg CaO^{-1}	Carrying Capacity
k	-	Deactivation constant
N	-	Number of cycles
%RH	%	Relative Humidity
p_v	Pa	Vapor Pressure

Nomenclature of the Random Pore Model

Symbol	SI Units	Description
k_s	$m^4.mol^{-1}.s^{-1}$	Rate constant for the surface reaction
S	$m^2.m^{-3}$	Reaction surface area per unit of volume
Ɛ		Porosity
L	$m.m^{-3}$	Pore length per unit of volume
t	s	Time
D_p	$m^2.s^{-1}$	Apparent product layer diffusion
D	$m^2.s^{-1}$	Effective diffusion coefficient
X_{k-D}		Conversion in the begging of the slow stage
Z	-	Ratio volume fraction
α	$m^3.mol^{-1}$	Molar Volume

Subscripts

Symbol	Description
b	Bulk
p	Particle
t	Total
r	Residual
e	Equilibrium
0	Initial
N	Number of Cycles

Content

List of Figures

List of Tables

1. Introduction

Planet Earth faces one of its most challenging problems due to the anthropogenic pollution. The populations of developed countries have released large quantities of gases to the atmosphere since the industrial revolution. These gases, e.g. CO_2, CO, water vapour, CH_4 and NO_x, absorb the thermal radiation causing the Greenhouse effect and subsequently the Global warming. Indeed, the average global temperature has increased and the last decade (2001-2010) was the warmest decade ever with an increase of 0.18-0.22 ºC (Figure 1). Projections keep showing that the temperature will rise between 1.8-4 ºC until the end of 2100.[1] This rise of temperature on Earth has lead to a higher frequency of extreme events, such as heat waves, great variability of the winter temperatures and floods.

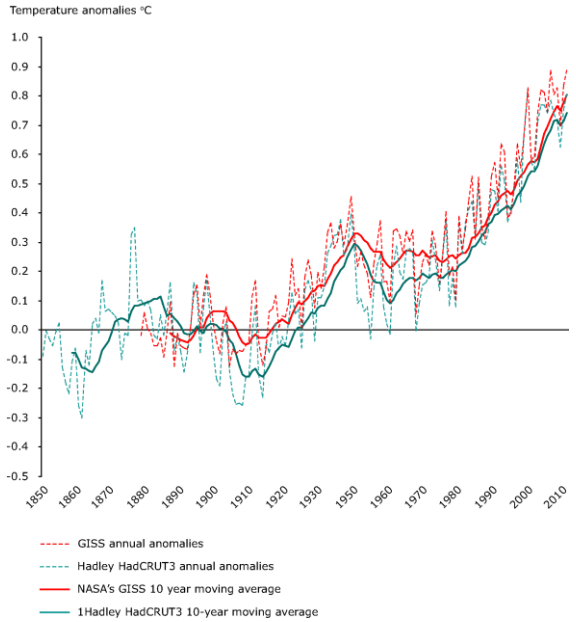

Figure 1: Observed global annual average temperature deviations in the period 1850-2010 (ºC) [1]

The GHG's emissions has increased exponentially through the years (Figure 2) and it has been sustained not only by the developed countries, but also by the rapid industrialization of other countries, especially China and India.[2] Of these GHG's, carbon dioxide has an important role, representing 80% of the total emissions.[2]

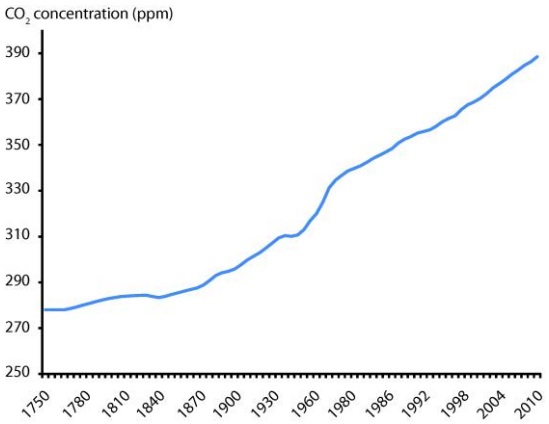

Figure 2: Atmospheric Concentration of CO_2 (ppm) [1]

About a third of the CO_2 emissions come from burning fossil fuels in power plants for electricity generation purposes.[3] Nevertheless, the utilization of fossil fuels (coal, oil, natural gas) continues to represent more than 80% of the primary energy supply [2]. The situation has no better forecast in the near future, because the utilization of fossil fuels has not reduced, indeed, coal, which has the highest emission intensity of conventional fossil fuels [2], is also the fuel with the higher growing rate of utilization. Coal's price, availability and the location of coal reserves, encourage its great utilization in electricity productions, especially in China and Asia (developing countries). Also, with the continuous improvement of oil extraction techniques the reliance on fossil fuels is expected to continue at least in the next decade [4].

Different ways of curtailing greenhouse gases emissions have been explored, such as switching to lower carbon fuels (e.g. nuclear power or renewable sources), reducing energy consumption by improving energy efficiency and employing carbon sequestration techniques. During the present work, the technology of Carbon capture and Storage (CCS) was approached. This technology relies on separating the CO_2 from an exhaust gas from the energetic and industrial activities (named as stationary emission sources) into a pure CO_2 stream for sequestration in geological formations.[4] A number of governments (U.S, E.U, and Australia) are supporting technology development and commercial deployment, because it is considered essential to mitigate climate change.[4] However, CCS technology still needs a significant amount of research related to cost reduction and energy efficiency improvements.[5]

1.1 Motivation

The present work focuses on a post-combustion carbon capture and storage technology (CCS) called calcium-looping, which consists in the removal of CO_2 from flue gas with a solid sorbent, limestone. This technology has attractive advantages such as the cheap and abundant carrier, low energy

penalty and mature large-scale technology equipments. Also, the possible synergy with cement manufacturing has become the CaO-looping one of the most promising CCS technologies. Therefore, there is an immense R&D with the aim of achieving an efficient and inexpensive process. [4, 5]

The main drawback of CaO-looping technology is the rapid deactivation of the sorbent reactivity after several cycles of CO_2-capture-and-release. Different methods to either reduce the rate decay in reactivity or to reactivate the sorbent have been investigated.[6] However, most research has been performed using a gas mixture comprising of solely CO_2 and N_2 as the gas reactants, leaving an uncertainty about how others flue gas components affect the reactivity of the sorbent. Therefore, the present work aims to study the influence of steam on the sorbent reactivity given that steam is an important compound in a flue gas (e.g. 5-10% in a flue gas from coal). The presence of steam during the calcium-looping process is known to increase the rate of sintering and the rate of calcination.[4] However, the steam effect on carbonation conversion is still unclear. Donat et al.[4] reported an improvement in the sorbent reactivity when steam was present whereas a later paper from Arias et al.[7] only noticed a small influence of steam on the carbonation conversion. Thus, the main goal of this work is to clarify if the presence of steam has a positive or negative influence on the carbonation reaction.

1.2 Objectives

The aim of the present work is to improve understanding about steam influence on the CaO sorbent performance, more specifically how steam affects the kinetics of the carbonation reaction. Briefly, the main objectives of this work are:

- Study the sorbent behaviour during repeated calcination/carbonation cycles;

- Elucidate the influence of steam on carbonation reaction during multi-cycle experiments, for different types of limestone;

- Compare conversions and carrying capacities obtained for experiments performed with and without steam;

- Analyse the sorbent decay when steam is present;

- Apply a pore model in order to obtain the intrinsic reaction rate constant for the carbonation reaction.

1.3 Thesis Outline

This text is organized as follow. Chapter 2 presents a literature review on the subject, focusing on information previously available about the different processes to capture CO_2 including a detailed description of the calcium-looping cycle. Chapter 3 presents the materials and methods used in the experimental work and the experimental set-up is also described. Chapter 4 shows all the results obtained and a thorough discussion of these is made. Results of experiments performed with and without steam for two limestones, Havelock and Purbeck, are compared. Also in this chapter a short modelling exercise is done in which the Random Pore Model is fitted to the experimental results. Chapter 5 presents the conclusions of the present work and Chapter 6 presents the suggestions for future work.

2. Literature Review

2.1 Carbon Capture and Storage (CCS)

Carbon Capture and Storage (CCS) refers to the set of technologies developed to capture CO_2 from the exhaust gases of power stations or other industrial sources. [2] This technology consists of three steps, the capture of CO_2, the transportation of the high purity CO_2 stream and its storage. The CCS techniques are described by the EU as a way to reduce CO_2 emissions and to achieve the goals proposed for all EU countries in 2020. [1]

The CO_2 Capture Technologies are classified in three different types of technologies, which are: (i) pre-combustion, (ii) oxy-combustion and (iii) post-combustion. The main objective is the same: to obtain a high-purity CO_2 stream suitable for storage, followed by other stream depleted in CO_2 that also results from the implemented process.[8]

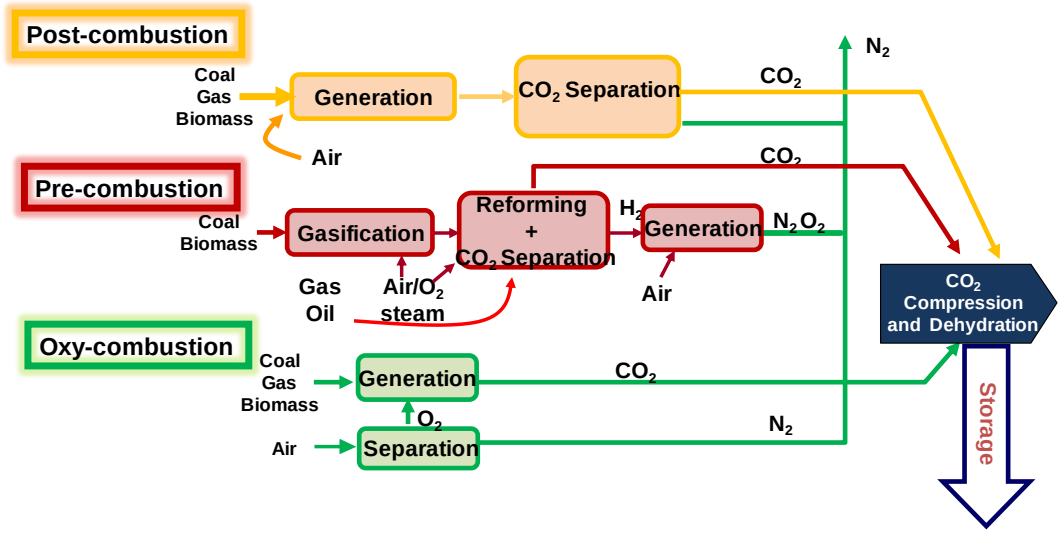

Figure 3: Classification of CO_2 capture processes

2.1.1 Pre-Combustion

Pre-combustion technologies consist of removing CO_2 before the combustion step. This specific CCS technology involves the gasification of the fuel, reacting the fuel with insufficient oxygen in order to produce synthetic gas or “syngas”, by incomplete combustion. The syngas comprises predominantly

carbon monoxide, hydrogen, methane and carbon dioxide. These gases are converted into a mixture of CO_2 and H_2, by passing the gases through a series of catalyst beds and through a reforming process. The CO_2 and H_2 are separated with the goal of proceeding with the transport and CO_2 storage, and thus the remaining H_2 can be used as fuel.[2, 9] Pre-combustion processes have the advantage of requiring less energy than post-combustion, however the gasifier has a high capital cost, making the total capital costs higher. [2, 9]

2.1.2 Oxy-Combustion

Oxy-combustion involves combustion of fuel with a pure oxygen stream (with recycled CO_2 from the exhaust), which results in a flue gas comprising of mainly CO_2 and water vapor. The recycled CO_2 is in order to moderate the high flame temperature in the boiler. After this, the CO_2 is easily separated by a condensation process. The major cost and energy penalty of this process is the previous cryogenic separation of air. On the other hand, the high-purity CO_2 stream obtained (99.9%)[8] is the stronger advantage of oxy-combustion technology.

2.1.3 Post-Combustion

The Post-combustion capture is an “end of pipe” technology, which enables its deployment without drastically affecting the process operations. Post-combustion processes aim to remove CO_2 from a flue gas resulting of a combustion, constituted mainly of nitrogen, water, CO_2 and other impurities (SOx, NOx and dust), depending on the fuel used. There are different separation technologies being analyzed, such as membranes, cryogenic separation, solvents and sorbents. A high purity stream is achieved and approximately 90% of the CO_2 from the flue gas CO_2 is absorbed. On the other hand, this technology reduces the power station efficiency, since it requires about 20% of the electricity generated in the power station.[2]

Post-combustion processes are a promising technology and the post-combustion calcium-looping using calcium oxide as a sorbent is the leading technology being developed.[2] Currently, there are no industrial plants of solid sorbent post-combustion capture, there are only pilot or laboratory plants for research purposes. For example, in Oviedo, Spain, a 30kW test facility comprising two interconnected circulating fluidized bed (CFB) reactors was developed by INCAR-CSIC and CO_2 capture efficiencies of 70-90% were reached. [10]

The closest-to-market post-combustion process is based on amine-based solvent scrubbing and it is already implemented in some power plants, as in the case of Sleiper power plant in Norway and in Salt Creek, USA.[2, 8]

CCS research has been focused on two areas: (i) improvement of the capture step regarding the energy efficiency; (ii) improvement of the infrastructures for transporting/storage of the CO_2 stream. Overall, for the future development of this technology, a reduction of processes costs (separating, compressing, transporting and storing) is necessary. Also, government financial support (e.g. increase the price of emission taxes) is necessary in order to motivate the energy producing and the industrial sector in deploying the CCS installations. One of the CCS main goals is reducing the emissions of intensive industries, such as cement industry, oil refineries, pulp and paper production, and others.

Further investigations are trying to find some application for the CO_2 pure stream. Presently, enhancement of the hydrocarbon recovery is the only application recognized. A future application in plastic and fuels production (e.g. methanol) has been investigated. [2] . Though, it is difficult to come across with a significant market because of the large amount of CO_2 generated. Mainly, the storage of carbon dioxide is done in geological structures, such as saline aquifers, depleted oil and gas fields.

2.2 Calcium Looping Technology

The utilization of calcium oxide as a sorbent to separate the CO_2 from an exhaust gas has shown to be a very promising technology for mitigating the CO_2 emissions. This technology takes advantage of the reversible reaction between CaO and CO_2 to form $CaCO_3$. Calcium oxide is supplied by limestones, which are attractive CO_2 carriers because they are cheap and abundant materials in the nature.[5] Calcium-looping technology has other key advantages, which are: (i) low energy penalty, (ii) synergy with cement manufacturing, (iii) use of mature large-scale equipment (reduces scale-up risk).It also has the advantage of reducing the thermal efficiency associated with the CO_2 capture, to about 6-8%, compared to 8-10% for MEA-scrubbing.[2] However, the decay of the sorbent reactivity after several cycles of CO_2 capture-and-release, affects the cost efficiency.[4] Nevertheless, if the exhausted sorbent is used as feedstock for cement industries, reactivity loss becomes a minor problem[2]. Significant research efforts have been done to improve the long-term capacity of calcium oxide sorbents.

2.2.1 Comparison between Calcium-Looping and other technologies

Limestone has a higher equilibrium capacity which allows to have higher capacities of CO_2 absorption than other processes in development. Actually, 1kg of CaO can capture 393g CO_2 for only 50% conversion, much higher than the capacities shown by MEA scrubbing and activated carbon. [9, 11] This new technology can also achieve less cost per gCO_2 captured. Furthermore, calcium looping cycle is expected to have a lower energy penalty when compared to MEA scrubbing for example. [2] Carbonation/calcination cycles not only can be applied in post-combustion capture but also can be used for pre-combustion capture, associated with hydrogen production. [12]

Regardless of all the points referred above, it is necessary to continue the progress in understanding the kinetics of the calcium-looping reactions to accomplish sorbent optimization. Also the scaling-up of the process remains a challenge due to the existing attrition and due to the sorbent decay. [13]

2.2.2 Calcium-looping Combustion systems

The principle of this technology is the reversibility of the capture reaction between the sorbent, calcium oxide, and the carbon dioxide. In order to do this it is necessary to have at the same unit the carbonation reaction, which captures in fact the CO_2, and the reverse reaction named calcination. Thus, this cycle technology is based on the use of lime-based sorbents in a dual fluidized bed combustion (FBC), constituted by a carbonator and a calciner reactor.[3, 14]

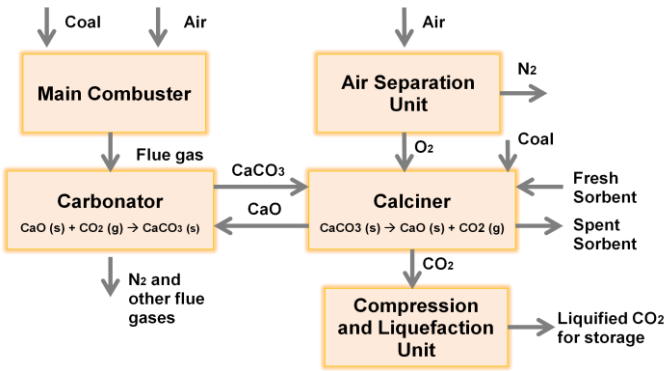

Figure 4: Calcium looping technology applied to capturing CO_2 from a combustion flue gas [4]

Figure 4 shows the complete process of calcium-looping technology. Firstly, the flue gas originated in the combustion on a power station enters the first fluidized bed reactor, the carbonator. Here, CO_2 is separated from the other gases by reaction with CaO being converted to $CaCO_3$, at 650ºC. In the second reactor, $CaCO_3$ (product of the first reaction) is converted again into CaO, regenerating the sorbent. This regeneration step requires input of energy in order to accomplish the required temperature (900ºC) to drive the endothermic calcination reaction. Thus, it is necessary to perform the calcination reaction in an oxy-combustion process.

Calcium looping cycle is based on the reaction between the calcium oxide (sorbent) and the carbon dioxide (Equation 1).

$$\boldsymbol{CaO}\,(\boldsymbol{s}) + \boldsymbol{CO_2}(\boldsymbol{g}) \leftrightarrow \boldsymbol{CaCO_3}(\boldsymbol{s}) \quad (1)$$

The direct reaction is called *carbonation* and it is responsible for the capture of CO_2. It is an exothermic reaction and it is carried out in a temperature around ~650ºC, at atmospheric pressure. The reverse reaction, *calcination*, produces the high-purity CO_2 stream that is directed to the storage step and, at the same time, the sorbent calcium oxide is regenerated. It is an endothermic reaction, carried out at high temperatures around ~900ºC.

It is important to understand how these reactions behave when different conditions are applied. Thus, it is necessary to understand the equilibrium between the carbonation and calcination reaction, to enable its utilization in the optimum way.

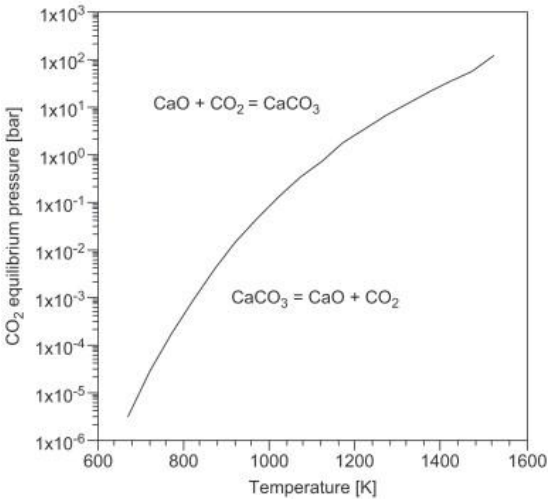

Figure 5: Equilibrium partial pressure of gaseous CO_2 above CaO as function of temperature[15]

Baker [16] in 1962 developed an expression to describe the equilibrium (Equation 2).

$$\log_{10} P_{CO_2}[atm] = 7.079 - \frac{8308}{T[K]} \quad (2)$$

In Equation 2, the CO_2 partial pressure is displayed as P_{CO2} and expressed in *atmospheres* and *T* is the temperature of the system expressed in *kelvin*.

The equilibrium (Figure 5) can be understood very briefly with a simple example selecting a given concentration of gaseous CO_2 at a given pressure. In these conditions there is an equilibrium temperature and above it the calcination is preferred (as it occurs at higher temperatures), or else, below the same temperature the carbonation reaction is preferred. This way it becomes clear that for a calcium-looping cycle two different temperatures should be used. Instead of varying the temperature two different CO_2 partial pressures can also be used such as two different absolute pressures.[9]

2.2.3 Calcination Reaction

The calcination reaction is the sorbent regeneration reaction and produces also a pure CO_2 stream. The mechanism of this reaction depends on many variables, such as the type of limestone, the particles size, CO_2 partial pressure, structural changes and diffusion rate.[8] Particularly, the atmosphere in which the calcination reaction takes place has a great impact in the sorbent performance, because the atmosphere may determinate the surface area, pore volume and the pore structure. The structure of the sorbent determines the internal surface area available, and therefore, it determines the total conversion of the next cycle. Nevertheless, a high surface area is associated with very small pores and these can be not available for the subsequent carbonation reaction due to some drawbacks, as sintering. [5]

Khinast et al. [17] reported that the calcination reaction has an induction stage, followed by a fast reaction stage controlled by chemical reaction and a last step controlled by particle diffusion resistance. It was also shown that under the investigated conditions the product layer diffusion and the heat transport were not limiting steps. However, the calcination reaction decayed exponentially with increasing CO_2 partial pressure, under the same experimental conditions. It is widely accepted that for atmospheres with high CO_2 partial pressures, the calcination reaction rate decreases.[18] Concerning the ideal temperatures for the calcination, a balance has to be done between high temperatures that promote fast reaction rates, and the structural problems caused by sintering (see also Chapter 2.2.6.2). Other important factor for the calcination rate is the size of the limestone particles. Larger particles can cause problems related to mass and heat transfer reducing the velocity of the reaction.

2.2.4 Carbonation reaction

The carbonation reaction is an exothermic reaction and it is an incomplete reaction. This is due to structural limitations of the sorbent, and so, depending on the reaction conditions, different degrees of conversion can be achieved. According to Bhatia and Perlmutter [19] in the end of the first cycle the conversion is already restricted to around 70%. This is due to the fact that the reaction is dominated by the small pores contained in the calcine that start to narrow at about 60% of conversion. Further conversion is thus restricted only to the larger pores which react slowly. [3]

Bhatia and Perlmutter described the carbonation reaction as a first-order reaction with respect to the CO_2 partial pressure.[19] This reaction consists of a first stage when carbonation is rapid and chemically controlled and a second stage where the rate is diffusional controlled (diffusion through the $CaCO_3$ layer). The transition between the fast and slow regimes takes place suddenly at a given level of conversion, relying on the experimental conditions. As the number of carbonation/calcination cycles increase the transition to the lower regime happen at lower conversions. [13]

Small conversions in the carbonation reaction are mainly caused by the formation of a product layer that covers the surface available for the CO_2 capture and the coverage of the small pores mainly responsible for the fast reaction. What is believed to happen is that there is a lack of space hampering the growth of the product. Experimental studies driven by Alvarez and Abanades[20] have demonstrated that for different types of limestone textures a product layer of $CaCO_3$ is formed with about 50nm thick. The slow step is thus due to the diffusion of CO_2 through this layer before contacting with the solid sorbent.

Despite the formation of this impeditive layer there is a characteristic conversion that remains active even after many carbonation/calcination cycles. Florin and Harris [21] studied this residual sorbent capacity for multi-cycle experiments. They concluded that the decay asymptote in the carbonation conversion trend represents the establishment of equilibrium between the pore volume and surface area loss during thermal sintering, and the pore volume and surface area regeneration as a consequence of a solid-state diffusion mechanism. As soon as this equilibrium is established, there will be the same residual conversion of carbonation for all cycles.

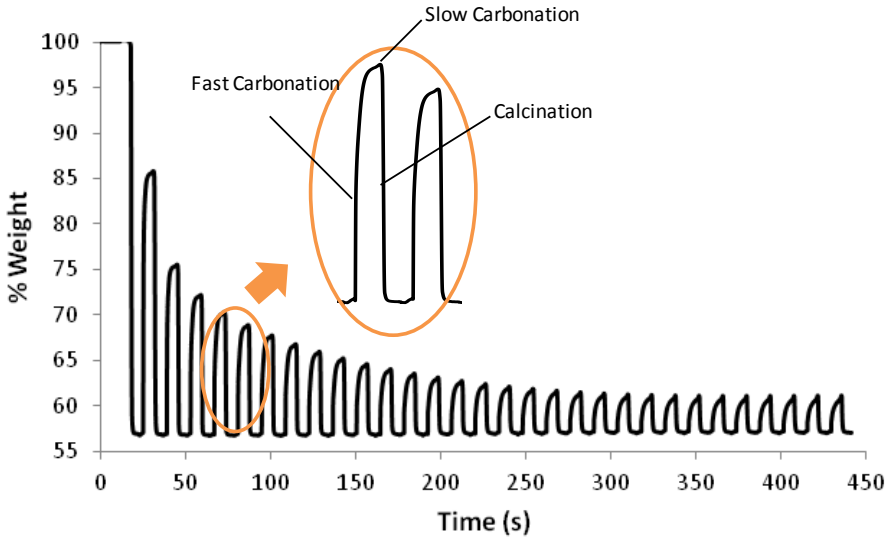

Figure 6: Calcination/carbonation cycles (data obtained with the TGA)

2.2.5 Sorbent Performance

It is extremely important to understand how some operating variables affect the sorbent capacity of absorbing CO_2, such as sorbent type, particle size, calcination time and calcination temperature. To analyze the effect of these variables a new concept named *carrying capacity* is introduced.

2.2.5.1 Sorbent type

Some literature showed that the type of sorbent, limestone or dolomite, affects the performance in the sulphation reaction, diminishing the $CaSO_4$ formation. This is because different limestones generate different textures in calcinations, what leads to different conversions in the sulphation reaction. Hence, Abanades and Grasa [13] decided to study the effect of this variable on the carbonation reaction to see if its influence was also important in the reaction conversion. Their experiments were performed in different conditions and the sorbents were subjected to multi-cycles up to 500. It was shown that among all the 6 limestones studied, one behaved differently showing a poor performance in the first cycles. However, all the different types of limestone had a similar decay in the rate of conversion. Therefore, the most important factor to bear in mind is to select limestones from the same origin in order to simplify the scale-up of the technology, because the same sorbent behavior will be achieved. Nevertheless, the selection of the sorbent should be based in other important factors as their availability, cost, mechanical stability and so on.

2.2.5.2 Particle size of the sorbent

It was shown that the particle size of the sorbent has influence in the sorption capacity in the fast reaction stage. However, this variable did not show to have a meaningful influence when the sorbent is taken to multiple carbonation/calcination cycles.[13]

2.2.5.3 Calcination Temperature

To study the effect of calcination temperature is important, because finding an optimum range will allow to achieve better results. Particularly, high temperatures promote high conversion rates, although it also promotes deactivation processes such as sintering. It was shown that for temperatures up to 950ºC the sorbents performance did not change. On the other hand, calcinations temperatures in the range of 950 up to 1000ºC made the activity of the sorbent decrease. Other authors work argue against this because their experimental results showed that, if operating in a continuous mode, high temperatures promote high conversion rate.[13] In this case, the temperature effects in the rate of conversion have overcome the sintering process. Further investigation has to be made to explain this discrepancy. Though, systems working at atmospheric pressure, as post-combustion systems, calcinations at 950ºC are already feasible enough, since they do not deteriorate the sorbent.

2.2.5.4 Calcination Time

The importance of the calcination time has to do with its influence on the sorbent texture. Since the calcines' texture determines the maximum level of conversion, it is necessary to understand the influence of time in the initial properties of the sorbent. Previous studies revealed that the duration of the calcination reaction affects the maximum conversion, although for multiple cycle experiments this effect becomes negligible.[13] Alvarez and Abanades [5] visualized during their experiments with extended residence times, that important changes in the pore network happened during the first calcinations. Nevertheless, after 30 cycles the effect of time on the sorbent disappears (becomes the same as samples subjected to shorter times). It is important to notice that increasing calcination times cause the decay in the sorbent activity, however the effect caused is much lower than sorbents subjected to sintering mechanisms.

Summarizing all said before, the most important variables for a good sorbent performance are the temperature and the time of the calcination reaction. High values of these variables accelerate sorbent

degradation, reaching the residual conversion at a lower number of cycles. However, the residual conversion of the sorbent seems to be insensitive to extreme conditions.[13]

2.2.5.5 Carrying capacity

In order to measure the efficiency of a sorbent it was introduced a parameter called *carrying capacity*. This parameter is used to quantify the amount of CO2 absorbed by the sorbent in the carbonation reaction taking into account the quantity of CaO in the original sorbent. It is defined through the following equation:

$$\boldsymbol{Carrying\ Capacity} = \frac{(m_{CO_2})_i}{m_{CaO,initial}} \quad (3)$$

Where m_{CO_2} corresponds to the mass of carbon dioxide absorbed by the sorbent for cycle *i* and $m_{CaO,initial}$ is the quantity of calcium oxide present in the initial amount of limestone. The calcium oxide quantity is determined by the knowledge of the limestone purity. From the stoichiometry of the carbonation reaction it is observed that 1g of CaO would capture 0.79g of CO_2 if a complete reaction were achieved. However, the ability of CaO sorbents to take up CO_2 decays rapidly upon cycling.

Many experiments were made to determine the carrying capacity of natural limestone in fluidized or fixed bed reactors under conditions similar to the reality, i.e., atmosphere containing CO_2 and calcination performed at high temperatures.[22-25] No more than 30% (molar basis) of carbonation conversion was achieved after 15 or 20 cycles.[9] Pore blockage is assumed to be the reason for the degradation in the carrying capacity by causing changes in the initial pore network.[23] However, a residual carrying capacity was shown to be kept after multiple-cycles, becoming constant around a specific value.[13] This asymptotic value was found to be about ~8% of carbonation conversion for natural limestones. [10, 26, 27]

2.2.6 Deactivation Processes

Carbonation reaction has showed through many studies to be far from being complete. Additionally, the CO_2 capture reaction has revealed to be sensitive to some imposed conditions, making its results even worse. Hence, it is important to look at some effects that can originate the sorbent decay. Mainly the sorbent decay is related to the exposure to extreme experimental conditions (temperature, pressure…) or related to the composition of the surrounding atmosphere.

2.2.6.1 Sulphation Reactions

When calcium-looping cycle technology is applied in a post-combustion system, the CaO will be contacting an exhaust gas from a power station. This exhaust gas comprises more compounds besides carbon dioxide. Hence, the calcination/carbonation cycles must be optimized within these conditions. Unfortunately, SO_2, a product of sulphur combustion competes with CO_2 in the solid-gas contact with the sorbent. Indeed, calcined limestones have already been used to capture SO_2. [9] Since coal contains typically 0-8 % (wt) of sulphur [18], it is possible to have sulphation competing against the carbonation reaction.

$$\boldsymbol{CaO}\,(\boldsymbol{s}) + \boldsymbol{SO_2}(\boldsymbol{g}) + {}^{\boldsymbol{1}}\!/_{\boldsymbol{2}}\,\boldsymbol{O_2} \leftrightarrow \boldsymbol{CaSO_4}(\boldsymbol{s}) \qquad \Delta\boldsymbol{H_{r,298K}} = \boldsymbol{-502\ kJ/mol} \tag{4}$$

$$\boldsymbol{CaCO_3}(\boldsymbol{s}) + \boldsymbol{SO_2}(\boldsymbol{g}) + {}^{\boldsymbol{1}}\!/_{\boldsymbol{2}}\,\boldsymbol{O_2}(\boldsymbol{g}) \leftrightarrow \boldsymbol{CaSO_4}(\boldsymbol{s}) + \boldsymbol{CO_2}(\boldsymbol{g}) \qquad \Delta\boldsymbol{H_{r,298K}} = \boldsymbol{-324\ kJ/mol} \tag{5}$$

Equation 4 is known as indirect sulphation and it occurs when CO_2 partial pressure in the reaction vessel is less than the equilibrium vapor pressure of CO_2. On the other hand, direct sulphation (Equation 5) occurs when CO_2 partial pressure is greater than the equilibrium vapor pressure of CO_2.[18] This $CaSO_4$ formed makes the sorbent not useful for calcination/carbonation cycles and the sorbent has to be replaced. Therefore, different authors tried to find how SO_2 affects the CO_2 conversion into $CaCO_3$. They observed that the presence of higher CO_2 partial pressures led to a lower sulphation rate.[9] The same effect was seen when partial pressures of SO_2 were higher, i.e. the carbonation rate diminished. [28] This was explained by the formation of sulphate products, such as $CaSO_4$. The high molar volume of $CaSO_4$, bigger than CaO and even bigger than $CaCO_3$, is thought to be responsible for causing pore blockage. In fact, Sun *et al* [28] reported a faster loss of conversion during calcination/carbonation cycles when SO_2 was present.

Although, the ability of absorbing SO_2 seems to be an disadvantage of calcines when the key objective is the reaction with CO_2, some authors suggested that it could be a good option to valorize the spent limestone, given the appreciable conversion to SO_2 after reaching the residual conversion in CO_2 capture.[8, 29] Using this property of the calcine could be a good solution for take the sulphur present and thus protect the calcination/carbonation cycles. Other option suggested is the installation of a desulphurisation unit before the calciner.[30]

2.2.6.2 Sintering

Sintering is caused by high temperatures and it is responsible for changing CaO initial texture by causing changes in the pore structure, such as grain growth or pore shrinkage. This effect happens

when the sorbent is in contact with high heating during high times of calcination. It also happens when the calcination/carbonation cycles occur in the presence of higher partial pressures of steam and/or carbon dioxide, and in the presence of impurities[18].

Borgwardt in 1989 [31] noticed in his experiments with CaO from ultrapure $CaCO_3$ and with CaO derived from limestone (contain impurities) that sintering is strongly dependent on temperature and impurities. Moreover, impurities accentuate the sintering effect at a specific temperature. The porosity decline, also reported by this author, showed a logarithmic decay during the sintering process. This supports the intrinsic idea of sintering causing grain growth on the sorbent. More recent studies made by Alvarez and Abanades[5] showed that pre-sintered samples achieved lower carbonations conversions compared to fresh calcines. The fresh CaO presented a conversion 10-15% higher after the first carbonation. The authors suggested that this result was caused by an increase in the pore size and caused by the parallel reduction in the surface area, which must have occurred in the pre-sintered samples.

2.2.6.3 Pore blockage

Besides the sintering causing grain growing in the sorbent physical structure, other textural effect happens during calcination/carbonation cycles. The deposition of $CaCO_3$ formed during the carbonation causes the pore blockage effect. A product layer starts to grow, filling up the superficial pores, and thus, the interior pore network is not available for further carbonations. [13] The formation of these narrow bottlenecks in the pore mouths is responsible for the continuous loss of sorbent surface area, reducing continuously the rate of carbonation. Indeed, it was found that the carrying capacity of the CaO after experiments comprising multi-cycles of calcination/carbonation was roughly proportional to the voidage inside pores with diameters less than 150nm.[23]

2.2.6.4 Attrition

Limestones have a lot of impurities and different compounds in its composition. Due to this, limestones are affected by attrition in the cracks existing in the limits between different compounds. That creates structural weaknesses and thus some facility in breaking into smaller pieces.

The attrition problem begins with the scale-up of the calcium looping process. The best reactors for these reactions (carbonation and calcination) are the fluidized bed reactors (FBR). The FBR operation is already well understood, however the strong contact between sorbent particles promotes high rates of attrition. Hence, attrition is another cause for the carrying capacity decay. When submitted to attrition, limestone particles start to have changes in properties and material is lost due to elutriation of

fines.[9] With the elutriation of material from the reactor the overall efficiency will be affected since less material is available for the reaction. [18]

2.2.7 Enhancement of Calcium-Looping Technology

In Chapter 2.2.6 it was reported the main effects responsible for the carrying capacity sorbent decay. Since this is a drawback in the calcium-looping cycle future industrial application, researchers have tried to find ways to overcome these difficulties. This has been done in three different paths: (i) determination of optimal operating conditions; (ii) development of synthetic sorbents, and (iii) study of sorbent enhancement techniques.[27]

The operating conditions and its relationship with the conversion of the carbonation reaction were already described in the Chapter 2.2.5, so they will not be discussed further here. Though, this chapter will briefly embrace the points (ii) and (iii). The methods that have showed some potential in solving the sorbent decay are the reactivation by steam/water (hydration), thermal pre-treatment, chemical doping of the sorbent and the production of synthetic sorbents.[3]

2.2.7.1 Thermal Activation

The Thermal Activation consists in the application of a prolonged calcination before starting cycling the sorbent at different temperatures. The main purpose of this treatment is to stabilize the sorbent morphology, because this aids in maintaining the CO_2 carrying capacity along cycles.[3]

To test the effect of thermal activation in protecting the carrying capacity, Manovic et al [32] performed pre-treatments at temperatures between 800-1300ºC and also with different durations, 6-48h. The results showed that pre-heated sorbents have lower conversion in the first cycle. However, the conversion of the pre-heated samples increases during cycles, and they actually achieved better results in the next cycles. This effect is called self-reactivation of the sorbent.[32]

Indeed, the thermally pretreated sorbents were found to be more reactive at higher number of cycles. This effect was found especially pronounced for powdered samples, pre-treated at 1000ºC. After 30 cycles these samples had 50% of carbonation conversion, comparing to the only ~25% of the non pre-treated samples.[3, 18, 32]. However, since the composition of the sorbents is so different, there are some sorbents that do not show enhance performance after pre-treatment at high temperatures, e.g. La Blanca limestone.[3]

A recent study developed by Arias et al [33] concluded that self-reactivation may not be expected under typical reaction conditions of a circulating fluidized-bed carbonator, because the reaction time is

only limited to few minutes. So, the implementation of thermal pre-treatment does not seem possible in a real capture system, because it is also known to decrease the mechanical resistance and the sorbent elutriation.[32]

2.2.7.2 Hydration

Sorbent hydration is based on the chemical reaction displayed below (Equation 6). The direct reaction is exothermic ($\Delta_r H_{298K} = -109\ kJ.mol^{-1}$) whereas the backward step denominated as dehydration reaction is an endothermic reaction.

$$\boldsymbol{CaO + H_2O \leftrightarrow Ca(OH)_2} \quad (6)$$

Since this method is accepted to be the most promising to solve the decay problems, many researchers have been studying how this reaction behaves under different experimental conditions, how the rate of carbonation is improved and also how it affects the sorbent structure. Because this reaction is not the main focus of this report only the most important studies will be presented to give a general idea of the work that has been done.

Two different groups of researchers reported that the reactivity of spent sorbent can be doubled following hydration.[18] Manovic and Anthony[34] performed their experiments in a TGA and the sorbent hydration was made in a pressurized reactor containing steam at 200ºC. They observed that the reactivated sorbents achieved about 70% carbonation conversion after 10 cycles, compared to the 35-40% for the original sorbent. [3, 34] It has shown thus that hydration improves sorbent characteristics and that may enable the use of the sorbent for prolonged time. Other experiments realized by Blamey et al [24] with hydrated limestone particles that had already experienced 13 calcination/carbonation cycles also showed an improvement in carbonation conversion.

Other author, Zeman[35] studied the application of the hydration technology to a capture plant. Zeeman discussed the employment of a third reactor between the calciner and the carbonator, in which the hydration occurs. The third reactor operates at 300ºC in order to minimize the thermal load of cycling. Nevertheless, these experiments have a drawback, since the improvement in carbonation conversion only was studied for ten cycles.[18]

The advantage of pre-treated samples with hydration processes is thought to be due to a larger specific surface. The particle core swells with the water, which make the particle to break into small fractures. After the dehydration, it is achieved a CaO with higher surface area and thus more

reactive.[36] However, this same effect induced the attrition of the particles, as it was observed by Fennel et al.[22] in experiments in a fluidized bed reactor.

2.2.7.3 Synthetic Sorbents

The manufacture of synthetic CaO-based sorbents tries to overcome the morphological disadvantages of the natural sorbents. It is aimed to increase the surface area or to do improvements concerning the sorbent mechanical stability.

Currently, the calcium aluminate-based pellets are reported to be the most efficient and inexpensive sorbents for CO_2 capture.[3, 37] These sorbents can aid with the sintering reduction, attrition and the consequent elutriation. Furthermore, these aluminate-based pellets can be reactivated/reformed by water, which results in mean conversions of ~35%. However, this synthetic sorbents lose their activity with high temperatures.[3] Other synthetic sorbent prepared using a sol-gel method was reported to achieve improvements in reactivity and sintering resistance. Santos et al. [38] synthesized a CaO sorbent with a coral-like morphology. This different structure gives a higher surface area to the sorbent with a value of 45 m^2/g, 5 times higher than a CaO obtained from a commercial $CaCO_3$. Concerning carrying capacity, the sorbent showed a constant reactivity throughout 18 cycles (0.58 $gCO_2/gCaO$). The residual conversion was also improved with a value of 0.24 $gCO_2/gCaO$ achieved after 70 carbonation/calcination cycles.

There is also a possibility of creating synthetic sorbents by dispersing CaO across an inert matrix or support. For example, Li et al. [39, 40] reported that their $CaO/Ca_{12}Al_{14}O_{33}$ sorbents were characterized by having a high cyclic stability with conversions of more than 40% through 13 cycles and conversions about 20% after 56 cycles. On the other hand, Pacciani et al. [41] have prepared CaO on a mayenite matrix, but no significant improvement was noticed. However, a strong point of this synthetic sorbents is that the sorbent reactivity increases with increasing concentration of CO_2. This favors the implementation of synthetic sorbents in a real industrial system. [18]

An overall view allows to understand that synthetic sorbents are very promising candidates to achieve higher conversions in the CO_2 capture reaction. The major drawback in its use is the high cost of manufacture.

2.2.7.4 Doping

Doping is a chemical pre-treatment in order to enhance the cyclic stability of a sorbent. There are many different methods, such as mixing with solids or aqueous salt solutions. In 2003, Salvador et al.

[42] used two salts, Na_2CO_3 and NaCl, with the key objective to reactivate the lime and enhance CO_2 capture. The experiments were performed in a TGA and in a fluidized bed reactor. In the TGA experiments, only the addition of NaCl achieved good results, since the overall capacity was raised to an almost constant value of 40% through 13cycles. On the other hand, the experiments in the FBR did not achieved any promising results, moreover these additives (Na_2CO_3 and NaCl) had the reverse effect of severely reducing the CO_2 capture capacity.[42] However, Fennell et al. [23] did experiments with the same dopants in a FBR and observed a small improvement in the long-term carrying capacity for small amounts of salt (<0.1 mol/l). The reason why salts may affect the limestone behavior during reactions seems to be due to different valences of the salt ions that can cause defects in the limestone lattice, thus improving diffusion transport mechanisms.[9, 31]

Other salts were studied, e.g. Gonzalez et al. [43] studied limestones doped with KCl and K_2CO_3 in a fluidized bed reactor. Although the doped limestones had showed a slower initial reaction rate (measured in a TGA), limestones doped with small amount of salt (~0.05 mol/l) obtained higher conversions than the undoped limestones. [9] By the same time, Florin and Harris [12] performed doping experiments using a lithium compound, Li_2CO_3. Although an increase in the rate of CO_2 capture was observed, the long-term carrying capacity conversion was not improved. Further studies with alkali metals showed to improve the sorption capacity with the increase of atomic radii of the alkali metals (Li< Na< K< Rb<Cs), although studies covering multi-cycles are still missing.[9] More recently, Beruto et al. [44] found that metal ions smaller than Ca^{2+} were useful as doping agents since they reduce the sintering rate.[9] For the time being, none doping agent proved to significantly improve the long-term reactivity of the CaO.

2.2.8 Effect of steam on CaO-based sorbents

In calcium-looping experiments, researchers usually choose to simplify the atmosphere in which the reactions take place, to facilitate the analysis of the experimental results[45]. However, CaO sorbent behaves differently in different atmosphere compositions, as when SO_2, H_2S or CO_2 are present. Individual effects of both SO_2 and CO_2 have been widely investigated, however the flue gas composition has a more extensive range of compounds. Steam is generally present at significant percentages in any flue gas from fuel combustion. For example, in a flue gas from coal steam can be between 5-7% of the total composition of the stream (total composition:10-15%CO_2, 3-4% O_2, 5-7% H_2O, 500-3000ppm of SO_2, 150-500 ppm of NO_x) [9, 46]. Thereby, the purpose of this study is to improve understanding about the steam influence in the CaO sorbent performance. A review about the previous findings on the effect of steam is done here, mentioning the most relevant papers.

Since the effect of steam in the calcination/carbonation reactions with a calcium oxide sorbent is not very developed yet, it is necessary to start by studying the effect of steam in other similar processes. Namely, it is important to start observing the effect caused on dolomites and in the sulphation reaction.

The first publication about the effect of steam on calcium compounds was reported by Berger [9, 47]. This paper describes that limestone was calcined in less than half of the time in the presence of steam instead of air. The same author showed that the enhancement of calcination could be attributed to the higher thermal conductivity and heat capacity of steam compared to air. [9] Later on, other authors, e.g. Borgwardt [48] noticed the importance of heat transfer for limestones with particle sizes <6 mm. However, good heat transfer properties seem not to be responsible for the enhancement of calcination by steam, at least they are not the only effect counting. Indeed, following research reported higher calcination reaction rates and also higher conversions at lower temperatures for small particles (<1mm) in the presence of steam where heat transfer effects are neglected. [9]

Although steam showed to enhance calcination conversion of limestone, detailed investigations about sintering of calcium oxide particles revealed that steam aids in the sintering phenomena. It is known that steam aids sintering of CaO and consequently, reduces the surface area available for reaction, even if it is present at lower concentrations (<2%).[9, 49, 50] On the other hand, steam also enhances the solid state diffusion in CaO.[45] Since the majority of studies were made with dry gas mixtures, i.e without steam present in the flue gas, there is no much reliable information about the reactions in the presence of steam. However, some work was made for the sulphation reaction and it may help to understand the calcination-carbonation reactions. Stewart et al. [51] reported that the conversion of both direct and indirect sulphation reactions were enhanced by the presence of steam. Thus, there is a contradictory effect observed: despite the fact that steam enhances sintering of CaO particles, steam enhances calcination[4] and it may as well enhance the carbonation reaction.

In 1977, an investigation realized by Dobner et al. [52] found that the carbonation reaction between CaO from dolomites and CO_2 was promoted by steam. The author justified this effect with the property of steam in “catalyze” the reaction at low temperatures (~550ºC). Similarly, Symonds et al. [45, 53] found an increased CO_2 absorption when steam was present, but this time with limestones. This author hypothesized that the reaction was catalyzed by H_2O due to the formation of a transient specie $Ca(OH)_2$, which is more reactive than CaO[25]. However, other studies verified that the activation energy of the carbonation reaction is higher in the presence of water, what makes this hypothesis of the catalytic effect of water inconsistent.[45] Also, Yan and Xiao[54] studied the carbonation reaction of commercial CaO (150-250μm) in presence of steam, in a pressurized TGA. For the analyzed temperatures (550-650ºC) the results were very promising. The carbonation conversion achieved after 30minutes was about 50%, while the conversion without steam was only 10%. However, other authors have showed contradictory facts. Sun et al.[55] with experiments conducted in a TGA at 850ºC concluded that the carbonation of limestone did not show any improvements owned to the presence of steam. Moreover, Lu et al. [56] stated a decrease in the carrying capacity in tests made with a synthetic sorbent (<10μm) when steam was presented.

Recently, researchers have made efforts to find explanations about the influence of steam on carbonation reaction. Manovic and Anthony [45] studied 7 different types of limestone (samples with ~30mg and size fractions range between 250-500μm) in a TGA under post-combustion capture conditions (gas mixture with 20%CO_2 and 10-20% of steam). They found that carbonation is enhanced

by steam, but is more pronounced at lower temperatures and for more sintered samples. For example, in an atmosphere containing steam the carbonation conversion was more than doubled at 400ºC. These authors justified this behavior with the enhancement of the solid-state diffusion in the product layer, as already reported by other authors. Other experiments also showed that higher steam concentrations do not affect the conversion profiles in the temperature range of 500ºC to 600ºC. A similar view is reported by Donat et al.[4]. A significant increase in reactivity of CaO-sorbents from natural limestone after 30 cycles in presence of steam (1-20%) was noticed. A synergistic effect was also observed, i.e. the highest reactivity was observed when steam was present for both calcinations and carbonation. Steam showed to influence the sorbent reactivity in two ways: (i) promoting sintering during calcinations that lead to larger pores in the sorbent (~50nm diameter), which appear to be more stable; (ii) reducing the diffusion resistance through the $CaCO_3$ layer.

There is much more to be investigated in this specific field of calcium-looping cycle. Indeed, Arias et al. [7] performed a wide range of experiments to develop a further comprehension. The experiments were made in the TGA, with limestone with smaller particle sizes (<50μm) and mass (<3 mg). Using post-combustion conditions for both calcination and carbonation, it was reported that the steam had no influence on the diffusion of CO_2 in the diffusion-controlled step. Moreover, they found that steam has little influence in the carbonation conversion (fast and slow reaction stages). However, the same experiments have indicated that different limestones can produce different results. It was noticed that steam may have a slightly positive influence by increasing the end of the carbonation step. This statement goes in agreement with Manovic and Anthony [45]and Donat et al.[4] papers. Despite this, Arias et al [7]explained that the use of bigger particles of limestone in Manovic and Anthony [45] experiments did not eliminate the external and internal diffusion effects, which make the results unclear.

Briefly, there is general agreement that the presence of steam, even at low concentrations, increases the rate of sintering and the rate of calcination.[4] So, the remaining problem is how steam influences the conversion of the carbonation reaction (CO_2 capture reaction).

3. Materials and Methods

In this chapter, the experimental set-up and the procedure as well as the materials used are described. Also, some techniques used to analyse the final samples are briefly described.

3.1 Experimental set-up

In this work, all the experiments were performed in a thermogravimetric analyser (TGA). The experiments of calcination/carbonation cycles were divided in two different groups: experiments with and without steam. Therefore, two different experimental set-ups were necessary.

3.1.1 Set-up: Experiments without steam

The thermogravimetric analyser, TA Q5000 IR was used to simulate continuous operation by changing the temperature for the carbonation and calcination reactions. The main parts of this system are the furnace where the reactions take place, the balance in the top part of the structure and the flow controllers. The reaction starts when a small platinum pan containing the limestone particles is automatically loaded to the electrical heated furnace.

This TGA has two flow controllers inside, but there is also an external flow controller which allows more than two gases to be connected at the same time. In these first experiments, “gas 1” was used as nitrogen and it splits between the balance and the furnace. A mixture of 15%(v/v) CO_2 in nitrogen was used as “gas 2” connected directly to the sample. It is essential to have a continuous flow of an inert gas (N_2) through the balance in order to avoid damaging it. The mixing effects of the purge gas in the balance and the 15%(v/v) CO_2 gas running in the furnace were assumed to be negligible.

The changes in the sample mass show the reaction progress. Both temperature and sample weight were continuously recorded by the computer and the results were simultaneously visualised in software called *Universal Analysis 2000*.

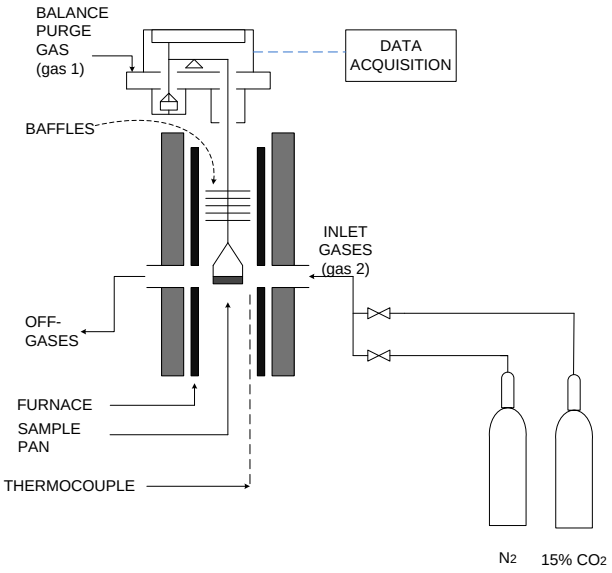

Figure 7: Schematic diagram of the experimental apparatus necessary to perform the no-steam experiments in TGA

3.1.2 Set-up: Experiments with steam

In order to introduce steam in the system a different method was necessary. Only small concentrations of steam can be used in the TGA to avoid damage to the balance. To introduce the steam in a safe way, the external flow controllers were used to introduce the *gas 2*, while *gas 1* (purge) continued to come directly from the TGA. The external rotameters (*TA Instruments*) have two ports where N_2 and the 15%(v/v) CO_2 mixture were connected. A bubbler system or a saturator of 100 ml volume was used to saturate the stream with water. In this case, external rotameters were required. The wet gas adopted the temperature of the water in the bubbler and then passed into the furnace. The higher the temperature in the bubbler, the higher the potential load of water in the gas flow. It was assumed that when exiting the bubbler the gas was saturated. A K thermocouple placed in the middle of the saturator monitored the temperature inside and it was recorded using a software, *Agilent VEE Pro 7.0*.

Steam concentrations were around ~1%. In order to monitor the steam concentration a humidity probe was introduced in the outlet line immediately after the TGA. This sensor recorded the relative humidity that was used to follow the steam concentration. Relative humidity could not be higher than 60-70%, to avoid the water condensation which would damage the sensor and also the TGA equipment. If higher concentrations of steam were desired, the lines in the system would have to be heated up which would require changes in the experimental set-up.

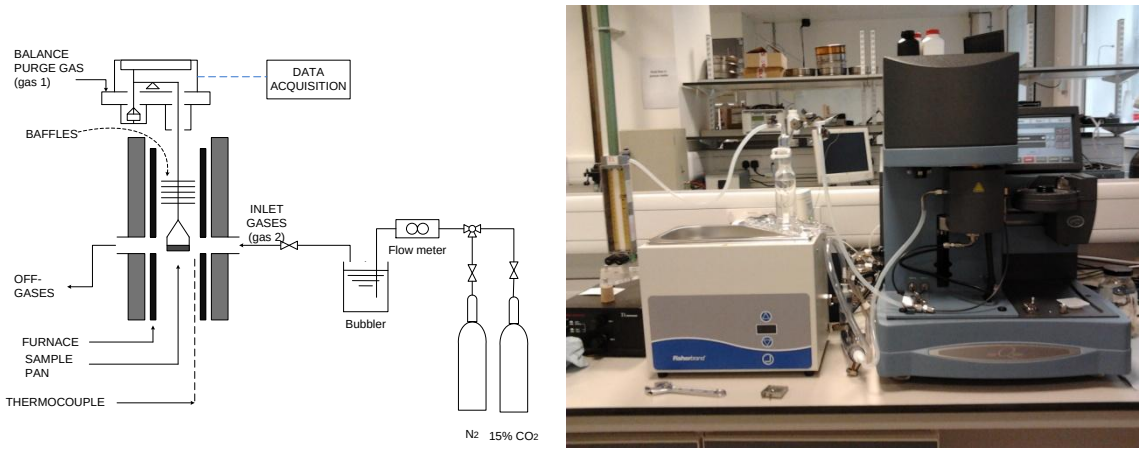

Figure 8: Schematic diagram of the experimental apparatus necessary to perform the steam experiments in TGA. Real pictures of the experimental set-up

3.2 Calibration

For the experiments carried out in the TGA in presence of steam, the external rotameters and the humidity probe had to be calibrated following the procedure explained in this section.

3.2.1 Rotameters

The external rotameters were calibrated with the experimental gases, nitrogen and 15%(v/v) CO_2. A gas line exiting these flow controllers was connected to the bottom of the bubble column filled with a mixture of detergent and water. The calibration was carried out measuring how long it took to a layer of soap to pass through a certain volume in the bubble column. Each rotameter position tested was subjected to 3 repetitions. A calibration graph was created for both gases (nitrogen and 15%(v/v) CO_2) (Figure 39 and Tables 13-14).

3.2.2 Humidity Probe

A humidity probe was used to measure the steam concentration in the flow gas. It allows temperature measurements between -40-85 ºC with an accuracy of ± 0.3 K (at 23 ºC). Relative humidity is also measured by the probe with an accuracy of ± 2%rh. The calibration method proposed by the supplier implies to use a saturated salt solution given that the variation of its relative humidity with temperature is known. Nevertheless, it was difficult to get a stable temperature in the bubbler, using the water bath

(*Fischerbrand*) so a different procedure had to be used. Five saturated salt solutions (magnesium chloride; magnesium nitrate; sodium chloride; potassium chloride; potassium nitrate) with different values of relative humidity at 23ºC were used in order to get 5 points of calibration.

An isolated plastic vessel containing the saturated solution and the humidity probe were placed in a water bath at 23ºC. After around 2 hours, the relative humidity value was stable and therefore, the container well equilibrated. The “true value” that the solution should have in accordance with the literature at that temperature was compared with the probe software in order to correct the small deviations. This procedure was repeated for all the saturated solutions.

In Appendix A the relative humidity of the salt solutions used is shown summarized in a table (Table 15).

3.3 Materials

3.3.1 Limestone

Two types of limestone were used in the experiments, Havelock and Purbeck. However, Havelock was used in most of the tests. In the last part of this work, Purbeck limestone was used to be compared with Havelock in terms of conversion enhancement with steam. These two types of limestone were selected because of their relative purity in terms of $CaCO_3$ and also because there is a significant quantity of data in previous works that could be compared with these results.

The elemental composition of the limestones was determined by X-ray fluorescence and it is summarized in Table 16. It is necessary to know the composition of the limestone for the calculation of the carrying capacity.[13]

With the aim of obtaining the desired particle sizes, both limestones were sieved twice in a sieve shaker for about ~1 hour each time. Given that the Purbeck limestone has a lot of impurities (dust) is needed to wash it with deionised water after sieving it and then dry it all night in an oven at 110ºC.

3.3.2 Gases

Gases provided by BOC were N_2 and a gas mixture containing 15% (v/v) of carbon dioxide balance nitrogen. No moisture was detected in the gases.

3.3.3 Salt Solutions

Five salt solutions were used to calibrate the humidity probe. These solutions were prepared with a small quantity of water compared to the quantity of salt used in order to guarantee the saturation of the solution.

Table 1: Salt compositions and its purities (*Supplier: Fischer Scientific*)

	Magnesium Chloride	Magnesium nitrate	Sodium Chloride	Potassium Chloride	Potassium Nitrate
Chemical Formula	$MgCl_2.6H_2O$	$Mg(NO_3)_2.6H_2O$	NaCl	KCl	KNO_3
Assay	>98 %	>98%	99.5%	99% min	>99%

3.4 Reaction Conditions

Three different set of experiments were performed in this work. Preliminary experiments of five cycles were performed to optimize the experimental conditions for the kinetic study. Then, thirty cycle experiments with both Havelock and Purbeck were carried out. The first set of these experiments were done without steam and the second set of experiments were done in presence of steam. Reaction conditions for each of these set of experiments is showed in Table 2 below. Both calcination and carbonation were performed for five minutes.

Table 2: Reaction conditions and operational parameters of the experiments

	Five cycles Experiments	Thirty cycles Experiments	Thirty cycles Experiments with Steam
Data Logging (seg)	0.5	0.5	0.5
Calcination/Carbonation time (seg)	300	300	300
Carbonation Temperature (ºC)	600; 650; 700	650	650
Calcination Temperature (ºC)	900	900	900
Heating/Cooling rate (ºC/min)	120	120	120
Limestone	Havelock	Havelock/Purbeck	Havelock/Purbeck
Gas Composition	15%CO_2 (v/v), balance N_2	15%CO_2 (v/v), balance N_2	15%CO_2 (v/v), steam, balance N_2
Flowrate[1]	100; 120; 130; 140; 160; 200	140	140
Mass (mg)	2; 2.5; 3; 4; 6	3	3
Particle Size	150-355 µm;355-500 µm;500-710µm	355-500 µm	355-500 µm
Steam Concentration (%)	-	-	~1

[1] The same flowrate was used for 15%(v/v) CO_2 mixture and for the nitrogen used in the cooling part.

It is important to highlight that during the cooling down the 15%(v/v) CO_2 gas mixture was switched to nitrogen to guarantee that the carbonation reaction only started at the exact temperature. After achieving the carbonation temperature the 15%(v/v) CO_2 gas was switched on again.

3.5 Experimental Procedure

Before running an experiment, a profile is needed to be created in the TGA software *Universal Analysis 2000 (*Table 17*).* This profile will be different depending on the type of experiment required (number of cycles, temperatures, times, steam or not,...). The platinum sample pans were tared automatically below 50 ºC under the gas flow and then about 5mg of limestone were loaded and equally distributed in the pan. Calcination/Carbonation cycles started afterwards. All experiments ended with a last calcination to facilitate posterior SEM analysis. Once the experiment has finished, the sample was poured into a sample vial and stored in a desiccator, for future analysis.

For steam experiments, the bubbler was connected with the TGA. These experiments started by adjusting the external rotameters with the flow rate wanted. This adjustment was made with the needle valves of the rotameters. For the rest of the experiments, it was desired not to change the position of the valve of the 15%(v/v) CO_2 gas mixture, to avoid changes in the flow rate. After setting this up, the auto mode of the rotameters was switched on and the experiment started, although with a different method (Table 17). The bubbler had to be always filled up with water to assure a constant wet gas flow.

Reaction times, reaction temperatures and ramping rates were set according to Table 2. Time, sample mass and temperature were recorded by the integrated software. For further analysis, matlab was used.

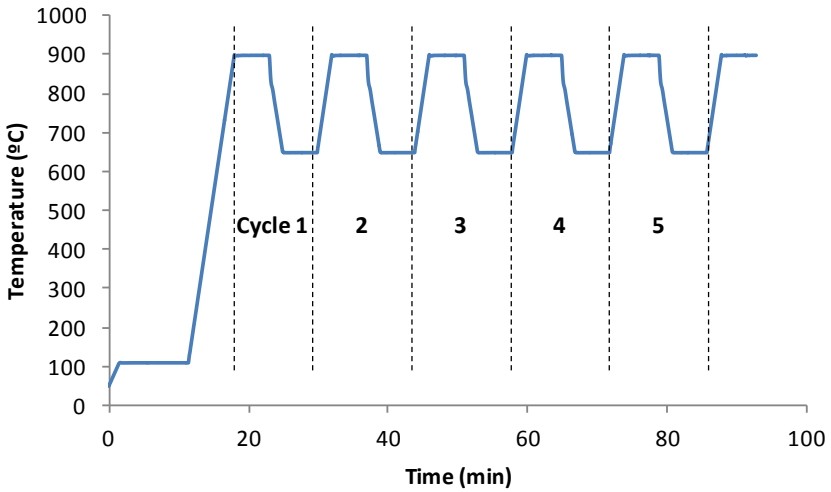

Figure 9: Temperature Program for the carbonation and calcination cycles in the TGA

3.6 Sample Analysis

After the experiments, samples were preserved with the aim of analysing them. A scanning electron microscope (SEM) was used to analyse the variation in the limestone morphology after it had been exposed to calcination/carbonation cycles. Also, a comparison between samples from experiments with and without steam was done.

3.6.1 Scanning electron microscope

The morphology of CaO samples was studied with a Hitachi TM-1000 scanning electron microscope (SEM) with a built in energy dispersive X-ray spectroscopy (EDX) analyser. This allows the calcined limestone surfaces to be high magnified. Before the observation, the samples were placed on alumina stubs and then coated with 30nm gold to avoid charging of the nonconductive CaO which could affect the results negatively. The microscope magnification was limited to 10,000 times.

4. Results and Discussion

4.1 Determination of the suitable experimental conditions for the kinetic study

Experiments were performed in order to determine the optimum conditions to study the carbonation reaction kinetics. The ideal flow rate, weight of the sample, particle size and carbonation temperature were analyzed. However, it must be pointed out that these experimental conditions are only suitable for the experimental setup used.

In order to study the kinetics of the carbonation reaction, it is essential to minimize the mass transfer resistance, which prevents an understanding of the true intrinsic reaction kinetics. High turbulence around the sample basket, lower temperatures and small amounts of sample, reduce the mass transfer resistance [57].Additionally, the experiments should be performed under isothermal conditions to avoid the influence of heat transfer in the reaction.

4.1.1 Key Concepts

Carbonation is a heterogeneous reaction between CO_2 and CaO. The reaction begins with the mass transfer of the reactant from the bulk fluid to the external surface of the limestone sorbent. Then, the reactant diffuses from the external surface into and through the pores, with the reaction taking place on the pore surfaces. At the end of the carbonation reaction, the formation of the product ($CaCO_3$) will cause an extra resistance - solid-state diffusion. Hence, the carbonation reaction has two distinct stages during the reaction. The initial and rapid stage of the reaction is chemically controlled whereas the slower regime is controlled by diffusion in the product $CaCO_3$ layer[4]. In this work, the focus is on the fast reaction phase, because extending the carbonation reaction through the slower stage causes a requirement for high residence times and large equipment in an industrial setting.

Carbonation is a first order reaction[19] and the overall rate of carbonation is described as:

$$\boldsymbol{r_{CO_2} = k_o C_b} \tag{7}$$

Where k_o is the overall rate coefficient, C_b is the CO_2 concentration in the bulk of the gas and r_{CO2} is the observed rate of reaction. This observed rate of reaction includes all the steps in the carbonation

reaction, such as diffusion and chemical reaction. Thus, the overall rate coefficient is the sum of these mechanisms resistances.

$$\frac{1}{k_o} = \frac{1}{k_g S_m} + \frac{1}{\eta k_r} \tag{8}$$

Equation 8 describes the overall rate coefficient (k_o) where k_g is the external mass transfer coefficient and k_r is the rate coefficient for the chemical reaction. Also, the specific surface area of the particle (S_m) and the effectiveness factor (η) are fundamental in the k_o calculation. These variables are described further below.

Substituting Equation (8) in Equation (7), we get the final expression for the carbonation rate of reaction:

$$r_{CO_2} = \left(\frac{1}{k_g S_m} + \frac{1}{\eta k_r}\right)^{-1} C_b = k_o C_b \tag{9}$$

There are two limiting steps that control the rate of reaction. When the mass transfer step is much more rapid than the surface reaction step ($k_g >> k_r$) the reaction is said to be “reaction controlled”. When the intrinsic reaction kinetics are fast in comparison to diffusion ($k_r >> k_g$) the reaction is controlled by the external mass transfer.[58] In addition to this, there is another resistance that can influence the velocity of the carbonation reaction, the internal mass transfer. Since the limestone is a porous solid, the concentration of CO_2 varies across its interior. For example, the concentration at the pore mouth will be higher than that inside the pore. The effectiveness factor, η, is introduced in order to account with the difference in concentration between the sorbent surface and its interior.

The importance of internal diffusion in the reaction limitations can be understood by the magnitude of the effectiveness factor. Equation 10 represents the definition of the effectiveness factor.

$$\eta = \frac{Actual\ overall\ rate\ of\ reaction}{Reaction\ rate\ when\ the\ concentration\ of\ reactants\ on\ the\ surface\ is\ the\ same\ as\ in\ the\ bulk\ gas\ phase} \tag{10}$$

The Effectiveness factor has values between 0 and 1. When the effectiveness factor approaches 1 the reaction is surface-reaction-limited. On the other hand, when $0<\eta<0.5$ it is considered that the diffusion inside the pores is the controlling mechanism.

For a first-order reaction in a spherical particle the Effectiveness Factor is given by Equation 11. In order to do this calculation, the Thiele Modulus, ϕ, has also to be determined (Equation 12). This variable is also dependent of the geometry of the sorbent.

$$\eta = \frac{1}{\phi}\left[\frac{1}{\tanh 3\phi} - \frac{1}{3\phi}\right] \tag{11}$$

$$\phi = \frac{d_p}{6}\sqrt{\frac{k_v}{D_{eff}}} \quad (12)$$

In this equation, d_p is the particle diameter, D_{eff} is the Effective Diffusivity and k_v is the first-order, intrinsic, volumetric rate constant (s^{-1}) given by the product of k_r and m_v, the mass per unit volume of the sorbent. The determination of m_v is explained thoroughly in Appendix B. The effective diffusivity (Equation 13) takes into account the mechanism for diffusion within the pores.[59] Therefore, this diffusivity has two components, the Knudsen Diffusivity and the Molecular Diffusivity, shown in Equations 14 and 15 respectively.

$$D_{eff} = \frac{\varepsilon^2}{\frac{1}{D_K}+\frac{1}{D_G}} \quad [60] \quad (13)$$

$$D_k(\mathbf{cm^2.s^{-1}}) = 9700 \times \overline{r_p}(\mathbf{cm})\sqrt{\frac{T\,(K)}{MM_{CaO}(\frac{g}{mol})}} \quad [60] \quad (14)$$

$$D_{AB}(\mathbf{cm^2.s^{-1}}) = 0.00186\frac{\left[T^3(\frac{1}{M_A}+\frac{1}{M_B})\right]^{1/2}}{P_T\sigma_{AB}^2\Omega_{AB}} \quad [61] \quad (15)$$

Some preliminary calculations were necessary to determine the porous radius value, $\overline{r_p}$, and the Molecular Diffusivity. In these Equations, the relative molar mass is expressed in (g/mol), the pore radius, $\overline{r_p}$, comes in (cm), the temperature is expressed in *kelvins* and P_t in atm. These preliminary steps can be visualized in the Appendix B.

4.1.2 Calculations

4.1.2.1 Conversion and reaction rate

The conversion was calculated for the different reaction conditions used (flow rate, sample weight, particle size and temperature of carbonation). The main aim was to determine which experimental conditions allow an improvement in carbonation conversion. The conversion can be determined using the following equation:

$$Conversion\ at\ time\ t = \frac{weight_{at\ time\ t} - weight_{at\ the\ start\ of\ carbonation}}{weight\ of\ limestone \times purity} \times \frac{MM_{CaCO_3}}{MM_{CO_2}} \quad [9] \quad (16)$$

Reaction rate is accomplished by the derivation of conversion with time (Equation 17). Calculations of both conversion and reaction rate were made using the Program Matlab.

$$Reaction\ Rate_{at\ time\ t}\left(1/s\right) = \frac{\Delta\ Conversion\ t}{\Delta\ time\ t} \quad (17)$$

4.1.2.2 Reaction rate coefficients

In order to determine the reaction rate coefficients (k_o, k_r and k_g) using the equations presented above, the concentration of CO_2 in the bulk gas stream and the concentration at the particle surface had to be determined. Although the inlet gas concentration was 15% (v/v) of CO_2 in nitrogen, losses in the TGA may cause a decrease in the CO_2 concentration inside the furnace. To solve this question a global mass balance and a CO_2 mass balance were done.

- Global mass balance:

$$\boldsymbol{F_{out} = F_{in} - R} \tag{18}$$

- CO_2 mass balance:

$$\boldsymbol{F_{CO_2,out} = F_{in} x_{CO_2,in} - R_{CO_2}} \tag{19}$$

In these equations F_{out} and F_{in} are the molar flow of the outlet and the molar flow of the inlet respectively and *R* represents the changes due to reaction. The molar fraction of CO_2 is described by x_{CO2} and its value on the inlet stream is equal to 0.15. The reacted CO_2 is obtained from the reaction rate calculated in *Matlab*.

$$\boldsymbol{Reaction\ Rate\ (s^{-1}) = r\left(\frac{mol\ CO_2}{mol\ CaO.s}\right) \times \left(\frac{gCaO}{MM\ (CaO)}\right) = r\left(\frac{mol\ CO_2}{s}\right)} \tag{20}$$

The Molar Mass of CaO is 56 g/mol. The (*gCaO*) is the mass obtained after the calcination, assuming that only calcium oxide is obtained.

At this stage it is possible to determine the quantity of CO_2 that leaves the furnace at every instant. It is noteworthy that the TGA only allows us to know the volumetric flow rate and it was necessary to obtain the molar flow rate. The density of the inlet gas stream was calculated by the Ideal Gas Law and it was assumed that the density is equal to that of nitrogen, since the gas mixture comprises 85% nitrogen.

$$\boldsymbol{\rho \approx \rho_{N_2}} \tag{21}$$

$$\boldsymbol{\rho_{N_2} = \frac{P_t \times MM_{N_2}}{R \times T}} \tag{22}$$

The total Pressure, P_t, inside the furnace was 1 atm and R= 8.314 (m^3.Pa.K^{-1}.mol^{-1}). For the temperature (expressed in *Kelvins*) it was considered an average of the temperatures reached in the furnace until the carbonation temperature was achieved (650ºC). The molar flow rate was given by:

$$\boldsymbol{F_{in} = \frac{Q_v \times \rho}{MM}} \tag{23}$$

Where, Q_v is the volumetric flow rate. The relative molar mass (MM) used was the average between the relative molar mass of CO_2 and N_2.

If the furnace was assumed to be an ideal reactor, so that the outlet concentration was equal to the concentration inside the reactor, the concentration of CO_2 in the bulk is calculated for each time t[2] by the following equation:

$$\boldsymbol{x_{out}} = \frac{\boldsymbol{F_{CO_2,out}}}{\boldsymbol{F_{out}}} \tag{24}$$

However, for the reaction rate coefficients calculation it is necessary to find an average concentration during the reaction time. This average was done between the concentration in the gas inlet (15 % v/v CO_2) and the minimum CO_2 concentration obtained in the furnace during the carbonation reaction (Equation 25).

$$\boldsymbol{x_{out,average}} = \frac{\boldsymbol{0.15 + x_{out,minimum}}}{\boldsymbol{2}} \tag{25}$$

It is now possible to determine the overall reaction rate coefficient, k_o, using Equation 7. The velocity of reaction considered was the maximum value achieved in the experiment.

$$\boldsymbol{k_o} = \frac{\boldsymbol{r_{experimental\ maximum}}}{\boldsymbol{C_b}} \tag{26}$$

The other reaction rate coefficients were also determined. The mass transfer coefficient was calculated by a correlation and all the steps taken are briefly described in Appendix B. The velocity of external mass transfer from the gas bulk to the particle surface was then determined by:

$$\boldsymbol{r_{exterior}} = \boldsymbol{k_g S_m (C_{bulk} - C_{surface})} \tag{27}$$

Where $C_{surface} \approx 0$ because when the mass transfer is the limiting step the chemical reaction occurs instantaneously at the particle surface. These calculations are only valid when the partial pressure of CO_2 is low (0.15atm), otherwise the calcination would have to be considered as well. The specific surface area, S_m is calculated considering the geometry of a CaO particle similar to a sphere.

$$\boldsymbol{S_m} = \frac{\boldsymbol{\pi \frac{d_p^2}{4}}}{\boldsymbol{m_{particle}}} \tag{28}$$

[2] To determine the concentration of CO_2 in the bulk it was first determined the CO_2 molar fraction.

To apply this equation it was necessary to determine the mass of a single particle of calcium oxide. (Appendix B)

By an iterative calculation of the effectiveness factor we can get the final value of the rate coefficient for the chemical reaction (k_r). A value between 0 and 1 is attributed to the effectiveness factor and the value of k_r is calculated by Equation 8. Then, the Thiele Modulus is calculated as well as the Effectiveness Factor by Equations 11-12. These steps are repeated several times until the iterative process is completed.

4.1.3 Analysis of the Results

4.1.3.1 Flow rate determination

Different flow rates were tested while other experimental parameters were kept constant. In these experiments 5mg of Havelock was used, with a particle size of 500-710μm. Before the tests, an experiment with an empty pan was performed in order to determine possible disturbances in the weight readings.[62] This blank test was used to correct all the following experiments.

In these set of experiments five calcination/carbonation cycles were performed. By analysing the results of conversion and reaction rate, the best flow rate to study kinetics was selected.

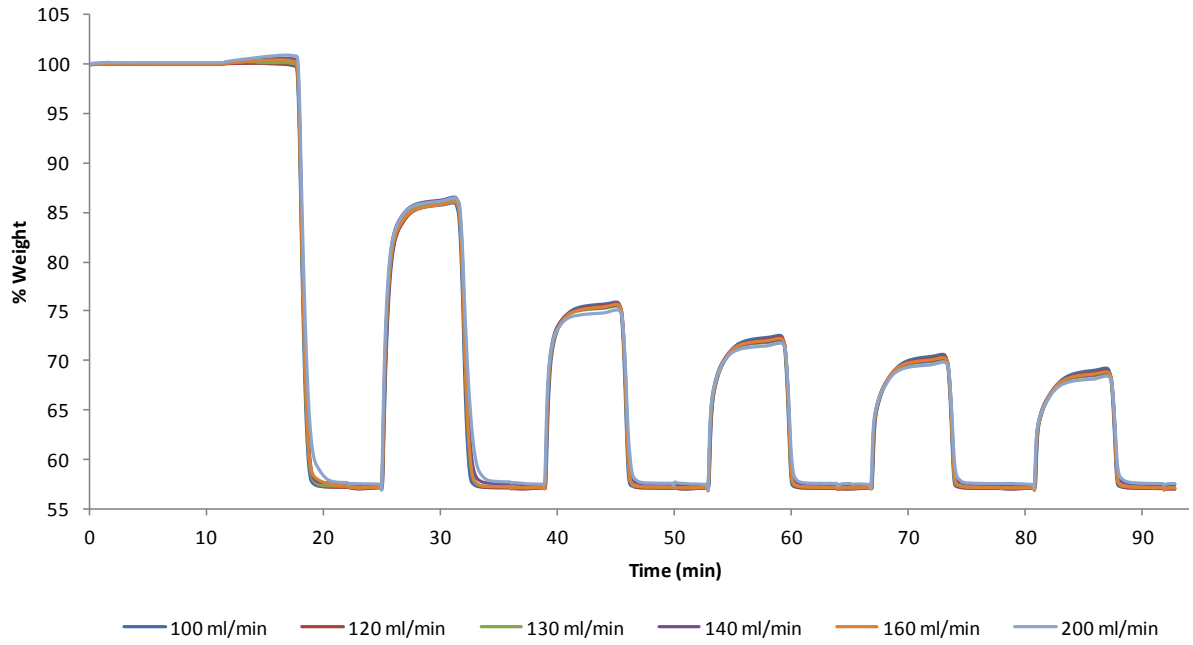

Figure 10: Graphical representation of the percentage of weight with time for different flow rates

Figure 10 shows that the reactions have the same behaviour regardless of the different flow rates. There are small differences that might cause different conversions and reaction rates. The experiment with a flow rate of 200ml/min shows a different behaviour from all others. This is caused by minor experimental errors. With this high flow rate, the platinum pan is confronted with strong vibrations. Also, the small limestone particles can leave the pan due to the high flow. Both of these factors are responsible for the difficulty in getting consistent results with this flow rate.

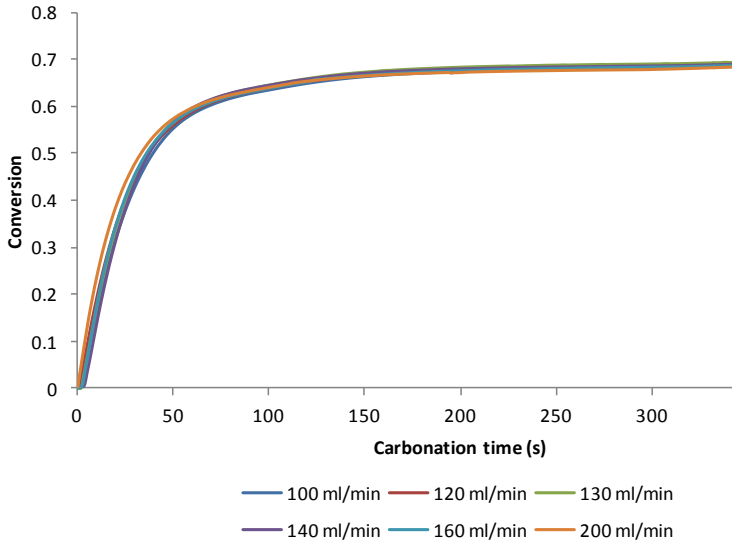

Figure 11: Carbonation conversion for the first cycle, plotted for different flow rates

The conversion results were similar for all the flow rates (Figure 11). The difference in the final conversion value was never higher than 10%. This way, it is concluded that the gas flow variation does not have influence in the conversion result.

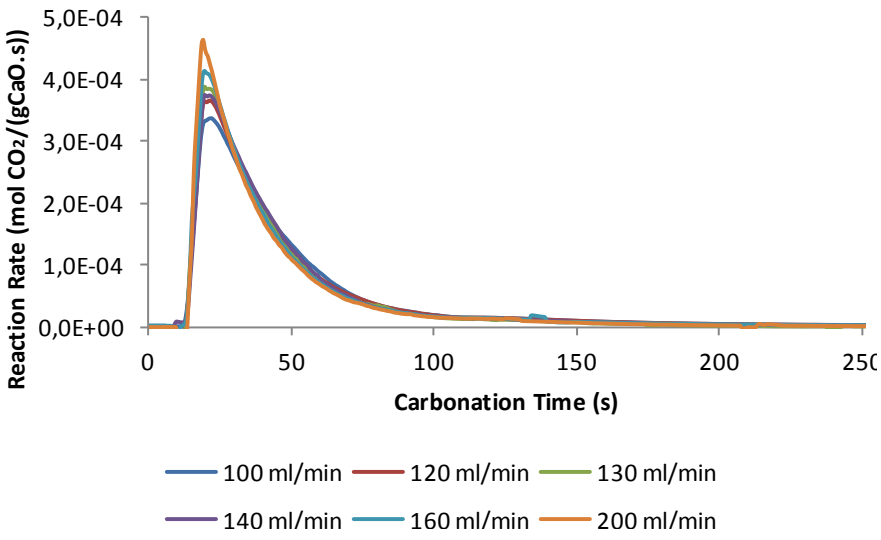

Figure 12: Reaction rate of the first carbonation reaction plotted for each flow rate tested.

As expected, higher flow rates produced higher reaction rates. Higher reaction rates mean that the overall reaction is faster (>> k_o) and this may be due to a reduction in the mass transfer resistance. High flow rates generate more mixture around the sample pan and higher concentrations of CO_2 will be found at the particle surface (Table 22-23). Figure 12 shows that in general, the rate increases with increasing flow rate, but that there is also experimental error in the results.

Table 3: Values of reaction rate coefficients and the effectiveness factor for the flow rates studied

	Fow rates (ml/min)					
	100	**120**	**130**	**140**	**160**	**200**
k_g ($m^3.gCaO^{-1}.s^{-1}$)	7.88E-04	7.98E-04	8.13E-04	**8.13E-04**	8.28E-04	8.38E-04
k_r ($m^3.gCaO^{-1}.s^{-1}$)	1.13E-03	1.35E-03	1.53E-03	**1.41E-03**	1.75E-03	2.33E-03
k_o ($m^3.gCaO^{-1}.s^{-1}$)	1.82E-04	1.96E-04	2.08E-04	**2.01E-04**	2.20E-04	2.46E-04
(k_g-k_r)	-3.45E-04	-5.49E-04	-7.21E-04	**-5.95E-04**	-9.21E-04	-1.49E-03
η	0.209	0.193	0.182	**0.189**	0.171	0.149

In order to study kinetics it is important to eliminate as far as possible or quantify if not possible, any resistance made by mass transfer. In these experiments where different flow rates are tested we expect to reduce the external mass transfer resistance and therefore, it is desired that k_g >> k_r. However, this did not happen for the flow rates tested. Nevertheless, it is observed a reduction in the external mass transfer for the higher flowrates (Table 3). Flow rates higher than 140 ml/min made the performance of the experiments more difficult due to oscillations of the sample pan. Therefore, 140 ml/min was the maximum flow that caused a small external mass resistance and a good consistency in the results simultaneously.

4.1.3.2 Determination of the Sample Mass

The same procedure as in the flow rate tests was followed to determine the quantity of limestone that reduced the mass transfer resistances. The experimental conditions were the same, but this time the flow rate was fixed, 140 ml/min.

Observing Figure 40 where % weight against time is represented it is possible to notice that the experiment with 2mg of limestone was a little different to the other experiments. This tendency has to do with the difficulty in conducting an experiment with such a small mass. To use 2 mg with this particle size (500-710μm) requires only a few particles. With a flow rate of 140 ml/min the vibration in the pan is high compared to the total mass. Therefore, even with a large number of repetitions it was very difficult to achieve good results.

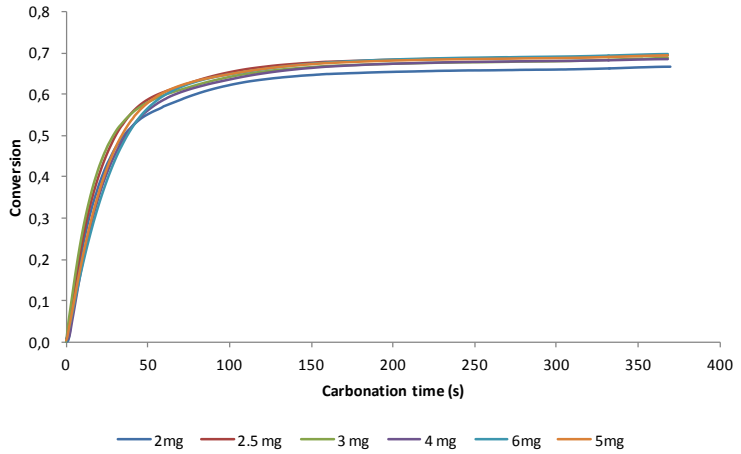

Figure 13: Conversion calculated for the first carbonation in the sample weight tests.

Although a small difference is noticeable between the result of the 2mg test and the others (Figure 13), the final conversion is similar. On the other hand, in the beginning of the experiment it is clear that some samples reacted slightly faster than the others. Visibly, the 2.5 and 3mg tests achieved the final value of conversion quicker.

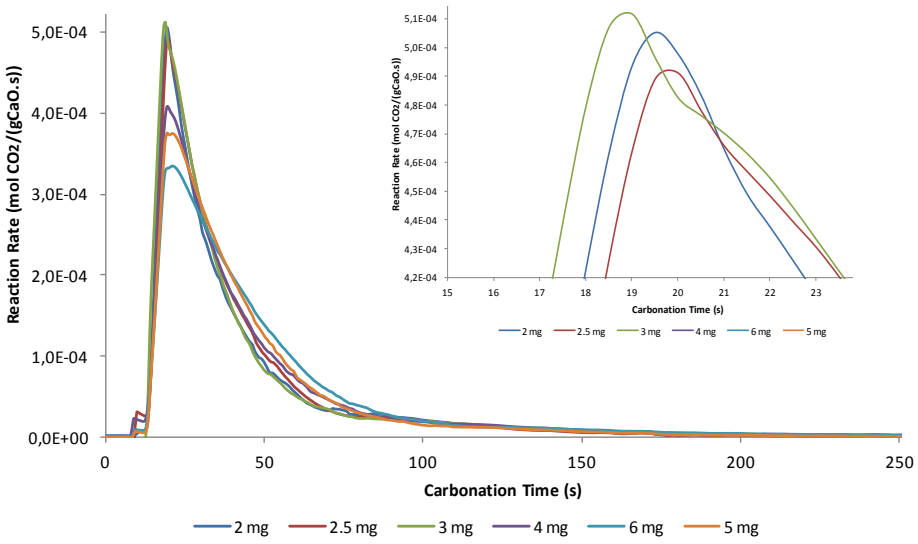

Figure 14: Reaction rate of the first carbonation reaction calculated for the sample weight experiments

Examining Figure 14, it is possible to see that experiments with higher sample mass (4mg and 6mg) show somewhat smaller values. This was expected, since higher quantity of particles in the pan can create an extra resistance for carbonation reaction. The closeness of the particles in the pan can reduce the external surface area available for the reaction. This extra resistance is called interparticle diffusion and it has to be avoided. [9] In the zoomed picture (Figure 14) we can see that the 3mg test achieved the highest reaction rate. Also, the coefficient related to the chemical reaction (k_r) presents a

higher value for this mass, as it is showed in Table 4. Moreover, the 3mg test showed to have the smallest external mass transfer and so this quantity was selected to be used in the next experiments.

Table 4: Values of reaction rate coefficients and the effectiveness factor for the sample mass tests

	Masses (mg)					
	2	2.5	3	4	5	6
k_g ($m^3.gCaO^{-1}.s^{-1}$)	7.90E-04	8.18E-04	**8.05E-04**	8.14E-04	8.13E-04	8.15E-04
k_r ($m^3.gCaO^{-1}.s^{-1}$)	2.94E-03	2.67E-03	**3.13E-03**	1.70E-03	1.41E-03	1.07E-03
k_o ($m^3.gCaO^{-1}.s^{-1}$)	2.63E-04	2.57E-04	**2.57E-04**	2.16E-04	2.01E-04	1.79E-04
(k_g-k_r)	-2.15E-03	-1.85E-03	**-2.33E-03**	-8.90E-04	-5.95E-04	-2.53E-04
η	0.134	0.140	**0.130**	0.173	0.189	0.215

4.1.3.3 Determination of the Particle Size

Different particle sizes of Havelock limestone were tested. In these experiments internal mass transfer has more importance. The diffusion resistance inside the particles is easily compared through the effectiveness factor.

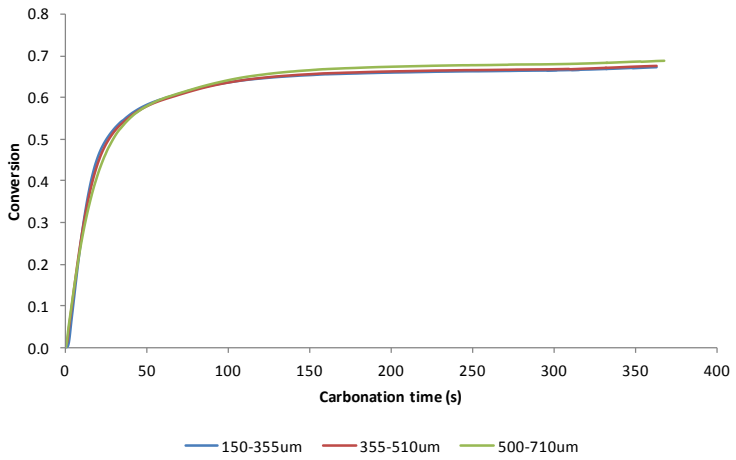

Figure 15: Conversion of the first carbonation in the particle size tests

Figure 15 represents the conversion calculated for different particle sizes. It was decided to use particles with small diameters, because in previous studies regarding the carbonation kinetics, small particles have achieved better results.[9] Concerning all particle sizes, the particles with 500-710μm of diameter achieved very marginally higher conversions in the end of reaction. However, the same particles started to react later than particles with smaller sizes. The internal diffusion of the reactant (CO_2) can be delaying the beginning of the chemical reaction.

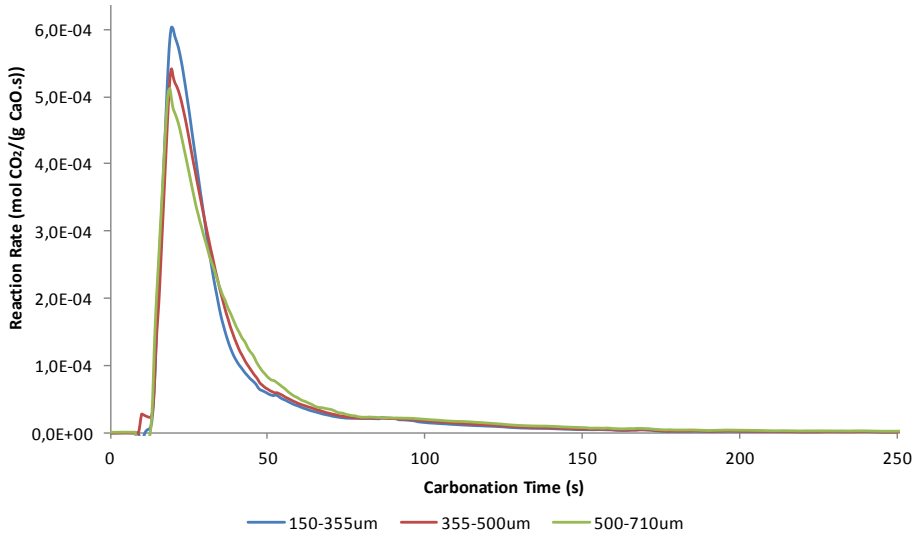

Figure 16: Reaction rate of the first carbonation reaction calculated for different particle sizes

Figure 16 shows that the smaller particle sizes accomplished slightly higher observed reaction rates. This confirms that smaller particles eliminate the internal mass transfer resistance, allowing the reaction to happen more rapidly. In order to verify this, the reaction rate coefficients were calculated and they are shown in Table 5.

Table 5: Values of reaction rate coefficients and the effectiveness factor for the particle size tests

	Particle Size (µm)		
	150-355	355-500	500-710
k_g ($m^3.gCaO^{-1}.s^{-1}$)	4.92E-03	**1.54E-03**	8.05E-04
k_r ($m^3.gCaO^{-1}.s^{-1}$)	5.57E-04	**1.24E-03**	3.13E-03
k_o ($m^3.gCaO^{-1}.s^{-1}$)	3.21E-04	**2.86E-04**	2.70E-04
(k_g-k_r)	4.36E-03	**2.95E-04**	-2.33E-03
η	0.616	**0.283**	0.130

The results obtained for k_r show clearly that given its higher external surface, particles with a higher diameter (500-710µm) will absorb more carbon dioxide. However, the particles that show a higher overall reaction rate coefficient are the particles with smaller sizes. What causes this improvement is the reduction in both external and internal diffusion resistance, as can be observed by k_g and η values. Particularly in the 150-355µm test, the effectiveness factor is much higher than the values obtained for the higher particle sizes.[62] On the other hand, particles of this size are a fine powder and they are potentially dragged out from the pan. Due to this fact, the particle size selected for the later experiments was the 355-500µm. The fact that, the largest particles (500-710µm) achieved the highest intrinsic reaction constant may indicate that the effectiveness factor calculations may be overestimating the importance of internal mass transfer.

4.1.3.4 Determination of the Carbonation Temperature

Carbonation reaction was studied at different temperatures, such as 600 ºC, 650ºC and 700ºC.

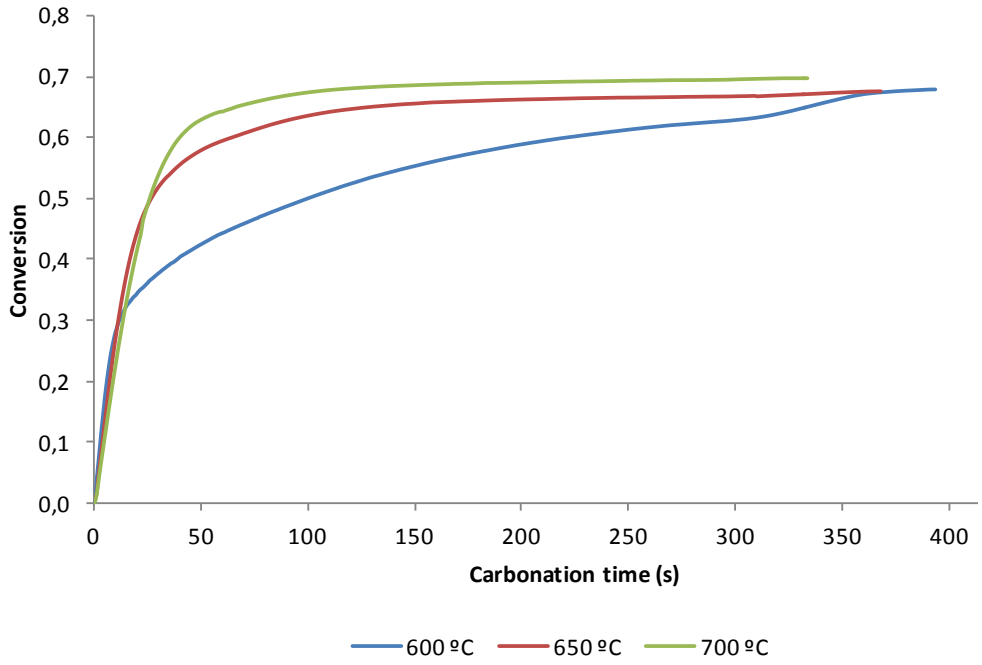

Figure 17: Conversion calculated for the first carbonation cycle in the carbonation temperature tests

Although the final conversion obtained for the first cycle is almost the same for all experiments, the trend followed by each series is very different (see also Figure 42). When carbonation is conducted at 600ºC it seems that the initial stage has a higher velocity. However, the similarity between the initial slopes of each series can be an indicative of the poor dependency of the carbonation kinetic parameter on temperature, as it was reported in the literature.[9]. It is clear that the diffusion rate is much more heavily dependent on temperature.

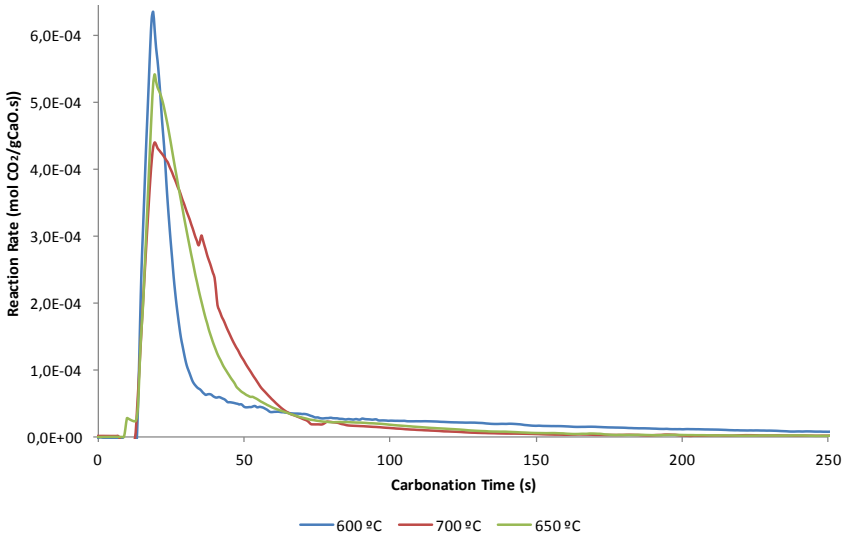

Figure 18: Reaction rates of the first carbonation calculated for experiments with different temperatures.

Figure 18 shows that the lowest temperature initially allows the system to react faster. This was expected since operating at lower temperatures reduces the equilibrium back pressure of CO_2.[58] Nevertheless, since the aim of this work was to achieve intrinsic parameters, it is important to check if this high observed velocity of reaction was due to a fast external diffusion or due to the chemical reaction.

Table 6: Values of reaction rate coefficients and the effectiveness factor for the carbonation temperature tests

	Temperature (ºC)		
	600	650	700
k_g ($m^3.gCaO^{-1}.s^{-1}$)	1.45E-03	**1.70E-03**	1.54E-03
k_r ($m^3.gCaO^{-1}.s^{-1}$)	1.95E-03	**1.24E-03**	7.51E-04
k_o ($m^3.gCaO^{-1}.s^{-1}$)	3.40E-04	**2.86E-04**	2.30E-04
(k_g-k_r)	-5.01E-04	**4.57E-04**	7.87E-04
η	0.228	**0.284**	0.355

When looking at the values of k_r, k_o and k_g of the experiments performed at 600ºC (Table 6) it becomes visible that the high value obtained for k_o is mainly due to the chemical reaction coefficient (high value of k_r). However, when looking at the difference between k_g and k_r, the temperatures of 650ºC and 700ºC appear as the best temperatures to obtain intrinsic parameters. Between these two temperatures it was decided to use 650ºC because it is reported to be the best temperature to use in a future scale-up of the technology.[63] Also, this temperature makes possible to compare our results with results from the literature.

4.2 Thirty cycle experiments with Havelock and Purbeck limestones

Experiments without steam were performed to determine the reactivity of both Havelock and Purbeck, under the reaction conditions shown in Table 2. Thirty calcination/carbonation cycles were performed, because the literature indicates that this allows a reasonable approximation to the conversion after many cycles to be made. [63]Manovic and Antony [32] reported that the sorbent most likely would not survive more cycles due to sulphation or attrition losses present in a large-scale system of CaO-looping. Also, the performance of more cycles would require a long time and fewer experiments would be realized. The reactivity study was made by calculating the conversion, reaction rates and carrying capacities of both limestones. A modelling process was done in order to see if the experimental data fitted well the Grasa equation [13] and also to determine the residual activity.

4.2.1 Conversion and Reaction rate

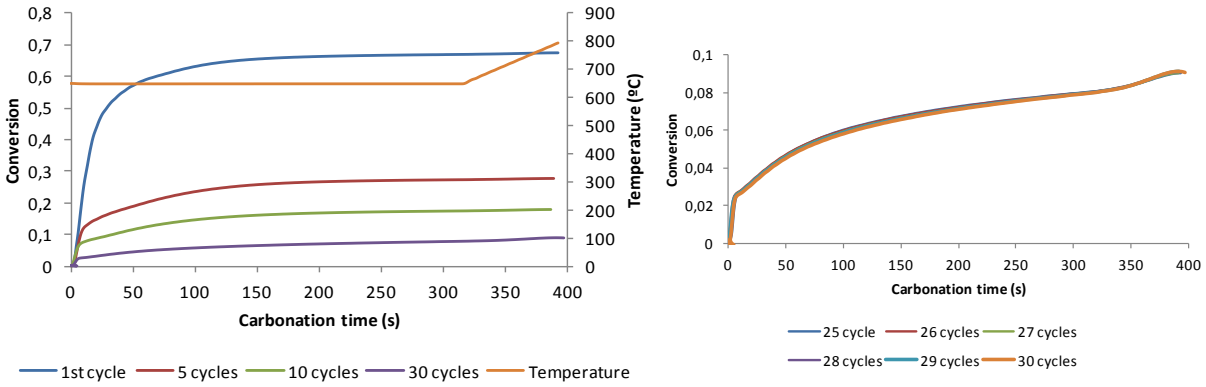

Figure 19: Conversion of Havelock in the thirty cycle experiments

The conversion of Havelock limestone was determined for different cycle numbers (Figure 19). Features of the carbonation reaction are present in every cycle (initial fast reaction period followed by a sudden change to a slower stage). As it was expected, conversion decreases with the number of calcination/carbonation cycles, what means that the sorbent loses CO_2 capture capacity.

In the end of the first carbonation, Havelock limestone accomplished ~67% conversion. After 5 cycles this value decreased almost 58% to a value of 28% of conversion. The decrease continued and in the end of the 30th cycle the carbonation conversion was only 9.1%. An important fact is that the conversion obtained in the last 5 cycles was the same (see Figure 19). Therefore, the reactivity seems to have already reached a decay asymptote by cycle 30. In fact, Grasa and Abanades [13] reported that after many hundreds of cycles a residual conversion of about 7-8% is achieved.

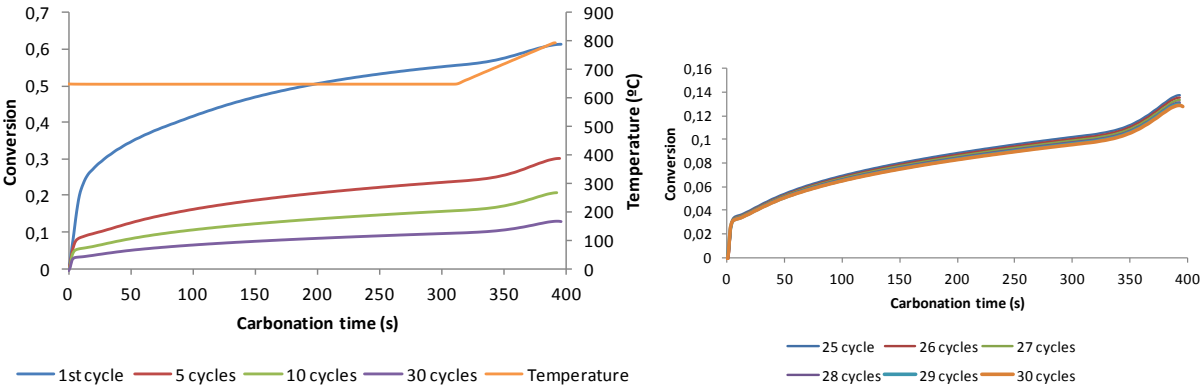

Figure 20: Conversion of Purbeck in a thirty cycle experiments

The same thirty cycle experiments were performed with Purbeck limestone. In the end of the first cycle, the carbonation conversion was about 61%. However, in the end of the 5th cycle the value achieved was 30%, marginally higher than the carbonation conversion of Havelock. Also, in the end of the thirty cycles, the carbonation conversion was around 13%, higher than that achieved by Havelock. These different levels of conversion between limestones are caused by existing differences in texture and morphology.[25]

Once again, the conversion result was the same for the last five cycles, suggesting that Purbeck limestone has a higher residual conversion than Havelock. A greater residual conversion after a large number of cycles allows the limestone to capture more CO_2, and it will also reduce sorbent purge rates in a real system[64]. However, in Figure 20 and also in Figures 43 and 44, where the thirty cycle experiments of each limestone are shown, it is possible to see that the format of cycles is different. It looks as if the Purbeck limestone starts off with a lower initial rate, but ends up with a higher one. The following carrying capacity analysis allows this to be checked.

Reaction rates for both limestones were also calculated in order to verify which one converted faster, keeping in mind the importance of a fast reaction in a industrial unit.

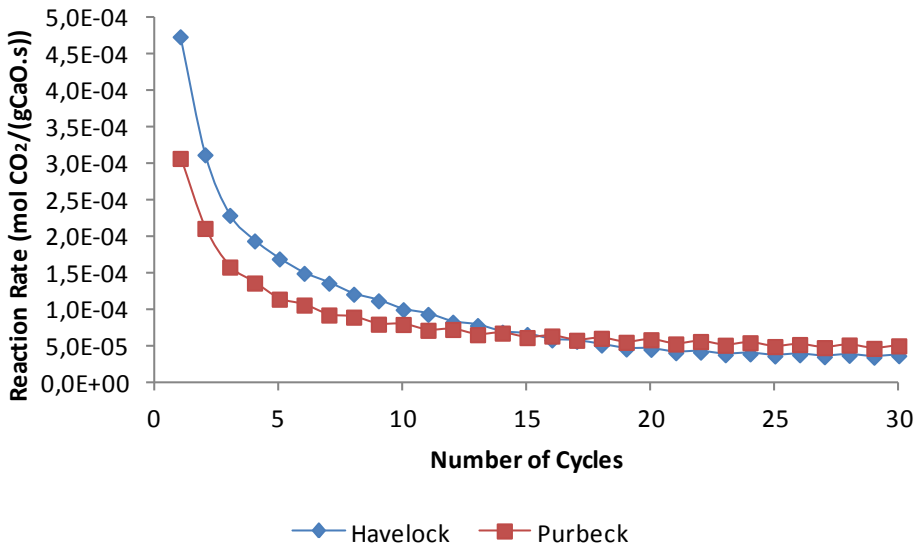

Figure 21: Maximum reaction rate obtained in the thirty cycle experiments for Havelock and Purbeck limestones

The first thing to be noticed in Figure 21 is that the reaction rate decay is very similar to that obtained in the carrying capacity (Figure 23). Initially, higher velocities of reaction were obtained by Havelock, but around the 15th cycle Purbeck limestone started to exhibit faster rates.

The maximum reaction rate of the first carbonation for Havelock was about 0.0266 s^{-1} and 0.017 s^{-1} for Purbeck limestone. These values were substantially higher than those reported by previous works. For example, Sun et al.[64]obtained a maximum reaction rate of 0.0048 s^{-1} in the first carbonation for a commercial limestone. This indicates the importance of minimising mass transfer resistances. Also, Donat [9] reported a value of 0.004 s^{-1} for Purbeck limestone, but this value was obtained in a fluidized bed reactor.

In order to understand why Purbeck limestone achieved a higher rate of reaction in the last cycles, a more detailed comparison between limestones is shown in Figure 22.

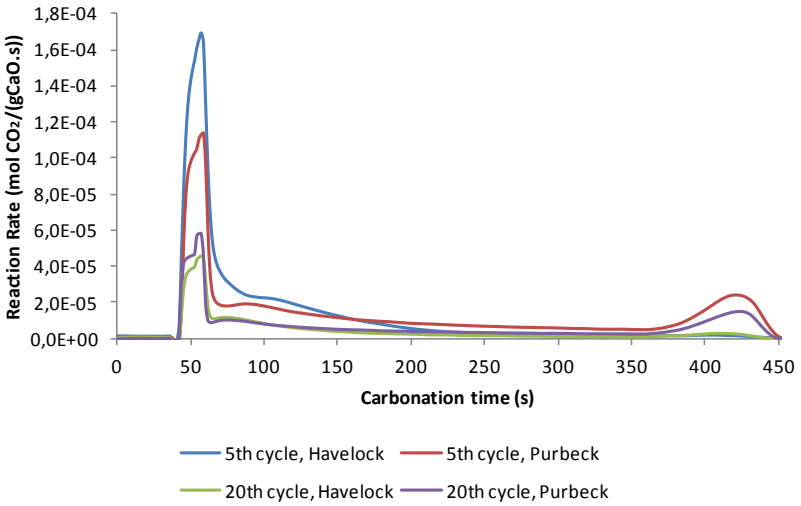

Figure 22: Variation of reaction rate with time (cycles 5 and 20), for Purbeck and Havelock

Figure 22 shows that after about 75 seconds the fast reaction stage was completed for both limestones. After this, the calcium oxide continues to react but more slowly because the reaction is constrained by diffusion resistances (see chapter 2.2.4). In the end of the carbonation reaction, the reaction was again accelerated during the diffusion controlled stage. This happened when temperature started to increase for the subsequent calcination step. This is mainly obvious for Purbeck as can be seen in Figure 22. The quantity of different elements in Purbeck's composition (higher than Havelock), may explain why this unusual effect is more pronounced. The different compounds (Table 16) may cause a inner morphological defect in the limestone that may enhance transport processes.[9] This effect along with the high velocities achieved by Purbeck in the last cycles demonstrate that this limestone has a more important diffusion controlled regime.[21]

4.2.2 Carrying Capacity

The carrying capacity of each limestone was calculated in order to determine which sorbent can absorb a higher quantity of CO_2.

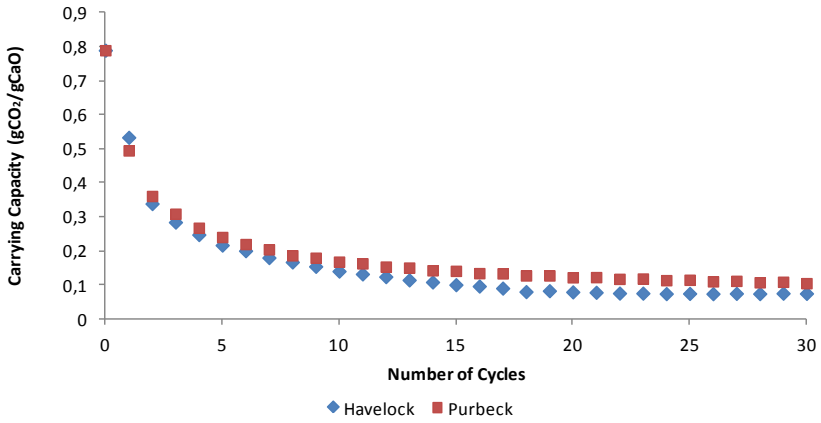

Figure 23: Carrying capacity of Havelock and Purbeck through thirty carbonation/calcination cycles

Figure 23 shows the decay of Havelock and Purbeck limestones' carrying capacities through thirty cycles. It can be seen that performance of both limestones is very similar. The observed fall in carrying capacity is due to pore blockage and due to the sintering process which are responsible for causing porosity reduction and loss of surface area (sees Chapter 2.2.5.5). Actually, Fennell et al.[23] found proportionality between the carrying capacity and the voidage inside pores narrower than ~150nm in the calcined limestone before carbonation began.

The limestones' uptake capacity decays severely in the first ten cycles and then it starts to have a slower decay rate. Around cycle 20, the carrying capacity of Havelock seems to stabilize around 0.075gCO_2/gCaO (corresponding to 9.5% of conversion). This value is very similar to the value reported by Grasa et al.[9, 13] in a multi-cycle experiment. These authors reported that when increasing the number of cycles the carrying capacity of limestones tend to stabilize around a residual conversion of 0.075-0.08. To ensure that the residual conversion was achieved in these experiments, tests with a more extensive number of cycles would have to be performed. These results agree with analysis of the conversion results, where a residual conversion also seems to have been achieved.

In the case of Purbeck limestone, although it has a smaller value for the carrying capacity in the first cycle, from the 2nd cycle, results exceeded those obtained by Havelock. Overall, Purbeck could absorb higher quantities of carbon dioxide. However, excluding the diffusion controlled stage from carrying capacity will allow a better comparison between the two limestones. An extension of the carbonation reaction through the slow diffusion controlled stage will lead to an only little enhancement of CO_2 absorption, considering the extra time it would take and the size required for reactors. So, only the fast carbonation stage is of interest for large-scale industrial application. In order to calculate carrying capacity excluding the diffusion stage it was necessary to define a transition point from the fast to the slow reaction stage. Since no definition was found in the literature, the transition point was defined as the conversion for which the reaction rate becomes less than 20% of the maximum reaction rate. [9]

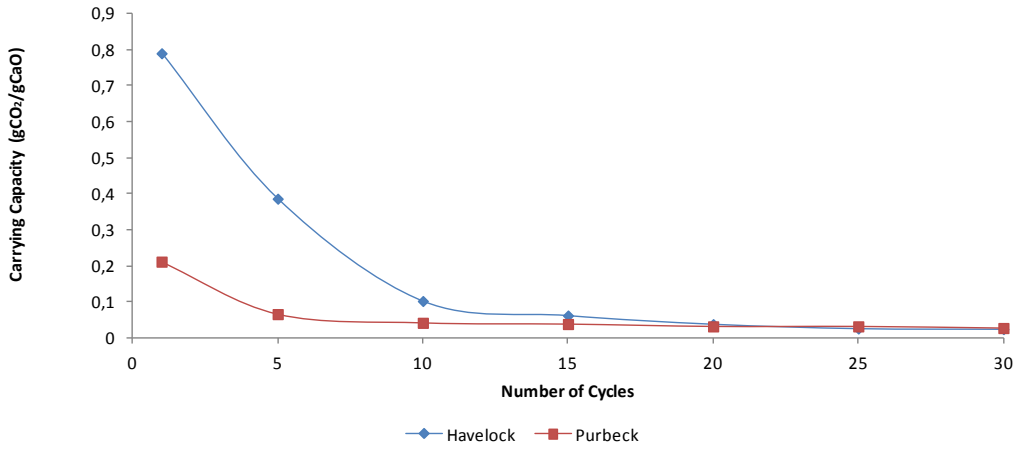

Figure 24: Carrying capacity of Havelock and Purbeck through thirty cycles for the fast carbonation stage only

The results in Figure 24 are substantially different from those shown previously. Purbeck in particular has reduced greatly its carrying capacity. It is possible to conclude that when only the fast carbonation stage is considered, Havelock limestone achieves better results until around the 20th cycle. In the last cycles, Purbeck limestone achieved similar results to Havelock. This is because in the last cycles the diffusion controlled regime gains importance in the carbonation reaction.

4.2.3 Grasa Equation

In order to perform a better study of the reactivity decay of limestones, the carrying capacity results were modelled using Grasa Equation. This equation was proposed by Grasa and Abanades[13] in order to try to understand the decay in conversion of limestones through carbonation and calcination cycles. Based on multi-cycle experiments up to 500 cycles, they proposed the following equation:

$$X_N = \frac{1}{\frac{1}{1-X_r}+kN} + X_r \quad (29)$$

Where X_N is the carrying capacity, k is the deactivation constant and X_r is the residual carrying capacity. The deactivation constant, k, increases with more severe calcinations conditions (i.e, longer times, higher temperatures...). The value of residual carrying capacity, X_r, is used as an indicator for the quality and sustainability of a sorbent to capture CO_2. Grasa and Abanades [13] found a couple of values for the constants (k=0.52; X_r=0.075) that seem to be valid for a wide range of sorbents and conditions.

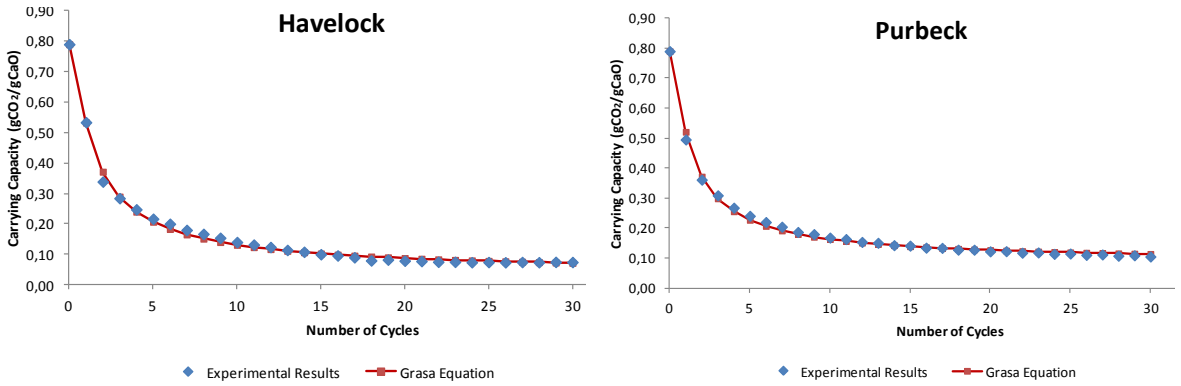

Figure 25: Comparison between experimental results and the Grasa Equation when applied for both Havelock and Purbeck.

Figure 25 shows that Grasa equation fits very well to our experimental results. The Grasa equation was calculated by Equation 29 and the fitting parameters X_r and k were determined using a least-square fitting. The coefficients used in the Grasa equation are shown in Table 7.

Table 7: Grasa equation coefficients obtained for Havelock and Purbeck

	Havelock	Purbeck
X_r	0.040	0.087
k	0.99	1.21

When Grasa Equation is applied to the experimental results it gives an idea how limestone would behave if the experiment continued through more cycles. Analysing the values obtained for Xr, Purbeck limestone had a higher value for the residual carrying capacity. This was expected since that in the end of the 30 cycles this limestone showed a higher capacity of CO_2 absorption. Nevertheless, the difference obtained in the end of the 30th cycle for carrying capacities was enhanced given that Purbeck limestone obtained a residual carrying capacity more than twice the value obtained by Havelock. This difference can be important when selecting a limestone to apply this process in a real industrial unit. The precision of these results would have been better if more cycles were performed. The values of the Grasa coefficients are similar to the values obtained by Grasa and Abanades[13] in tests with several limestones.

4.3 Effect of Steam in CaO-sorbents performance

In this Chapter, experiments of thirty calcination/carbonation cycles were performed with natural limestones (Havelock and Purbeck) under post-combustion capture conditions (carbonation temperature: 650ºC; calcination: 900ºC), but in the presence of steam in the gas composition. The

main purpose was to study how steam affects the CaO-sorbents performance, since steam is an important component of any flue gas. Previous works have started to study the carbonation performance under a wet flue gas, accomplishing good results. Moreover, these reaction conditions were already tested in a pilot-plant for calcium looping processes in Stuttgart. [4, 65]In this pilot-plat the CO_2 capture efficiency was significantly improved (from 80% to 95% at 600ºC) when compared to reactions performed with a dry gas.

In the present work, the experiments were performed using 1.5% steam in the reaction gas. Other concentrations could not be tested, however this is not a critical aspect since it was reported by Donat et al [4] an existence of an asymptotic reactivity at around 1% steam. This means that concentrations of steam higher than 1% do not bring any substantial improvement. Similar asymptotes were observed for Havelock, Cadomin and Purbeck. [4]

As it was referred in Chapter 3, a different experimental set-up had to be deployed in order to introduce steam. The system was commissioned, but the time necessary to change gases (between 15%(v/v) CO_2 and nitrogen) was longer than for experiments without steam. This caused a slightly decay in the weight during calcination (see Figures 46-47). Nevertheless, this has not influenced the results and subsequent calculations, so it was neglected. However, in the future, the rotameters should be installed in a different way to allow a faster change between gases. Two different limestones were tested, because the effect of steam may be different due to the different compositions of the limestones.

4.3.1 Determination of Steam Concentration

Partial pressure of water vapour was determined by Antoine Equation (Equation 30). In order to use this equation, the temperature of water inside the bubbler had to be known and it was measured by a K thermocouple in the bubbler. The gas passed through the bubbler and it was assumed that it was saturated with water vapor when leaving this equipment.

$$\boldsymbol{log_{10}P\ (mmHg) = A - \frac{B}{C+T(^{o}C)}} \quad (30)$$

Table 8: Antoine equation parameters for water[66]

A	B	C	T_{min} (ºC)	$T_{máx}$ (ºC)
8.07131	1730.63	233.426	1	100
8.14019	1810.94	244.485	99	374

With the mean value of relative humidity measured in the TGA effluent and with the vapor pressure obtained with Antoine Equation, the partial pressure of water was determined by Equation 31. The furnace was assumed to behave like an ideal reactor and therefore the concentration at the outlet is equal to the concentration inside the furnace.

$$\%\boldsymbol{RH} = \frac{\boldsymbol{partial\ pressure}}{\boldsymbol{p_v(T_{bubbler})}} \times \mathbf{100} \Leftrightarrow \ \boldsymbol{partial\ pressure} = \frac{\%\boldsymbol{RH} \times \boldsymbol{p_v(T_{bubbler})}}{\mathbf{100}} \quad (31)$$

In Equation 31, %RH is the relative humidity in the TGA outlet and p_v is the vapor pressure at the bubbler temperature.

4.3.2 Conversion

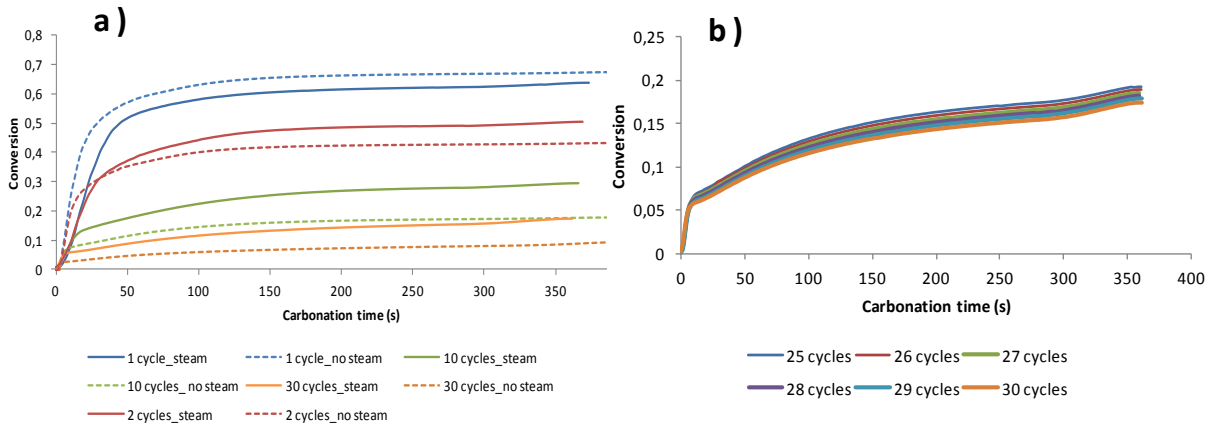

Figure 26: a) Conversion of Havelock in the thirty cycle experiments performed with and without steam; b) Conversion of the last 5 cycles in experiments performed with steam

The conversion obtained in the experiments with steam was calculated for both Havelock and Purbeck limestones. With the experimental set-up used, it was possible to achieve ~1.5% steam in the reacting gas (Appendix B). Experiments performed with steam achieved higher carbonation conversions, except in the first cycle (Table 30), where ~63.7% conversion was obtained. After this cycle, the enhancement by steam was noticeable and 37% conversion was accomplished in the 5th cycle (around a 34% increase) and in the 10th cycle the conversion was 29%.

Also in Figure 26, it is observed a significant improvement related to the residual conversion. While in experiments performed without steam an invariant (residual) conversion was obtained during the thirty reaction cycles, in the presence of steam the residual conversion was not achieved. Therefore, a higher conversion was kept by the sorbent during more carbonation reactions. In the 30th cycle, the conversion was 17%, almost twice the value obtained in the experiments without steam.

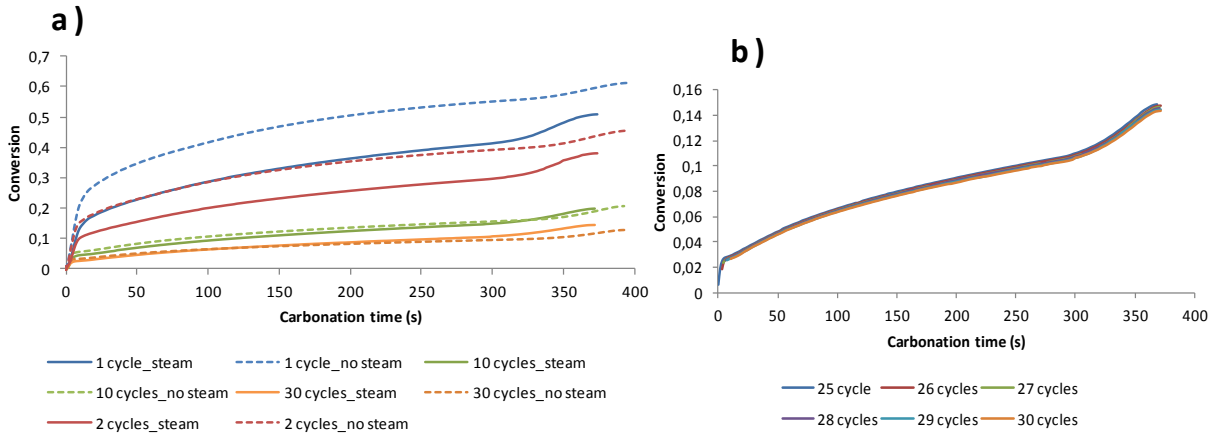

Figure 27: a) Conversion of Purbeck in the thirty cycle experiments performed with and without steam; b) Conversion for the last 5 cycles in experiments performed with steam.

Purbeck limestone exhibited very different behaviour. The value for the first carbonation was around ~50.9%, much lower than the value obtained without steam. It can be seen in Figure 27 and also in Table 31 that the results obtained with steam were gradually improving and slightly higher values were obtained from the 14th cycle. In the 30th cycle a value of 14.4% of conversion was achieved, higher than the correspondent conversion in the no steam experiments. This gradual enhancement was also observed for Havelock (see Table 30). Considering this, the idea that steam may improve the conversion by enhancing the diffusion controlled regime arises, since this regime becomes more relevant with increasing number of reaction cycles. Also, since the diffusion controlled stage of Purbeck was already higher it may be the reason for a lower improvement in the presence of steam.

Overall, the presence of steam seems to result in an increased CaO conversion over cycles, as reported by previous researchers, e.g. Symonds et al.[53]. Why this improvement did not happen for the first cycle it is not so clear, but it may be due to the fact that steam also increases the rate of sintering when present during the calcination reaction, even at low concentrations [9, 53, 67]. Sintering leads to larger pores limiting the particle surface sites available for carbonation. However, these larger pores also appear to be more stable in the next cycles [9, 53], because they are less susceptible to pore blockage.

Considering all experiments done, the highest conversions were obtained for Havelock limestone when steam was present in the reacting gas composition.

4.3.3 Maximum Reaction Rate

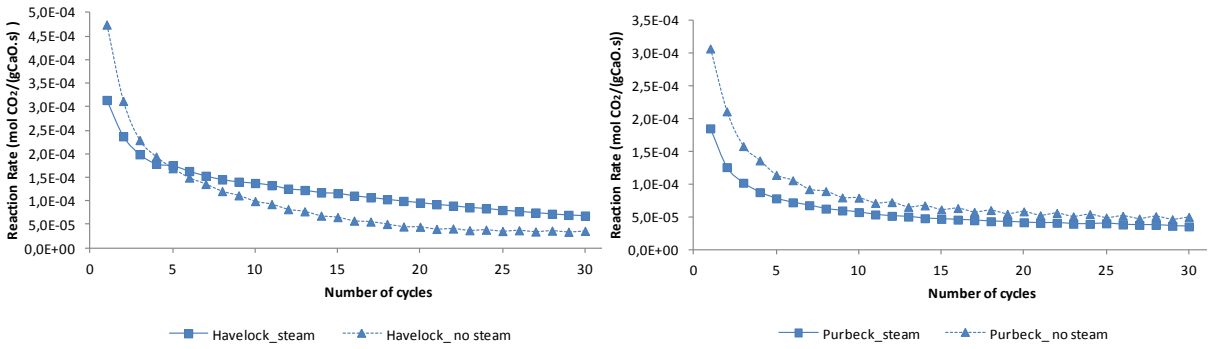

Figure 28: Maximum reaction rates of Purbeck and Havelock in experiments with 1.5 % of steam and in experiments without steam

In the steam experiments a reaction rate of 0.0176s^{-1} was achieved in the first carbonation of Havelock, which is smaller than the rate achieved without steam. However, around the 5th cycle this tendency changed and a higher value was achieved, 0.013 s^{-1} (Figure 28). In the next cycles, experiments with steam achieved always better results, because the decay with cycles was slower. Once again, in Purbeck limestone the enhancement with steam was not so pronounced. The reaction rate after the first carbonation has a value of 0.0104s^{-1}, which is smaller than the value achieved for the no steam experiments as can be seen in Figure 28. Experiments with no steam achieved higher reaction rates, but the values obtained for the two sets of experiments were similar in the last cycles. This also happened in the conversion results.

In previous works, such as in Donat [9], an enhancement of the fast reaction stage was noticed due to the presence of steam. Looking at Figure 49 it is possible to see that the fast carbonation stage was slightly prolonged. In Havelock, the fast stage was prolonged for 95seconds, while in the no steam experiments it only lasted 75seconds. This will cause an improvement in sorbent carrying capacity.

Overall, the experiments performed with steam and Havelock achieved the highest carbonation reaction rates.

4.3.4 Carrying Capacity

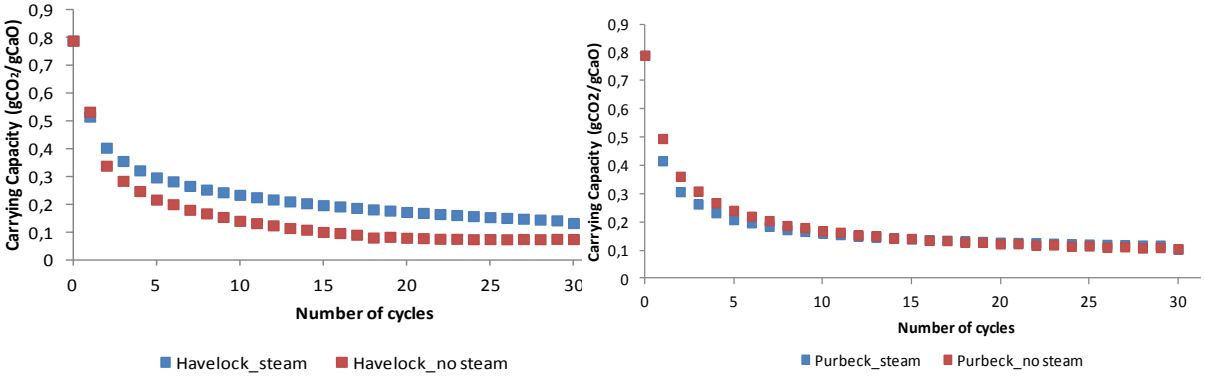

Figure 29: Carrying Capacity of Havelock and Purbeck in the thirty cycle experiments performed with and without steam

It is possible to notice in Figure 29 that Havelock achieved higher carrying capacities in the experiments performed with steam. As well as it was observed in the conversion results, it looks as if the decay asymptote was not yet achieved. However, more cycles would have to be done to confirm this statement. The carrying capacity after the 30th cycle was 0.13gCO_2/gCaO, a substantially higher value than that reported for experiments without steam. At the end, the quantity of CO_2 absorbed during the thirty cycles increased almost 49% when steam was present in experiments performed with Havelock.

In the case of Purbeck, the residual carrying capacity was achieved as in the experiments without steam, and the value obtained was the same for both experiments. Once again, it was confirmed that because the well developed diffusion controlled stage of Purbeck, the steam did not generate a significant improvement.

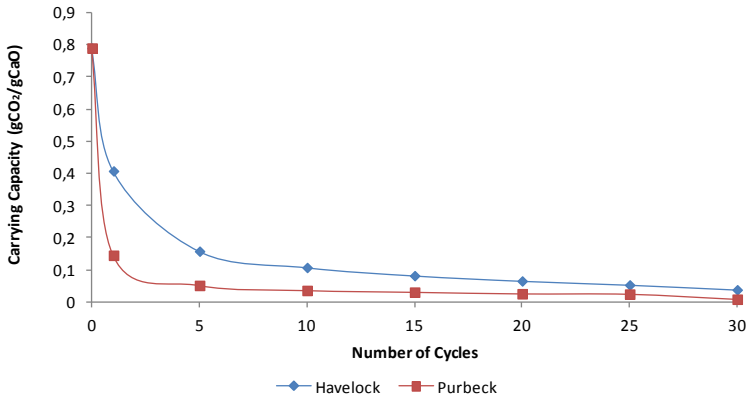

Figure 30: Carrying capacity of the fast reaction stage of Havelock and Purbeck in experiments performed with 1.5% steam

In the presence of steam, the fast carbonation stage was enhanced for Havelock (Figure 30). This shows that steam can also improve the carbonation fast reaction stage, although this was not noticeable for Purbeck limestone. More experiments have to be done using other types of limestone to verify the steam influence in this stage of reaction.

Summarizing, it can be said that steam enhances the diffusion controlled stage. Moreover, Donat [9] reported that the enhancement observed in the fast reaction stage was due to a reduction in the CO_2 diffusion resistance caused by steam. Manovic and Anthony [45]have reported as well an acceleration of the solid-state diffusion mechanism when steam was present during carbonation.

4.3.5 Grasa Equation

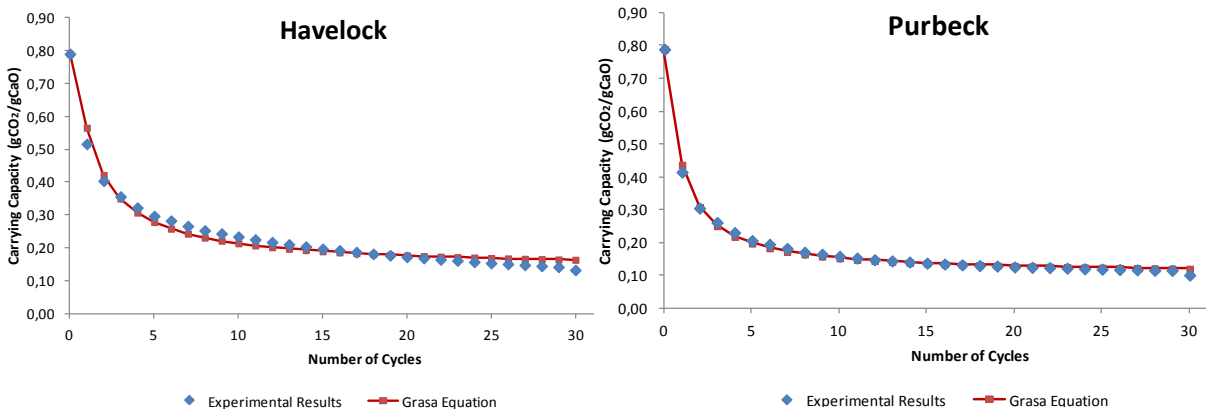

Figure 31: Comparison between experimental results and the Grasa Equation when applied for experiments performed with 1.5%steam in the gas composition

Figure 31 shows the fitting of Grasa Equation to the carrying capacity achieved for experiments carried out in presence of ~1.5% of steam. Grasa Equation fitted well to the experimental results, although with an adjustment not as good as in the experiments without steam. Particularly for Havelock, the Grasa Equation did not describe so well the limestone decay and because of this, the X_r value seems to be overestimated. A greater residual carrying capacity, X_r, was obtained compared to no steam experiments, as it was expected since the carrying capacity was always higher in the steam experiments. In contrast, Purbeck limestone had a better fitting exercise and therefore the Grasa coefficients achieved may be more reliable indicators of the final sorbent performance. Nevertheless, maybe Grasa Equation has to be changed in order to take into account the steam effects. Grasa coefficients are shown in Table 11 and the results are very similar to those obtained by Donat [9]. Those experiments were performed in a fluidized bed reactor and a residual carrying capacity of 11.5% was obtained for experiments with 1% steam and 13.5% was obtained for 6%steam.

Table 9: Grasa equation coefficients obtained for Havelock and Purbeck in the experiments performed with 1.5% steam

	Havelock	Purbeck
Xr	0.136	0.105
k	1.17	1.88

4.4 Scanning electron microscopy (SEM)

The main aim of this chapter was to clarify if the presence of steam in the reacting gas mixture affects the particles' morphology and therefore to explain the higher conversions and reaction rates obtained in the experiments performed with steam. Samples of Havelock limestone were observed in the scanning electron microscope after cycled five and thirty times in the TGA. All particles were observed in the calcine form (CaO).

The surface morphology of a limestone changes greatly over the course of reaction.[68] Because of this, a mechanism for pore evolution during the calcination/carbonation cycles was proposed by Sun et al.[68] in investigations using SEM analysis and mercury intrusion. This comprised an initial assumption that a calcined particle contains three different types of pores, type 1, type 2a and type 2b. Type 1 pores have diameters around 100nm, Type 2a pores are larger pores closer to the particle surface and Type 2b are larger pores in particle core, not available for the fast carbonation stage. Almost all surface area is provided by Type 1 pores and these pores also determine the apparent carbonation rates. Wu et al. [36]also reported that after the first calcination the limestones are an extremely porous solid with pores of about 2-3µm at the particle surface. Below, images of particles cycled under an atmosphere with and without steam are shown in order to allow a comparison.

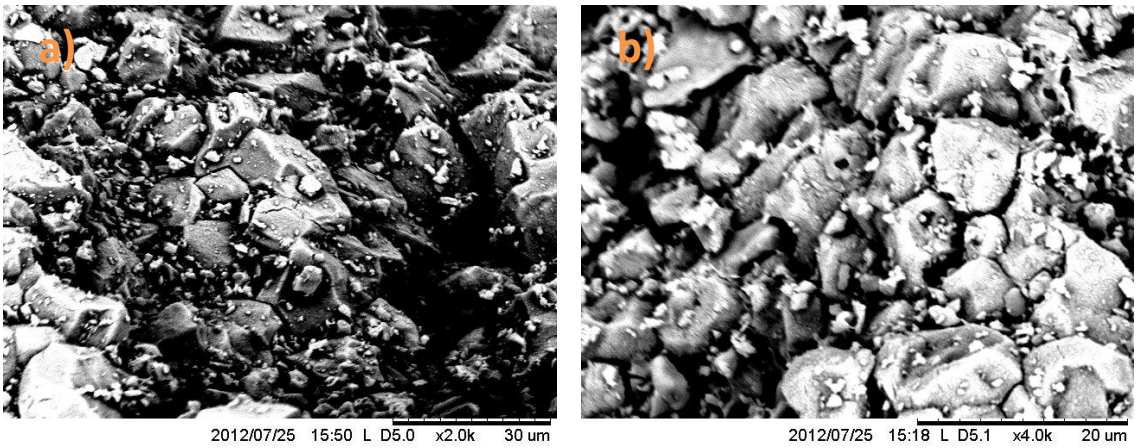

Figure 32: SEM images of Havelock particles after five calcination/carbonation cycles. (a) Particle cycled with no steam; b) Particle cycled in presence of steam)

Figure 32 shows limestone particles after five calcination/carbonation cycles in experiments performed with and without steam. In both images it is possible to see smooth areas caused by sintering. In Figure 32a) the particle shows some porosity and cracks to the particle interior can also be seen. In Figure 32b), despite the smooth areas the surface seems to be rougher and it appears to have smaller pores. This can be more clearly seen in Figure 33 where a picture of the same particle is shown with a greater magnification (1000x). In this Figure, the rough surface of the particle can be noticed, proving that the particle still has a complex porosity even after cycled five times. This way, the particle has a higher superficial area and therefore higher carbonation conversions are obtained.

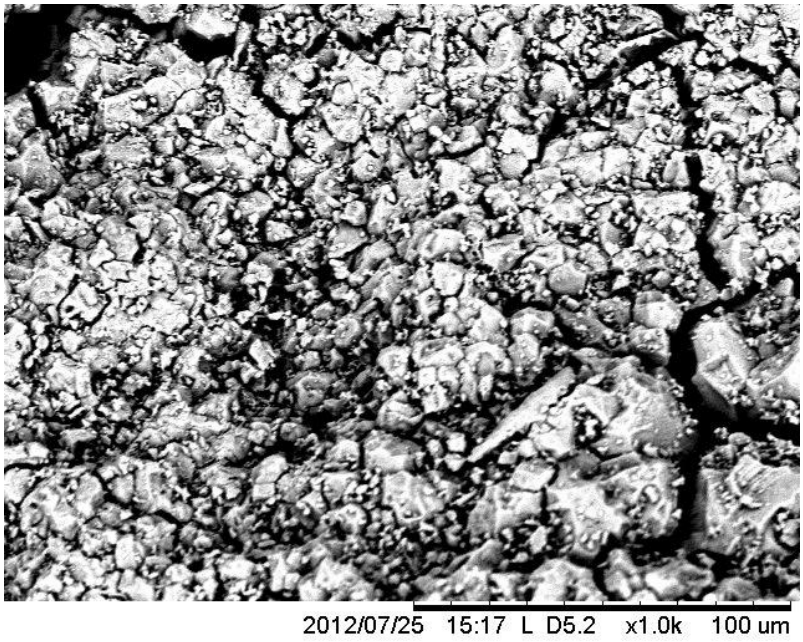

Figure 33: Particle cycled five times under an atmosphere with steam (same particle as in Figure 32b)

Although particles were cycled under a different gas composition, sintering processes occurred in both particles. Sintering is responsible of causing the coalescence of small grains and pores in the particle and therefore larger pores are obtained.

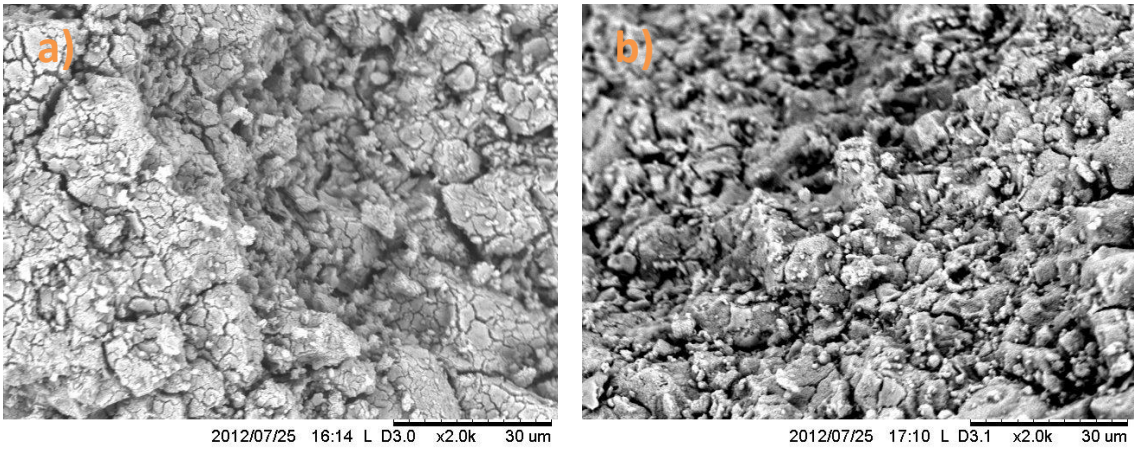

Figure 34: SEM images of Havelock particles after thirty calcination/carbonation cycles with a magnification of 2000x. (a) Particle cycled with no steam; b) Particle cycled in presence of steam)

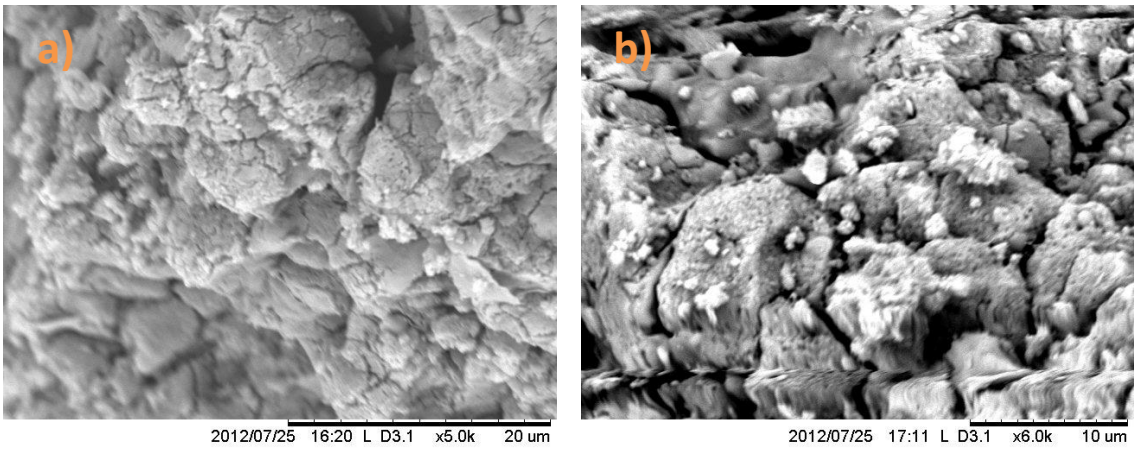

Figure 35: SEM images of Havelock particles after thirty calcination/carbonation cycles with a magnification of 5000x. (a) Particle cycled with no steam; b) Particle cycled in presence of steam)

Figure 34 and Figure 35 show particles after thirty calcination/carbonation cycles with and without steam present. Sintering processes are more pronounced after thirty cycles than after the 5th cycle. Particles cycled without steam have a smoother surface than particles cycled with steam, indicating that these particles suffered a more intense sintering process. Particles cycled with steam seemed to have retained higher porosity and therefore a higher surface area for the subsequent carbonations.

Unfortunately, it was not possible to do other analysis methods due to the small sample weight of limestone used in the TGA. For example, Gas adsorption analysis would give information about the BET surface area and information about the length and pore diameters. The BET surface area for particles cycled under presence of steam in a FBR was measured by Donat[9]. A reduction in the superficial area was reported, however particles had a smaller reduction in BET surface area in presence of steam, except for the first cycle. This might be caused by sintering, since this effect is known to proceed much faster and to a greater extent in presence of steam. As a result, smaller conversions and reaction rates were obtained for the first cycle, as it was shown in Chapter 4.3.

The reduction in BET area is related to a loss of porosity in particles. Donat et al. [4]reported that pores with 50nm of diameter were obtained after thirty cycles for particles cycled with steam instead of 30nm of diameter for particles cycled without steam. The pore diameter of 50nm corresponds to the critical carbonated product layer thickness associated with the transition from the fast to the slow reaction regime found by Alvarez et al.[20]. A further investigation has to be done in order to understand why this occurred.

At this point, the improvement in carbonation caused by steam seems to be related to the creation of greater porosity at the particle surface. In fact, Donat et al.[4] reported that this enhancement was due to a synergistic effect caused by the presence of steam during both calcination and carbonation. During calcination the presence of steam enhances the sintering process causing a shift to larger pores. These larger pores are less susceptible to pore blockage and thus higher surface areas and higher carbonation conversions are obtained. On the other hand, the presence of steam during carbonation maintains the tiny pores and it also reduces the diffusion resistance through the carbonate layer. This way, higher carbonation reaction rates are achieved, as it was seen in the previous Chapter 4.3.

4.5 Random Pore Model

In this Chapter a simple reaction model is used in order to try to quantify the enhancement caused by the presence of steam during the calcination/carbonation cycles. The Random Pore Model (RPM) was selected because it describes well multi-cycle experiments[57] and also because it was recently applied to experiments performed with steam by Arias et al.[7]. This model allows to derive reaction rate constants (k_s) and to determine the diffusion parameter (D). This way, it is possible to further discuss the effect of steam on reaction rates. The model was only applied to Havelock limestone.

According to this model the reaction rate of a gas-solid reaction in the presence of a product layer diffusion resistance is expressed by Equation 32. [19] This expression accounts with the internal pore structure of the particle by using the parameter ψ.

$$\frac{dX}{dt} = \frac{k_s S_0 C(1-X)\sqrt{1-\psi \ln(1-X)}}{(1-\varepsilon)\left[1+\frac{\beta Z}{\psi}\left(\sqrt{1-\psi \ln(1-X)}-1\right)\right]} \quad (32)$$

$$\psi = \frac{4\pi L_o(1-\varepsilon)}{S_0^2} \quad (33)$$

In these equations, k_s is the rate constant for the surface reaction, S is the reaction surface area per unit of volume, ε is the porosity of the particle, C is the CO_2 concentration and L_0 represents the initial pore length per unit of volume. So, Lo and ε can be directly calculated from mercury porosimetry data applied to fresh calcines. This method or other similar such as gas adsorption analysis could not be

performed, due to the small quantities of limestone used in the TGA. Therefore, through a literature data collection, some parameters were selected to be applied in the model (Table 10). These parameters were taken from experiments performed in presence of similar reaction conditions as those used in this work.

Table 10: Values used as porosity, surface area and pore length of the calcines

	No steam/Steam
ε	0.507 [36]
S_0 (m^2/m^3)	4.64×10^7 [59]
L_0 (m/m^3)	4.75×10^{14}

Both surface area and pore length ($L_0 = 1/ \pi \times r_p^2$) were calculated using values of pore radius, calcium oxide density and other limestone characteristic parameters shown in Table 20.

For a reversible first-order system the expression 34 can be simplified and integrated in the regime of chemical reaction control, which will allow to derive the reaction rate constant (k_s) (Equation 34) [57].

$$f(\psi) = \frac{1}{\psi}\left[\sqrt{1 - \psi \ln(1 - X)} - 1\right] = \frac{k_s S_0 (C_b - C_e) t}{2(1-\varepsilon)} \quad (34)$$

C_b is the concentration in the gas bulk and C_e is the equilibrium CO_2 concentration. This last concentration can be determined by Equation 2.

The determination of the reaction rate constant (k_s) is done by plotting the left side of Equation 34, f(ψ), against time. Adjusting a linear trend to the fast reaction regime, k_s can be determined by the slope. Figure 36 shows an example of this procedure applied to the conversion results of the experiments performed with and without steam. The values of k_s are presented in Table 11.

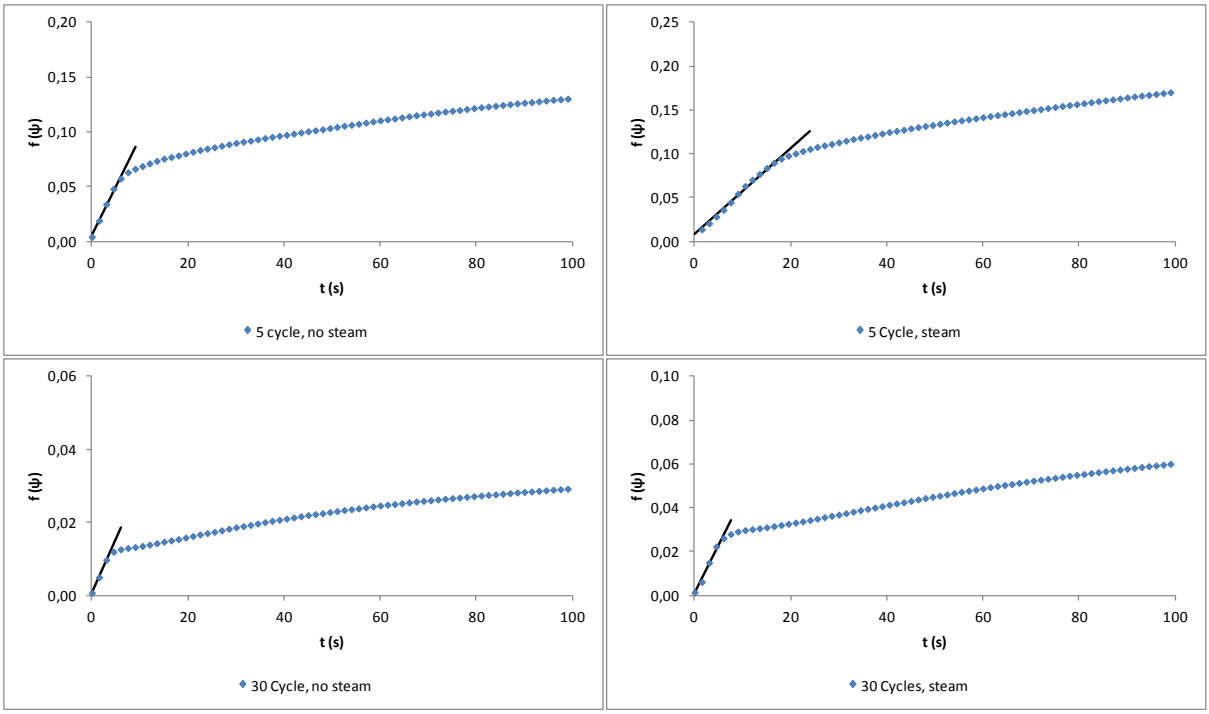

Figure 36: Representation of f(ψ) vs. time for the 5th and 30th cycles of the experiments with and without steam

As it was seen in Chapter 4.4, the sorbent texture evolves with the number of cycles to a larger pore size distribution achieving smaller surface areas. The evolution of these structural parameters complicates the RPM application. In order to allow the application of this model without the determination of these parameters, Grasa et al. [57] proposed a methodology to estimate the surface area and the pore length for the Nth cycle, S_N and L_N.

$$\boldsymbol{S_N = S_0 X_N} \tag{35}$$

$$\boldsymbol{L_N = L_0 X_N \frac{r_{p0}}{r_{pN}}} \tag{36}$$

In Equation 36, in order to determine the pore length it is assumed that r_{p0}/r_{pN} has a value of 0.1 for highly cycled particles. The maximum carbonation conversion (X_N) is determined using Equation 29 and the parameters already found for the Grasa Equation.

The Random Pore Model also allows determination of the effective diffusivity of the slow stage of the carbonation reaction. It is possible to compute this from the linear slope when the left hand side of Equation 37 is plotted against the square-root of time. Since the second and slow stage of carbonation reaction is controlled by a product layer diffusion the integration of Equation 32 gives:

$$\boldsymbol{\frac{1}{\psi}\left[\sqrt{1-\psi \ln(1-X)}-1\right] = \frac{S_0}{(1-\varepsilon)}\sqrt{\frac{D_p t}{2Z}}} \tag{37}$$

Where D_p is the apparent product layer diffusion. This parameter is related to the effective diffusion coefficient, D, as follows:

$$D_p = \frac{M_{CaO} D C_b}{\rho_{CaO}} \tag{38}$$

An example of the diffusion coefficient determination is shown in Figure 37.

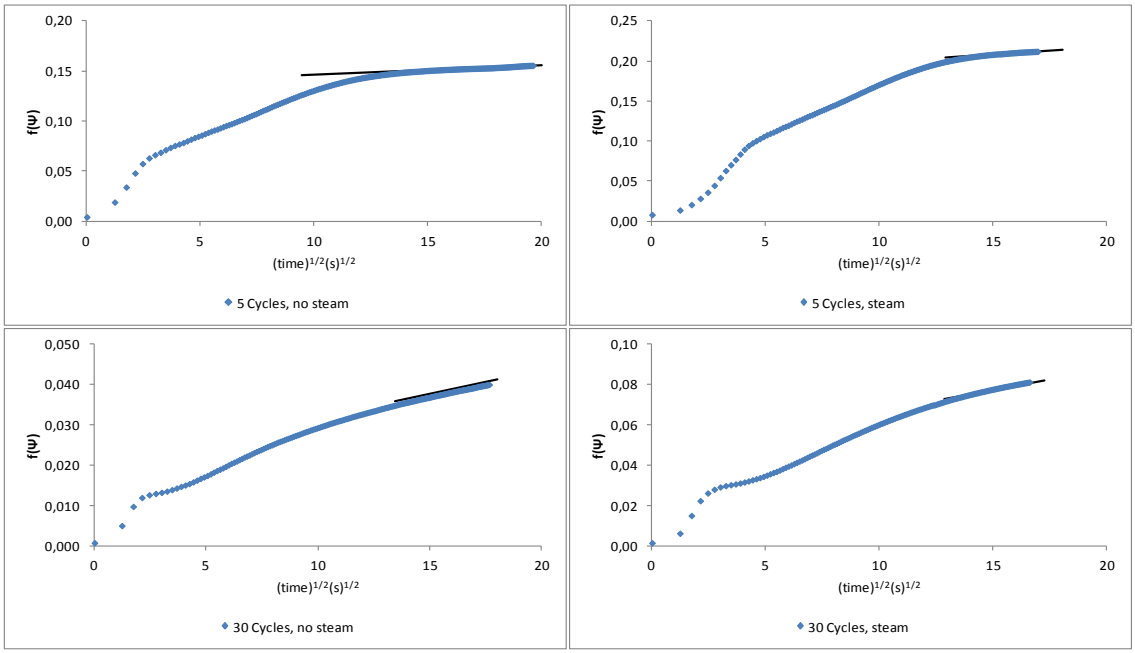

Figure 37: Representation of f(ψ) vs. the root of time used for the determination of D_p.

Having determined the parameters k_s and D_p it is now possible to determine the carbonation conversion using the RPM. In order to do this, it was required to differentiate the two stages of carbonation reaction: a first stage chemically controlled and a second stage where exists a combined control by chemical reaction and CO_2 diffusion through the product layer. For the chemically controlled reaction stage, conversion is calculated by [57, 69]:

$$X = 1 - exp\left(\frac{1-\left(\frac{\tau}{2}\psi+1\right)^2}{\psi}\right) \tag{39}$$

Where,

$$\tau = \frac{k_s(C_b - C_e)S_0 t}{(1-\varepsilon)} \tag{40}$$

The transition between regimes was obtained from the experimental results assuming that the transitory conversion happened when the reaction rate become less than 20% of the maximum reaction rate (Chapter 4.2). Grasa et al.[57] verified that the first chemically controlled stage lasted until a product layer of 30-40nm was formed on the particle surface. The product layer thickness is related with the transitory conversion and it can be obtained by Equation 41 [69]. In the last part of the

calculations, the product layer thickness was determined (Table 12) in order to be compared with the values reported in the literature.

$$\boldsymbol{h = \frac{X_{k-D} \times \rho_{CaO} \times \alpha_{CaCO_3}}{S_N \times M_{CaO}}} \quad (41)$$

Conversion of the diffusion controlled regime is calculated from Equation 42 after the transitory conversion is achieved. [57]The transitory conversion ($X_{k\text{-}D}$) of each cycle was later adjusted by a least-square fitting using the *Solver* function of *Excel* (Table 12) in order to improve the fitting exercise.

$$\boldsymbol{X = X_{k-D} + \left(1 - exp\left(\frac{1}{\psi} - \frac{\left[\sqrt{1+\beta Z\tau} - \left(1 - \frac{\beta Z}{\psi}\right)\right]^2 \psi}{\beta^2 Z^2}\right)\right)} \quad (42)$$

$$\boldsymbol{\beta = \frac{2 \times k_s \times \rho_{CaO} \times (1-\varepsilon)}{M_{CaO} \times D \times S_0}} \quad (43)$$

Equations 39 and 42 were plotted together with the conversions calculated for the experimental results. Figure 38 shows that overall the model predicted well the conversion, but the fitting was better to the initial cycles. For the 1st, 5th and 10th cycles the random pore model fitted well to the experiments performed with and without steam present. For the last cycles the fitting was not so good given that the model seems not to characterize so well the diffusion controlled stage. On the other hand, Arias et al.[69] when applying this model to the sulfation reaction in experiments up to fifty cycles observed a better fitting to the last cycles. The RPM model when applied to our results also showed difficulty in representing the transition between the two regimes of carbonation reaction. This may be because in this period the reaction is strongly controlled by both mechanisms (chemical reaction and diffusion through the product layer). Also, the textural parameters used as inputs in the RPM (ε, S0 and L0) were not determined for our particles. This, along with the simplifications introduced by Equations 35 and 38 can affect the reliability of the results.[69]

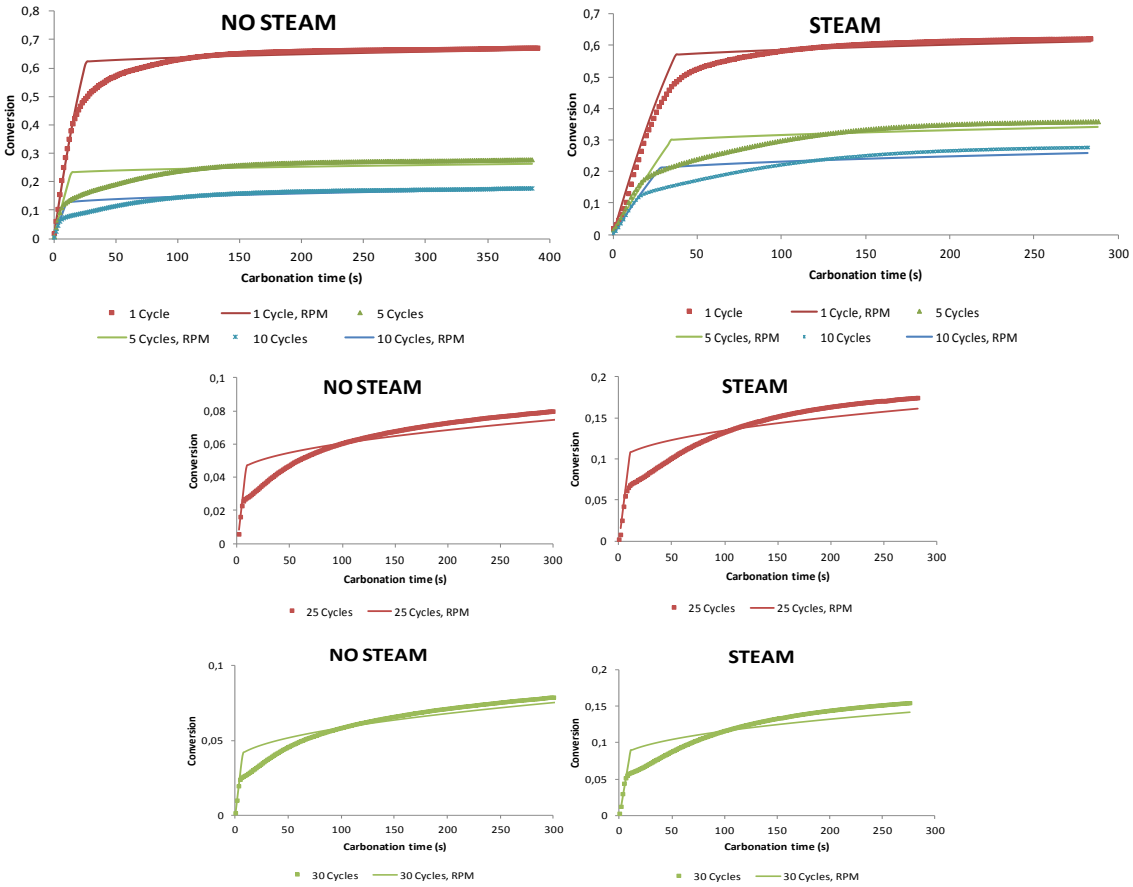

Figure 38: Comparison between the experimental conversion and the conversion calculated using the random pore model for experiments with and without steam

Table 11: Results obtained from the RPM application.

	No Steam					Steam				
	Number of Cycles					Number of Cycles				
	1	5	10	25	30	1	5	10	25	30
k_s ($m^4.mol^{-1}.s^{-1}$)	1.79E-10	5.13E-10	5.71E-10	4.15E-10	4.83E-10	1.10E-10	2.09E-10	2.26E-10	3.74E-10	3.15E-10
D ($m^2.s^{-1}$)	3.52E-17	3.54E-16	1.96E-15	2.42E-15	4.11E-15	6.76E-17	7.85E-16	1.60E-15	2.32E-15	2.48E-15
ψ	1.4	0.7	1.0	1.7	1.9	1.4	0.5	0.6	0.8	0.8
S_N ($m^2.m^{-3}$)	4.64E+07	9.60E+06	6.09E+06	3.65E+06	3.36E+06	4.64E+07	1.29E+07	9.92E+06	7.83E+06	7.59E+06
L_N ($m^2.m^{-3}$)	4.75E+14	9.82E+12	6.23E+12	3.74E+12	3.44E+12	4.75E+14	1.32E+13	1.01E+13	8.01E+12	7.76E+12
ε	0.507	0.507	0.507	0.507	0.507	0.507	0.507	0.507	0.507	0.507

Although the initial values of specific surface area (S_0) and pore length (L_0) were not determined for our particles, the behaviour of these two parameters with the number of cycles followed the expected trend (Table 11). The pore length diminished during cycles and the specific surface area had the same behaviour. Also, as it was referred to before in Chapter 4.4, experiments performed with steam showed higher values of specific surface area.

The values obtained for the structural parameter ψ are similar to the values presented by Bhatia and Perlmuter[7, 19, 57, 62]. The lack of porosity data made us assume a constant value for all cycles and therefore, this may be other factor of error.

The reaction rate constants and the diffusion coefficients determined by the model, achieved values in the same order of magnitude as in the literature. [4, 45, 69] Particles cycled without steam showed to be slightly more reactive during the fast stage of carbonation, since higher values of k_s were obtained. Experiments performed without steam had a mean reaction rate constant equal to $(4.37 \pm 1.50)x10^{-10} m^4.mol^{-1}.s^{-1}$ whereas the steam experiments obtained a value of $(2.47\pm0.86)x10^{-10} m^4.mol^{-1}.s^{-1}$. Looking at these values one would say that steam has no influence on the reaction rate constant. However, this has to be verified again by applying the model with the correct parameters of S, L and ε.

The mean effective diffusion achieved similar results in both experiments performed with and without steam with values of $(1.45\pm1.02)x10^{-15}$ $m^2.s^{-1}$ and $(1.77\pm1.65)x10^{-15}$ $m^2.s^{-1}$, respectively. Nevertheless, it is important to note that the model did not fit very well the diffusion controlled stage so the accuracy of these values is not assured. Except for the first cycles, the positive influence of steam in the product layer diffusion referred in chapter 4.3 was not very visible. However, the initial textural parameters used in the model belonged to Havelock particles cycled with a no steam atmosphere and it may have negatively influenced the results achieved in the steam experiments.

Finally, the transitory conversion (X_{k-D}) and the values obtained for the product layer thickness are shown in Table 12.

Table 12: Transitory conversion (X_{k-D}) used in the random pore model and the value achieved for the product layer thickness

	Cycles	1	5	10	25	30
X_{k-D} (%)	NO STEAM	60.66	22.68	11.83	4.14	3.57
	STEAM	54.69	27.79	19.10	9.57	7.73
h (nm)	NO STEAM	28.9	52.2	42.9	25.0	23.4
	STEAM	50.4	47.5	42.5	27.0	22.5

For the experiments performed with no steam present the product layer thickness achieved a mean value of 34.5 nm and a similar value of 38 was obtained in the experiments performed with steam. These values are within the range of 30-42 nm reported by Grasa et al.[57] as being the product layer thickness in which the transition between the fast and slow regimes happens. This suggests that the transitory conversions applied in the model should be correct.

5. Conclusions

The main focus of this work was to get a better comprehension on how steam influences the CaO-sorbents performance, mainly how it affects the carbonation reaction and its kinetics. The experimental procedure started with a reactivity study in order to determine the optimal conditions to avoid the influence of mass transfer resistances. After this, many experiments were performed with Havelock and Purbeck sorbents with and without steam present (1.5% concentration) in order to obtain results of conversion, carrying capacities and reaction rates. The results obtained were extensively analysed. The study was improved by the observation of particles using a scanning electron microscope and by the application of a random pore model.

The conclusions of this experimental study can be summarized in the next statements:

1. The reaction rates obtained in the experiments without steam were significantly higher than values reported in literature. For the first carbonation, Havelock achieved a reaction rate value of 0.0266 s^{-1} and Purbeck achieved a value of 0.017s^{-1}.

2. Higher conversions were achieved by Havelock limestone in presence of 1.5% of steam. A value of 37% of conversion was accomplished in the 5th cycle and in the end of the 30th cycle an 91% improvement was registered in comparison to no steam experiments.

3. In steam experiments, Havelock achieved a carrying capacity value of .0.13gCO_2/gCaO for the 30th cycle. Also, the quantity of CO_2 absorbed during the cycles was 49% higher than that absorbed without steam.

4. For Purbeck limestone, only a little enhancement of 12% was observed for the last cycle conversion. No significant improvements were registered for reaction rates and carrying capacities.

5. The enhancement caused by steam has different results in different types of limestones due to impurities and the CaO content of the limestone.

6. Higher improvements in presence of steam were obtained for higher cycle numbers in both limestones.

7. Steam proved to enhance the diffusion controlled stage of carbonation and this was already reported by other authors. [4]

8. An enhancement in the fast reaction regime in presence of steam was observed. Improvements in the carrying capacity for this stage were noticed for Havelock limestone.

9. The highest conversions, carrying capacities and reaction rates were obtained for Havelock in experiments performed with steam.

10. Particles cycled with steam kept higher porosities and surface areas through cycles. This explains the higher conversions and carrying capacities.

11. Sintering effects were more pronounced in the particles cycled without steam.

12. The RPM fit well to our experimental data, although it presented problems in characterizing higher calcination/carbonation cycles and in characterizing the diffusion controlled stage of carbonation. This model has to be repeated together with methods to determine the internal structure of particles (pore diameter, pore length, surface area), because these parameters have a strong influence on the model results.

13. The reaction rate coefficients obtained with the model had higher values for no steam experiments. A mean reaction rate of $(4.33 \pm 1.50) \times 10^{-10}$ $m^4.mol^{-1}.s^{-1}$was obtained and experiments performed with steam achieved $(2.47 \pm 1.01) \times 10^{-10}$ $m^4.mol^{-1}.s^{-1}$.

14. The mean effective diffusion coefficient was similar for both experiments achieving values of $(1.45 \pm 1.02) \times 10^{-15}$ m^2/s for the experiments performed with steam and $(1.77 \pm 1.65) \times 10^{-15}$ for experiments performed without steam.

6. Future Work

The effect of steam in carbonation reaction was the scope of this work. Two different limestones were tested and revealed to behave differently when cycled in a steam atmosphere. More limestones can be tested in the future to try to connect the enhancement caused by steam with the impurities and CaO content of limestones. Also, higher steam concentrations could be tested in the TGA. However, modifications should be incorporated in the experimental set-up in order to avoid the condensation of steam in the lines, such has supplying heat with a heating tape.

Similar experiments as those performed in this work should be done with steam present during only calcination or carbonation reactions. These will help to distinguish the effect of steam in each reaction. The application of a random pore model should be repeated to verify the reaction rate coefficients obtained in this work. It is essential to do gas adsorption analysis of the samples in order to study properly the internal pore structure evolution and to get accurate values for the particle surface area.

In the calcium looping research, realistic gas atmospheres simulating the conditions present in a post-combustion process should continue to be tested. Particularly, the combined influence of sulphur species and steam on CaO-sorbents performance should be studied.

.

References

1. *Atmospheric greenhouse gas concentrations (CSI 013) - Assessment published Jan 2012 — EEA*. Publish date: 2012-01-25T13:20:30+01:00; Available from: http://www.eea.europa.eu/data-and-maps/indicators/atmospheric-greenhouse-gas-concentrations-2/assessment.
2. Florin, N. and P. Fennell, *Carbon Capture technology: future fossil fuel use and mitigating climate change*. 2010, Grantham Institute for Climate Change.
3. Manovic, V. and E. Anthony, *Lime-Based Sorbents for High-Temperature CO_2 Capture - A Review of Sorbent Modification Methods.* Environmental Research and Public Health, 2010. **7**: p. 3129-3140.
4. Donat, F., N.H. Florin, E.J. Anthony, and P.S. Fennell, *Influence of High-Temperature Steam on the Reactivity of CaO Sorbent for CO2 Capture.* Environmental Science & Technology, 2012. **46**(2): p. 1262-1269.
5. Alvarez, D. and J.C. Abanades, *Pore-size and shape effects on the recarbonation performance of calcium oxide submitted to repeated calcination/recarbonation cycles.* Energy & Fuels, 2005. **19**(1): p. 270-278.
6. Blamey, J., E.J. Anthony, J. Wang, and P.S. Fennell, *The calcium looping cycle for large-scale CO(2) capture.* Progress in Energy and Combustion Science, 2010. **36**(2): p. 260-279.
7. Arias, B., G. Grasa, J.C. Abanades, V. Manovic, and E.J. Anthony, *The Effect of Steam on the Fast Carbonation Reaction Rates of CaO.* Industrial & Engineering Chemistry Research, 2012. **51**(5): p. 2478-2482.
8. Chambel, A., *Modelling of Solid Looping Cycle for Carbon Capture and Storage*, in *Engenharia Química*. 2009, Instituto Superior Técnico, Universidade Técnica de Lisboa: Lisboa.
9. Donat, F., *The influence of high-temperature steam on the rate and extend of reaction of CaO-sorbent for CO2 capture-and-release*. 2011, TU Bergakademie Freiberg.
10. Dean, C.C., J. Blamey, N.H. Florin, M.J. Al-Jeboori, and P.S. Fennell, *The calcium looping cycle for CO2 capture from power generation, cement manufacture and hydrogen production.* Chemical Engineering Research and Design, 2010.
11. Gupta, H. and L.S. Fan, *Carbonation-calcination cycle using high reactivity calcium oxide for carbon dioxide separation from flue gas.* Industrial & Engineering Chemistry Research, 2002. **41**(16): p. 4035-4042.
12. Florin, N.H. and A.T. Harris, *Screening CaO-Based sorbents for Co-2 capture in biomass gasifiers.* Energy & Fuels, 2008. **22**(4): p. 2734-2742.

13. Grasa, G.S. and J.C. Abanades, *CO2 capture capacity of CaO in long series of carbonation/calcination cycles.* Industrial & Engineering Chemistry Research, 2006. **45**(26): p. 8846-8851.
14. Abanades, J.C., E.J. Anthony, J.S. Wang, and J.E. Oakey, *Fluidized bed combustion systems integrating CO2 capture with CaO.* Environmental Science & Technology, 2005. **39**(8): p. 2861-2866.
15. Manovic, V., J.-P. Charland, J. Blamey, P.S. Fennell, D.Y. Lu, and E.J. Anthony, *Influence of calcination conditions on carrying capacity of CaO-based sorbent in CO(2) looping cycles.* Fuel, 2009. **88**(10): p. 1893-1900.
16. Baker, E.H., *The Calcium Oxide-Carbon Dioxide System Pressure Range 1-300 Atmospheres.* Journal of the Chemical Society, 1962. **87**: p. 464-470.
17. Khinast, J., G.F. Krammer, C. Brunner, and G. Staudinger, *Decomposition of limestone: The influence of CO2 and particle size on the reaction rate.* Chemical Engineering Science, 1996. **51**(4): p. 623-634.
18. Florin, N.H., J. Blamey, and P.S. Fennell, *Synthetic CaO-Based Sorbent for CO(2) Capture from Large-Point Sources.* Energy & Fuels, 2010. **24**: p. 4598-4604.
19. Bhatia, S.K. and D.D. Perlmutter, *EFFECT OF THE PRODUCT LAYER ON THE KINETICS OF THE CO2-LIME REACTION.* Aiche Journal, 1983. **29**(1): p. 79-86.
20. Alvarez, D. and J.C. Abanades, *Determination of the critical product layer thickness in the reaction of CaO with CO2.* Industrial & Engineering Chemistry Research, 2005. **44**(15): p. 5608-5615.
21. Florin, N.H. and A.T. Harris, *Reactivity of CaO derived from nano-sized CaCO(3) particles through multiple CO(2) capture-and-release cycles.* Chemical Engineering Science, 2009. **64**(2): p. 187-191.
22. Fennell, P.S., J.F. Davidson, J.S. Dennis, and A.N. Hayhurst, *Regeneration of sintered limestone sorbents for the sequestration of CO2 from combustion and other systems.* Journal of the Energy Institute, 2007. **80**(2): p. 116-119.
23. Fennell, P.S., R. Pacciani, J.S. Dennis, J.F. Davidson, and A.N. Hayhurst, *The effects of repeated cycles of calcination and carbonation on a variety of different limestones, as measured in a hot fluidized bed of sand.* Energy & Fuels, 2007. **21**(4): p. 2072-2081.
24. Blamey, J., N.P.M. Paterson, D.R. Dugwell, P. Stevenson, and P.S. Fennell, *Reactivation of a CaO-based sorbent for CO2 capture from stacionary sources.* Proceedings of combustion Institute, 2011. **33 (2)**: p. 2673-2682.
25. Blamey, J., N.P.M. Paterson, D.R. Dugwell, and P.S. Fennell, *Mechanism of Particle Breakage during Reactivation of CaO-Based Sorbents for CO(2) Capture.* Energy & Fuels, 2010. **24**: p. 4605-4616.
26. Abanades, J.C. and D. Alvarez, *Conversion limits in the reaction of CO2 with lime.* Energy & Fuels, 2003. **17**(2): p. 308-315.
27. Outeda, C., *CaO based sorbents looping cycles for CO2 capture*, in *Engenharia Química*. 2011, Instituto Superior Técnico: Lisboa.

28. Sun, P., J.R. Grace, C.J. Lim, and E.J. Anthony, *Removal of CO2 by calcium-based sorbents in the presence of SO2.* Energy & Fuels, 2007. **21**(1): p. 163-170.
29. Anthony, E.J., *Solid looping cycles: A new technology for coal conversion.* Industrial & Engineering Chemistry Research, 2008. **47**(6): p. 1747-1754.
30. Manovic, V. and E.J. Anthony, *Sequential SO2/CO2 capture enhanced by steam reactivation of a CaO-based sorbent.* Fuel, 2008. **87**(8-9): p. 1564-1573.
31. Borgwardt, R.H., *SINTERING OF NASCENT CALCIUM-OXIDE.* Chemical Engineering Science, 1989. **44**(1): p. 53-60.
32. Manovic, V. and E.J. Anthony, *Thermal activation of CaO-based sorbent and self-reactivation during CO2 capture looping cycles.* Environmental Science & Technology, 2008. **42**(11): p. 4170-4174.
33. Arias, B., J.C. Abanades, and E.J. Anthony, *Model for Self-Reactivation of Highly Sintered CaO Particles during CO(2) Capture Looping Cycles.* Energy & Fuels, 2011. **25**(4): p. 1926-1930.
34. Lu, D.Y., V. Manovic, R. Hughes, and E.J. Anthony, *Study of CO2 capture using CO2 looping combustion technology*. Proceedings of the 6th International Symposium on Coal Combustion, ed. X.X.M. Xu. 2007. 997-1007.
35. Zeman, F., *Effect of steam hydration on performance of lime sorbent for CO2 capture.* International Journal of Greenhouse Gas Control, 2008. **2**(2).
36. Wu, Y., J. Blamey, E.J. Anthony, and P.S. Fennell, *Morphological Changes of Limestone Sorbent Particles during Carbonation/Calcination Looping Cycles in a Thermogravimetric Analyzer (TGA) and Reactivation with Steam.* Energy & Fuels, 2010. **24**: p. 2768-2776.
37. Manovic, V. and E.J. Anthony, *CaO-Based Pellets Supported by Calcium Aluminate Cements for High-Temperature CO(2) Capture.* Environmental Science & Technology, 2009. **43**(18): p. 7117-7122.
38. Santos, E.T., C. Alfonsin, A.J.S. Chambel, A. Fernandes, A.P.S. Dias, C.I.C. Pinheiro, and M.F. Ribeiro, *Investigation of a stable synthetic sol-gel CaO sorbent for CO2 capture.* Fuel, 2012. **94**(1): p. 624-628.
39. Li, Z.S., N.S. Cai, and Y.Y. Huang, *Effect of preparation temperature on cyclic CO2 capture and multiple carbonation-calcination cycles for a new Ca-based CO2 sorbent.* Industrial & Engineering Chemistry Research, 2006. **45**(6): p. 1911-1917.
40. Li, Z.S., N.S. Cai, Y.Y. Huang, and H.J. Han, *Synthesis, experimental studies, and analysis of a new calcium-based carbon dioxide absorbent.* Energy & Fuels, 2005. **19**(4): p. 1447-1452.
41. Pacciani, R., C.R. Mueller, J.F. Davidson, J.S. Dennis, and A.N. Hayhurst, *Synthetic Ca-based solid sorbents suitable for capturing CO2 in a fluidized bed.* Canadian Journal of Chemical Engineering, 2008. **86**(3): p. 356-366.
42. Salvador, C., D. Lu, E.J. Anthony, and J.C. Abanades, *Enhancement of CaO for CO2 capture in an FBC environment.* Chemical Engineering Journal, 2003. **96**(1-3): p. 187-195.
43. Gonzalez, B., J. Blamey, M. McBride-Wright, N. Carter, D. Dugwell, P. Fennell, and J. Carlos Abanades, *Calcium looping for CO2 capture: sorbent enhancement through doping*, in *10th*

International Conference on Greenhouse Gas Control Technologies, J.H.C.T.W. Gale, Editor. 2011. p. 402-409.

44. Beruto, D.T., R. Botter, A. Lagazzo, and E. Finocchio, *Calcium oxides for CO(2) capture obtained from the thermal decomposition of CaCO(3) particles coprecipitated with Al(3+) ions.* Journal of the European Ceramic Society, 2012. **32**(2): p. 307-315.
45. Manovic, V. and E.J. Anthony, *Carbonation of CaO-Based Sorbents Enhanced by Steam Addition.* Industrial & Engineering Chemistry Research, 2010. **49**(19): p. 9105-9110.
46. Iyer, M.V., H. Gupta, B.B. Sakadjian, and L.S. Fan, *Multicyclic study on the simultaneous carbonation and sulfation of high-reactivity CaO.* Industrial & Engineering Chemistry Research, 2004. **43**(14): p. 3939-3947.
47. Berger, E.E., *Effect of Steam on the Decomposition of Limestone.* Industrial & Engineering Chemistry, 1927. **19 (5)**: p. 594-596.
48. Borgwardt, R.H., *CALCINATION KINETICS AND SURFACE-AREA OF DISPERSED LIMESTONE PARTICLES.* Aiche Journal, 1985. **31**(1): p. 103-111.
49. Beruto, D., A.W. Searcy, R. Botter, and M. Giordani, *THERMODYNAMICS AND KINETICS OF H2O(V) CHEMISORPTION AND SOLUBILITY IN NANOMETRIC AND SINGLE-CRYSTAL MGO PARTICLES DURING SINTERING.* Journal of Physical Chemistry, 1993. **97**(36): p. 9201-9205.
50. Borgwardt, R.H., *CALCIUM-OXIDE SINTERING IN ATMOSPHERES CONTAINING WATER AND CARBON-DIOXIDE.* Industrial & Engineering Chemistry Research, 1989. **28**(4): p. 493-500.
51. Stewart, M.C., V. Manovic, E.J. Anthony, and A. Macchi, *Enhancement of Indirect Sulphation of Limestone by Steam Addition.* Environmental Science & Technology, 2010. **44**(22): p. 8781-8786.
52. Dobner, S., L. Sterns, R.A. Graff, and A.M. Squires, *CYCLIC CALCINATION AND RE-CARBONATION OF CALCINED DOLOMITE.* Industrial & Engineering Chemistry Process Design and Development, 1977. **16**(4): p. 479-486.
53. Symonds, R.T., D.Y. Lu, R.W. Hughes, E.J. Anthony, and A. Macchi, *CO(2) Capture from Simulated Syngas via Cyclic Carbonation/Calcination for a Naturally Occurring Limestone: Pilot-Plant Testing.* Industrial & Engineering Chemistry Research, 2009. **48**(18): p. 8431-8440.
54. Yang, S. and Y. Xiao, *Steam catalysis in CaO carbonation under low steam partial pressure.* Industrial & Engineering Chemistry Research, 2008. **47**(12): p. 4043-4048.
55. Sun, P., J.R. Grace, C.J. Lim, and E.J. Anthony, *Investigation of attempts to improve cyclic CO2 capture by sorbent hydration and modification.* Industrial & Engineering Chemistry Research, 2008. **47**(6): p. 2024-2032.
56. Lu, H., E.P. Reddy, and P.G. Smirniotis, *Calcium oxide based sorbents for capture of carbon dioxide at high temperatures.* Industrial & Engineering Chemistry Research, 2006. **45**(11): p. 3944-3949.
57. Grasa, G., R. Murillo, M. Alonso, and J.C. Abanades, *Application of the Random Pore Model to the Carbonation Cyclic Reaction.* Aiche Journal, 2009. **55**(5): p. 1246-1255.

58. Froment, G.F., K.B. Bischoff, and J.D. Wilde, *Chemical Reactor Analysis and Design*.
59. Chao, L.-K. and J. Cegla, *The influence of carbonation/calcination cycles on the effectiveness factor of CaO particles during carbonation*, Imperial College London.
60. Chuang, S.Y., J.S. Dennis, A.N. Hayhurst, and S.A. Scott, *Kinetics of the chemical looping oxidation of CO by a co-precipitated mixture of CuO and Al(2)O(3).* Proceedings of the Combustion Institute, 2009. **32**.
61. Bird, R.B., W.E. Stewart, and E.N. Lightfoot, *Transport Phenomena*. 2nd ed. 2007.
62. Grasa, G.S., J.C. Abanades, M. Alonso, and B. Gonzalez, *Reactivity of highly cycled particles of CaO in a carbonation/calcination loop.* Chemical Engineering Journal, 2008. **137**(3): p. 561-567.
63. Rodriguez, N., M. Alonso, J. Carlos Abanades, A. Charitos, C. Hawthorne, G. Scheffknecht, D.Y. Lu, and E.J. Anthony, *Comparison of experimental results from three dual fluidized bed test facilities capturing CO2 with CaO.* 10th International Conference on Greenhouse Gas Control Technologies, 2011. **4**.
64. Sun, P., J.R. Grace, C.J. Lim, and E.J. Anthony, *A discrete-pore-size-distribution-based gas-solid model and its application to the CaO+CO2 reaction.* Chemical Engineering Science, 2008. **63**(1): p. 57-70.
65. Dieter, H. and C. Hawthorne, *-Demonstration of the Calcium Looping Process: High Temperature CO2 Capture with CaO in a 200 kWth Dual Fluidized Bed Pilot Facility*
66. *NIST Chemistry WebBook*.
67. Wang, Y. and W.J. Thomson, *THE EFFECTS OF STEAM AND CARBON-DIOXIDE ON CALCITE DECOMPOSITION USING DYNAMIC X-RAY-DIFFRACTION.* Chemical Engineering Science, 1995. **50**(9).
68. Sun, P., J. Lim, and J.R. Grace, *Cyclic CO2 capture by limestone-derived sorbent during prolonged calcination/carbonation cycling.* Aiche Journal, 2008. **54**(6): p. 1668-1677.
69. Arias, B., J.M. Cordero, M. Alonso, and J.C. Abanades, *Sulfation rates of cycled CaO particles in the carbonator of a Ca-looping cycle for postcombustion CO2 capture.* Aiche Journal, 2012. **58**(7).
70. *http://www.omega.com/temperature/z/pdf/z103.pdf*. [cited 2012 06/06/2012].

Appendices

Appendix A – Calibration

Table 13: Calibration of the Rotameter with the 15%CO_2 gas mixture

Rotameter Position	Time (seg)			Flow rate (ml/min)			Average Flow (ml/min)	Standard Deviation
	1	2	3	1	2	3		
120	54.0	54.0	54.0	111.1	111.1	111.1	111.1	1.7E-14
130	47.1	47.1	47.1	127.4	127.5	127.4	127.4	2.7E-02
140	42.1	42.1	42.1	142.6	142.6	142.6	142.6	3.9E-02
150	38.0	38.0	38.0	157.8	157.9	157.8	157.8	4.2E-02

Table 14: Calibration of the Rotameter with the N_2

Rotameter Position	Time (seg)			Flow rate (ml/min)			Average Flow (ml/min)	Standard Deviation
	1	2	3	1	2	3		
120	54.2	53.9	53.9	110.7	111.3	111.3	111.1	3.6E-01
130	47.1	47.3	47.2	127.4	126.8	127.1	127.1	2.7E-01
140	42.3	42.2	42.3	141.8	142.2	141.8	142.0	1.9E-01
150	37.9	37.8	37.9	158.3	158.7	158.3	158.5	2.4E-01

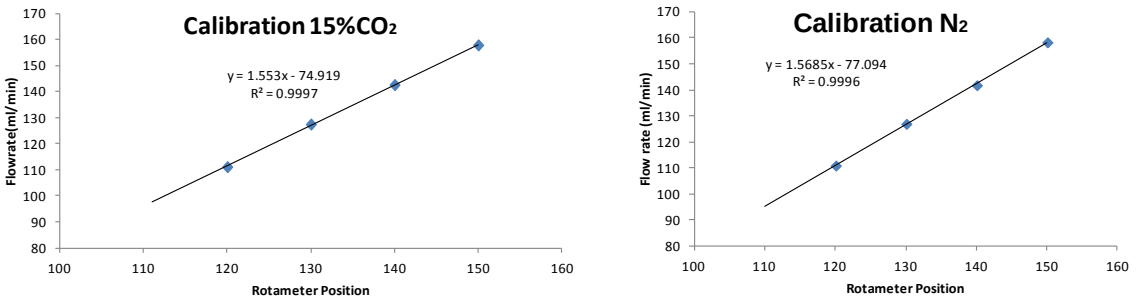

Figure 39: Results of rotameters calibration for the 15% CO_2 gas mixture and for nitrogen.

Table 15: Relative humidity of saturated salt solutions used to calibrate the humidity probe. The value for 23ºC was achieved by a linear regression.[70]

Temperature (ºC)	Magnesium Chloride		Magnesium Nitrate		Sodium Chloride		Potassium Chloride		Potassium Nitrate	
	%RH	Std Deviation	%RH	Std Deviation	%RH	Std Deviation	%RH	Std Deviation	%RH	Std Deviation
0	33.66	0.33	60.35	0.55	75.51	0.34	88.61	0.53	96.33	2.9
5	33.6	0.28	58.86	0.43	75.65	0.27	87.67	0.45	96.27	2.1
10	33.47	0.24	57.36	0.33	75.67	0.22	86.77	0.39	95.96	1.4
15	33.3	0.21	55.87	0.27	75.61	0.18	85.92	0.33	95.41	0.96
20	33.07	0.18	54.38	0.23	75.47	0.14	85.11	0.29	94.62	0.66
23	**32.90**	**-**	**53.49**	**-**	**75.36**	**-**	**84.65**	**-**	**94.00**	**-**
25	32.78	0.16	52.89	0.22	75.29	0.12	84.34	0.26	93.58	0.55
30	32.44	0.14	51.4	0.24	75.09	0.11	83.62	0.25	92.31	0.6
35	32.05	0.13	49.91	0.29	74.87	0.12	82.95	0.25	90.79	0.83
40	31.6	0.13	48.42	0.37	74.68	0.13	82.32	0.25	89.03	1.2
45	31.1	0.13	46.93	0.47	74.52	0.16	81.74	0.28	87.03	1.8
50	30.54	0.13	45.44	0.6	74.43	0.19	81.2	0.31	84.78	2.5
55	29.93	0.16	-	-	74.41	0.24	80.7	0.35	-	-
60	29.26	0.18	-	-	74.5	0.3	80.25	0.41	-	-
65	28.54	0.21	-	-	74.71	0.37	79.85	0.48	-	-
70	27.77	0.25	-	-	75.06	0.45	79.49	0.57	-	-
75	26.94	0.29	-	-	75.58	0.55	79.17	0.66	-	-
80	26.05	0.34	-	-	76.29	0.65	78.9	0.77	-	-
85	25.11	0.39	-	-	-	-	78.68	0.89	-	-
90	24.12	0.46	-	-	-	-	78.5	1	-	-
95	23.07	0.52	-	-	-	-	-	-	-	-
100	21.97	0.6	-	-	-	-	-	-	-	-

Table 16: Chemical composition (%wt) of Havelock and Purbeck limestones[9]

Compound	Havelock	Purbeck
Ca	97.64	97.67
Fe	0.20	0.49
Mg	0.27	0.61
Al	0.15	0.21
Si	1.20	0.65
Mn	0.43	0.14
K	0.04	0.09
S	0.00	0.11
Zr	0.00	0.05

Table 17: TGA profile followed in the experiments with and without steam.

	Experiments WITHOUT Steam	Experiments WITH Steam
TGA procedure method	Select gas 2 *(Gas 2: 15%CO_2)*	External Event On *(Gas 2: 15%CO_2)*
	Flow rate (ml/min) *(120/130/140/160/200 ml/min)*	Flow Rate = 0 ml/min *(No Gas coming from the internal TGA flow controller)*
	Equilibrate at 50 °C	Equilibrate at 50 °C
	Ramp 40 °C/min to 110 °C *(To vaporize any moisture present)*	Ramp 40 °C/min to 110 °C
	Isothermal for 10min	Isothermal for 10min
	Ramp 120 °C/min to 900°C	Ramp 120 °C/min to 900°C
	Isothermal for 4 min *(Calcination Reaction)*	Isothermal for 4 min
	Select gas 1 *(Gas 1: N_2)*	External Event Off *(Gas 1: N_2)*
	Isothermal for 1 min *(To do the cooling down under N_2)*	Isothermal for 1 min
	Ramp 120 °C/min to 650 °C	Ramp 120 °C/min to 650 °C
	Select gas 2	External Event On
	Isothermal for 5 min *(Carbonation Reaction)*	Isothermal for 5 min
	Repeat segment 6 for 4 times *(To do the cycling process)*	Repeat segment 6 for 29 times *(To do the cycling process)*
	Ramp 120 °C/min to 900 °C	Ramp 120 °C/min to 900 °C
	Isothermal for 4 min *(Last Calcination)*	Isothermal for 4 min
	Select gas 1	External Event Off
	Isothermal for 1 min	Isothermal for 1 min

Appendix B – Calculations

1. Weight of a calcium oxide particle:

After the calcination of $CaCO_3$ from the limestone, particles of calcium oxide were obtained. Firstly, the mass of each limestone particle was determined by the calculation of the number of particles and the particle volume. In order to do this, the density of calcium carbonate was necessary (2711 kg/m^3) and it was assumed the sphericity of the particles. Limestone porosity was assumed to be ε =0.1.

$$\boldsymbol{V_{particle} = \frac{4}{3}\pi\left(\frac{d_p}{2}\right)^3} \quad (44)$$

$$\boldsymbol{\rho_{limestone} = \rho_{CaCO_3 \times (1-\varepsilon)}} \quad (45)$$

$$\boldsymbol{n^{\circ}_{particles} = \frac{m_{initial}}{\rho_{limestone} \times V_{particle}}} \quad (46)$$

$$\boldsymbol{m_{\,limestone\,particle} = \frac{n^{\circ}_{particles}}{m_{initial}}} \quad (47)$$

The weight of a CaO particle is calculated by the determination of the reduction that a particle of $CaCO_3$ undergoes. It was considered that the calcination is a complete reaction and also that the limestone impurities can be neglected.

$$\boldsymbol{reduction = \frac{m_{CaO\ (end\ of\ calcination)}}{m_{inicial}}} \quad (48)$$

$$\boldsymbol{m_{CaO\ particle} = m_{CaCO3\ particle} \times reduction} \quad (49)$$

2. Mass per unit volume of the sorbent (m_v)

In order to determine the volume of a CaO particle, the volume that the pores occupy in the particle was considered,

$$\boldsymbol{V_{pores} = \frac{m_{CaO}}{\rho_{CaO}\left(\frac{1}{\varepsilon}-1\right)}} \quad (50)$$

Where the ρ_{CaO} has a value of 3350 kg/m^3. Consequently, the volume of the sorbent can be calculated by the porosity equation.

$$\boldsymbol{\varepsilon = \frac{V_{pores}}{V_{pores}+V_{solid}} \Leftrightarrow V_{solid} = \frac{V_{pores}-\varepsilon V_{pores}}{\varepsilon}} \quad (51)$$

After one calcination the mass per unit volume of the CaO is 3.35 x 10^6 (gCaO.m^{-3}).

3. Molecular Diffusivity (D_{AB})

The molecular diffusivity was determined using Equation 52 for an ideal gas.

$$D_{AB} = 0.0018583\sqrt{T^3\left(\frac{1}{M_A}+\frac{1}{M_B}\right)} \times \frac{1}{P\times\sigma_{AB}^2\times\Omega_{D_{AB}}} \quad (52)$$

$$\sigma_{AB} = \frac{1}{2}(\sigma_A + \sigma_B) \quad (53)$$

$$\varepsilon_{AB}/_k = \sqrt{\varepsilon_A/_k \times \varepsilon_B/_k} \quad (54)$$

The value of Chapman-Enskog constants was taken from the literature. [61]

Table 18: Values of the Chapman- Enskog for carbon dioxide and nitrogen.

σ_{N2} = 3.667 Aº	
σ_{CO2} = 3.996 Aº	
ε_{N2}/k = 99.8 K	
ε_{CO2}/k = 99.8 K	

$\frac{kT}{\varepsilon_{AB}}$	$\Omega_{D,AB}$
6	0.8129
7	0.7898

In order to calculate the velocity of the gas to determine de Reynolds number, it was necessary to know some dimensions of the Furnace. The dimension used was 5mm, value of the gas inlet diameter.

4. External mass coefficient (k_g)

The first step to determine k_g is to choose a suitable correlation. In this case a correlation for forced convection around spheres was selected. [61]

$$Sh_m = 2 + 0.60Re^{1/2}Sc^{1/3} \quad (55)$$

This equation assumes that the surface temperature and composition are constants. It also assumes that it has small net mass-transfer rates.

The Schmidt and Sherwood adimensional numbers are calculated with Equations 56 and 57.

$$Sh_m = \frac{k_g\times D_p}{D_{AB}} \quad (56)$$

$$Sc = \frac{\mu}{\rho\times D_{AB}} \quad (57)$$

$$Re = \frac{v\rho D_p}{\mu} \quad (58)$$

In these equations D_p, means the particle diameter, μ, represents the viscosity of the stream and D_{AB} is the molecular diffusivity of the reactant.

The particle diameter is determined by a geometric mean of the particle size (exemplified for the 500-710 μm particle size).

$$D_p = \sqrt{500 \times 710} \quad (59)$$

5. Porous radius

In order to calculate the Knudsen Diffusivity the porous radius, $\overline{r_p}$, has to be determined. This exact value can be known analysing the sorbent by means of mercury porosimetry or BET analysis. However, this was not possible to do in this work and therefore, some results from previous works were used. The BET surface area for Havelock limestone were taken from the literature[59], using the values correspondent to a similar particle size. The porosity used was taken from Wu et al. [36].

$$\overline{r_p} = \frac{2\varepsilon}{S_{BET}} \times \frac{1}{\rho_{CaO}} \quad (60)$$

Table 19: Porosity, BET surface area and the pore radius for Havelock limestone with a particle size of 500-710μm after one calcination

ε	0.507
S_{BET} (m^2/kg)	14933.6
ρ (kg/m^3)	3350
$\overline{r_p}$ (nm)	21.3

Table 20: Porosity, BET surface area and the pore radius for Havelock limestone with particle sizes of 150-355μm and 355-500μm after one calcination

ε	0.507
S_{BET} (m^2/kg)	13846.4
ρ (kg/m^3)	3350
$\overline{r_p}$ (nm)	25.6

6. Determination of the concentration of steam in the gas flow

In experiments performed with steam, the 15%(v/v) CO_2 gas mixture was introduced in the furnace after going through the bubbler to leave saturated with the water vapour. The total composition of the gas had to be determined. In order to do this it was used the Dalton's Law which says that the total pressure of an ideal gases mixture is equal to the sum of the partial pressures of the individual gases in the mixture:

$$\boldsymbol{p_T = p_{N_2} + p_{CO_2} + p_{H_2O}} \tag{61}$$

The steam partial pressure was determined by Equation 31, as previously describe in Chapter 4.3. Because of the steam introduction, the CO_2 and N_2 concentrations in the gas will be lower. Nevertheless, the proportion between CO_2 and N_2 in the wet gas will stay the same as the proportion already existent in the gas without steam.

7. Determination of parameters required for the RPM application

The ratio volume fraction, Z, can be determined by Equation 62.

$$\boldsymbol{Z = 1 + \frac{\rho(\alpha_C - \alpha_L)}{M_{CaO}}} \tag{62}$$

Where α_c is the molar volume of $CaCO_3$ with a value of 36.9 x 10^{-6} m^3/mol and α_L is the molar volume of CaO with a value of 16.9 x 10^{-6} m^3/mol.

Appendix C– Experimental Results

1. Determination of the optimum reaction conditions:

1.1 Flow rate Tests

Table 21: Results of the mass transfer and chemical reaction for the flow rate experiments

	Fow rates (ml/min)					
	100	120	130	140	160	200
$x_{out,\ average}$	0.140	0.141	0.141	0.142	0.142	0.143
$x_{out,min}$	0.130	0.132	0.132	0.134	0.135	0.136
$r_{external}$ (mol.gCaO^{-1}.s^{-1})	1.46E-03	1.48E-03	1.51E-03	1.52E-03	1.56E-03	1.59E-03
$r_{exp,max}$ (mol.gCaO^{-1}.s^{-1})	3.37E-04	3.65E-04	3.87E-04	3.76E-04	4.13E-04	4.65E-04
k_g (m^3.gCaO^{-1}.s^{-1})	7.88E-04	7.98E-04	8.13E-04	8.13E-04	8.28E-04	8.38E-04
k_r (m^3.gCaO^{-1}.s^{-1})	1.13E-03	1.35E-03	1.53E-03	1.41E-03	1.75E-03	2.33E-03
k_o (m^3.gCaO^{-1}.s^{-1})	1.82E-04	1.96E-04	2.08E-04	2.01E-04	2.20E-04	2.46E-04
(k_g-k_r)	-3.45E-04	-5.49E-04	-7.21E-04	-5.95E-04	-9.21E-04	-1.49E-03
ϕ	4.426	4.828	5.150	4.935	5.499	6.352
η	0.209	0.193	0.182	0.189	0.171	0.149

Table 22: Determination of the external mass transfer coefficient (k_g) for the flow rate experiments

	Flow rates (ml/min)					
	100	120	130	140	160	200
D_p (m)	5.96E-04	5.96E-04	5.96E-04	5.96E-04	5.96E-04	5.96E-04
Sh	2.41	2.45	2.47	2.49	2.52	2.58
Sc	9.91E-01	9.91E-01	9.91E-01	9.91E-01	9.91E-01	9.91E-01
Re	4.73E-01	5.68E-01	6.16E-01	6.63E-01	7.58E-01	9.47E-01
k_g (m.s^{-1})	4.36E-01	4.43E-01	4.46E-01	4.50E-01	4.56E-01	4.67E-01
S_m (m^2.gCaO^{-1})	1.81E-03	1.80E-03	1.82E-03	1.81E-03	1.82E-03	1.80E-03
k_g (m^3.gCaO^{-1}.s^{-1})	7.88E-04	7.98E-04	8.13E-04	8.13E-04	8.28E-04	8.38E-04

1.2 Sample Mass Tests

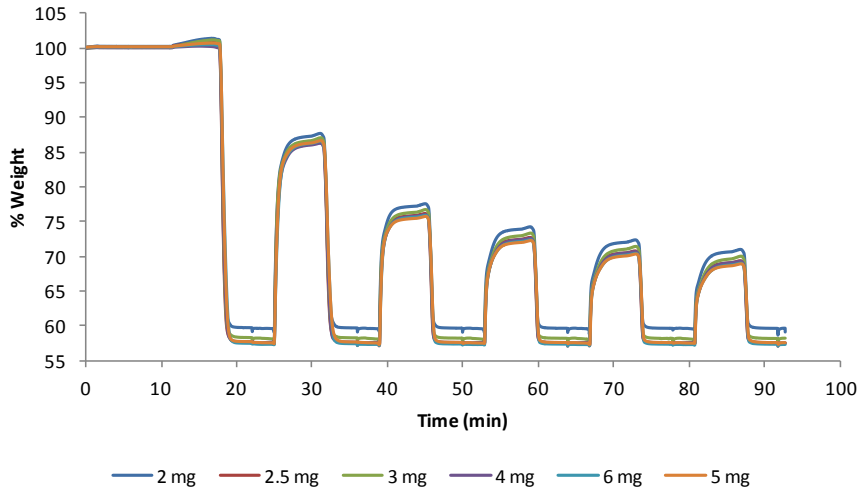

Figure 40: Percentage of weight versus time in the 5 carbonation/calcination cycle experiments for different samples masses (Havelock; 500-710µm; 140 ml/min)

Table 23: Results of the mass transfer and chemical reaction for the sample mass experiments

	Masses (mg)				
	2	2,5	3	4	6
$x_{out,\ average}$	0.146	0.145	0.143	0.143	0.141
$x_{out,min}$	0.141	0.139	0.137	0.136	0.132
$r_{external}$ (mol.gCaO^{-1}.s^{-1})	1.79E-03	1.89E-03	1.94E-03	1.99E-03	2.08E-03
$r_{exp,max}$ (mol.gCaO^{-1}.s^{-1})	3.37E-04	3.65E-04	3.87E-04	3.76E-04	4.13E-04
k_g (m^3.gCaO^{-1}.s^{-1})	7.90E-04	8.18E-04	8.05E-04	8.14E-04	8.15E-04
k_r (m^3.gCaO^{-1}.s^{-1})	2.94E-03	2.67E-03	3.13E-03	1.70E-03	1.07E-03
k_o (m^3.gCaO^{-1}.s^{-1})	2.63E-04	2.57E-04	2.57E-04	2.16E-04	1.79E-04
(k_g-k_r)	-2.15E-03	-1.85E-03	-2.33E-03	-8.90E-04	-2.53E-04
ϕ	7.128	6.796	7.362	5.427	4.298
η	0.134	0.140	0.130	0.173	0.215

Table 24: Determination of the external mass transfer coefficient (k_g) for the sample mass experiments

	Masses (mg)				
	2	2.5	3	4	6
D_p (m)	5.96E-04	5.96E-04	5.96E-04	5.96E-04	5.96E-04
Sh	2.49	2.49	2.49	2.49	2.49
Sc	9.91E-01	9.91E-01	9.91E-01	9.91E-01	9.91E-01
Re	6.63E-01	6.63E-01	6.63E-01	6.63E-01	6.63E-01
k_g (m.s^{-1})	4.50E-01	4.50E-01	4.50E-01	4.50E-01	4.50E-01
S_m (m^2.gCaO^{-1})	1.76E-03	1.82E-03	1.79E-03	1.81E-03	1.81E-03
k_g (m^3.gCaO^{-1}.s^{-1})	7.90E-04	8.18E-04	8.05E-04	8.14E-04	8.15E-04

1.3 Particle Size Tests

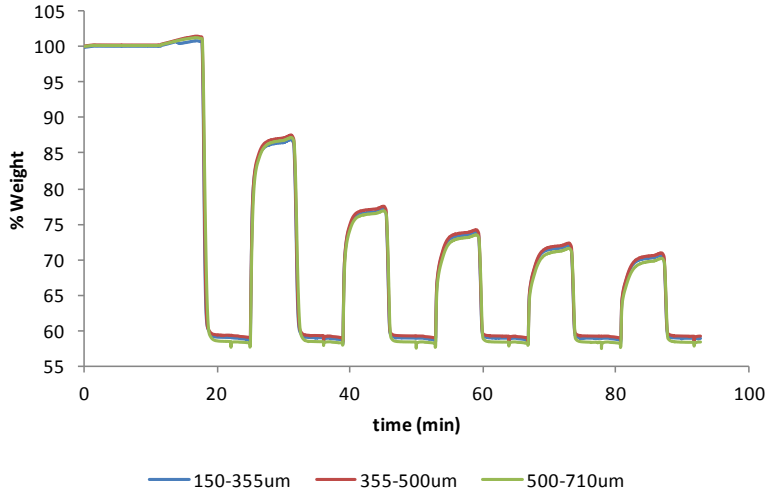

Figure 41: Percentage of weight versus time in the 5 carbonation/calcination cycle experiments for different particle sizes (Havelock; 3 mg; 140 ml/min)

Table 25: Results of the mass transfer and chemical reaction for the particle size experiments

	Particle Size (µm)		
	150-355	355-500	500-710
$x_{out,\ average}$	0.142	0.143	0.143
$x_{out,min}$	0.135	0.136	0.137
$r_{external}$ (mol.gCaO^{-1}.s^{-1})	9.25E-03	2.91E-03	1.52E-03
$r_{exp,max}$ (mol.gCaO^{-1}.s^{-1})	6.03E-04	5.41E-04	5.12E-04
k_g (m^3.gCaO^{-1}.s^{-1})	4.92E-03	1.54E-03	8.05E-04
k_r (m^3.gCaO^{-1}.s^{-1})	5.57E-04	1.24E-03	3.13E-03
k_o (m^3.gCaO^{-1}.s^{-1})	3.21E-04	2.86E-04	2.70E-04
(k_g-k_r)	4.36E-03	2.95E-04	-2.33E-03
ϕ	1.161	3.164	7.359
η	0.616	0.283	0.130

Table 26: Determination of the external mass transfer coefficient (k_g) for the particle size experiments

	Particle Sizes (µm)		
	150-355	355-500	500-710
D_p (m)	2.31E-04	4.21E-04	5.96E-04
Sh	2.30	2.41	2.49
Sc	9.91E-01	9.91E-01	9.91E-01
Re	2.57E-01	4.69E-01	6.63E-01
k_g (m.s^{-1})	1.08E+00	6.16E-01	4.50E-01
S_m (m^2.gCaO^{-1})	4.58E-03	2.50E-03	1.79E-03
k_g (m^3.gCaO^{-1}.s^{-1})	4.92E-03	1.54E-03	8.05E-04

1.4 Carbonation Temperature Tests

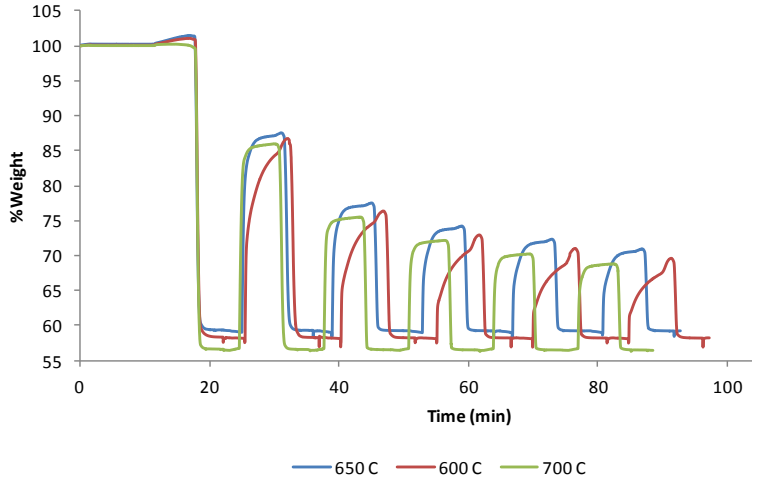

Figure 42: Percentage of weight versus time in the 5 carbonation/calcination cycle experiments for different carbonation temperatures (Havelock; 3 mg; 140 ml/min; 355-500µm)

Table 27: Results of the mass transfer and chemical reaction for the carbonation temperature experiments

	Temperature (ºC)		
	600	650	700
$x_{out,\ average}$	0.142	0.143	0.144
$x_{out,min}$	0.133	0.136	0.139
$r_{external}$ (mol.gCaO^{-1}.s^{-1})	2.71E-03	2.91E-03	3.23E-03
$r_{exp,max}$ (mol.gCaO^{-1}.s^{-1})	6.36E-04	5.41E-04	4.39E-04
k_g (m^3.gCaO^{-1}.s^{-1})	1.45E-03	1.70E-03	1.54E-03
k_r (m^3.gCaO^{-1}.s^{-1})	1.95E-03	1.24E-03	7.51E-04
k_o (m^3.gCaO^{-1}.s^{-1})	3.40E-04	2.86E-04	2.30E-04
(k_g-k_r)	-5.01E-04	4.57E-04	7.87E-04
ϕ	4.028	3.152	2.430
η	0.228	0.284	0.355

Table 28: Determination of the external mass transfer coefficient (k_g) for the carbonation temperature experiments

	Temperature (ºC)		
	600	650	700
D_p (m)	4,21E-04	4,21E-04	4,21E-04
Sh	2,43	2,41	2,40
Sc	1,02E+00	9,91E-01	9,66E-01
Re	4,96E-01	4,69E-01	4,45E-01
k_g (m.s^{-1})	5,70E-01	6,16E-01	6,63E-01
S_m (m^2.gCaO^{-1})	2,54E-03	2,50E-03	2,56E-03
k_g (m^3.gCaO^{-1}.s^{-1})	1,45E-03	1,54E-03	1,70E-03

2. Thirty Cycle experiments with Havelock and Purbeck limestones

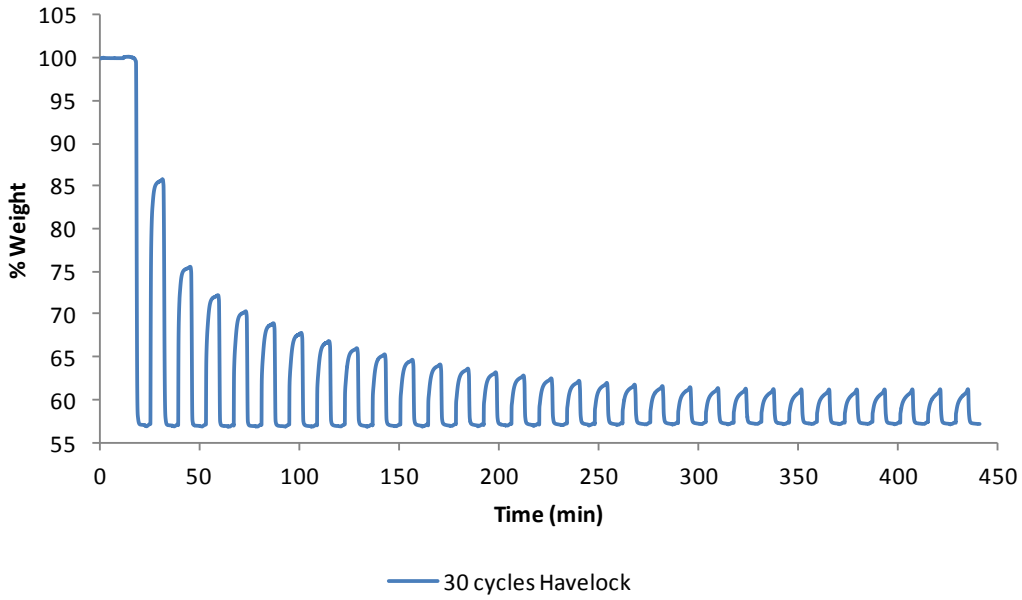

Figure 43: Variation of %weight with time for Havelock limestone in thirty cycle experiments

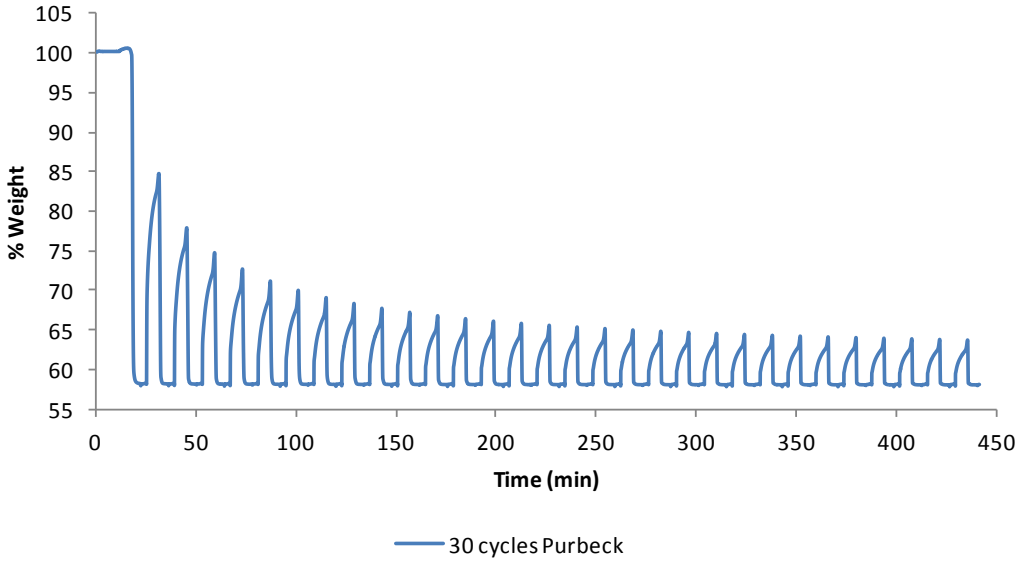

Figure 44: Variation of %weight with time for Purbeck limestone in thirty cycle experiments

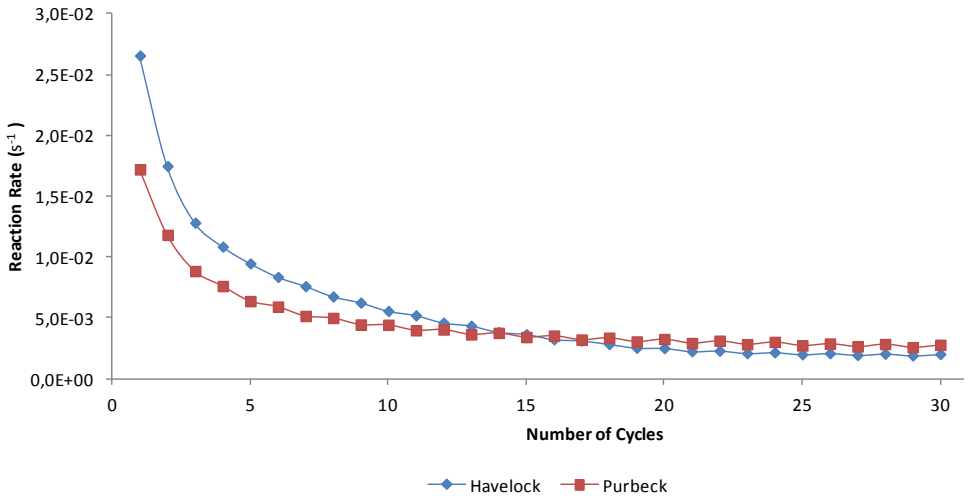

Figure 45: Maximum reaction rates (s^{-1}) for Havelock and Purbeck limestones in the thirty cycle experiments without steam

3. Thirty Cycle experiments performed with 1.5% steam in the gas flow

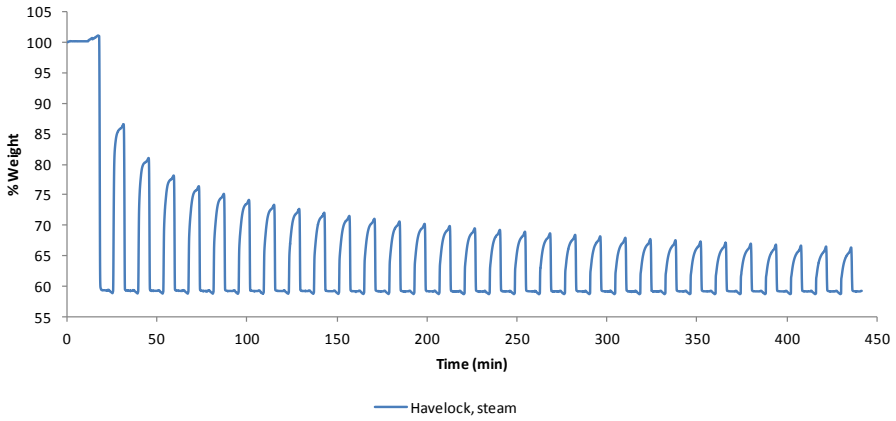

Figure 46: Percentage of weight vs time for the Havelock thirty cycle experiments performed with1.4% of steam

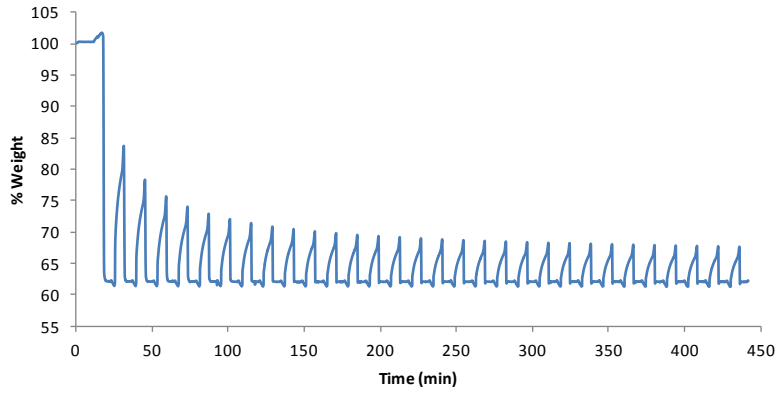

Figure 47: Percentage of weight vs. time for the thirty cycle experiments of Purbeck with 1.54% of steam

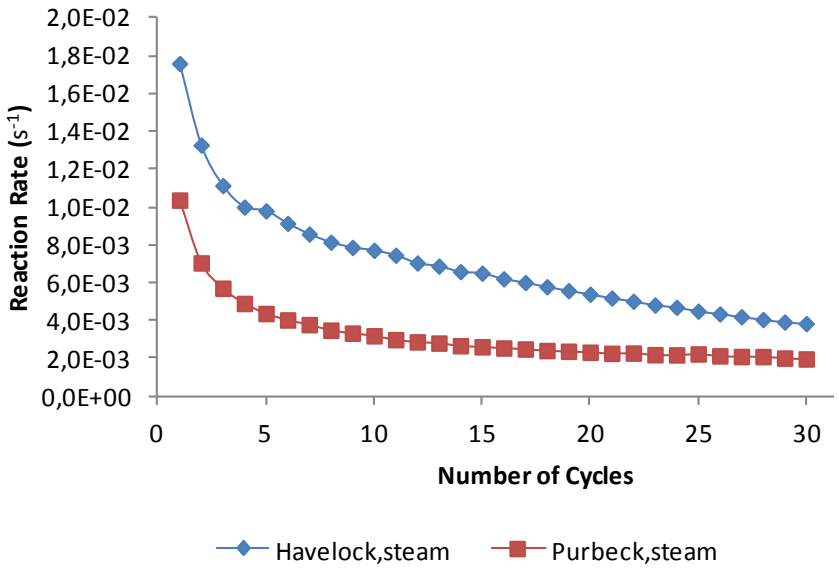

Figure 48: Maximum reaction rates (s^{-1}) for Havelock and Purbeck limestones in the thirty cycle experiments with steam

Table 29: (a and b) – Conversion of the thirty cycle experiments performed with and without steam with Havelock

a)

HAVELOCK	1	2	3	4	5	6	7	8	9	10	11	12	13	14	15
STEAM	64	51	45	41	37	35	33	32	32	29	28	27	26	26	25
NO STEAM	67	43	36	31	28	25	23	21	19	18	16	15	14	13	12
$\frac{"steam" - "no\ steam"}{"no\ steam"} \times 100$	5.2	16.6	25.3	30.1	34.1	39.9	45.6	51.6	66.5	64.7	71.5	78.1	85.1	91.9	98.2

b)

HAVELOCK	16	17	18	19	20	21	22	23	24	25	26	27	28	29	30
STEAM	24	23	23	22	22	21	21	20	20	19	19	19	18	18	17
NO STEAM	12	11	11	10	10	9	9	9	9	9	9	9	9	9	9
$\frac{"steam" - "no\ steam"}{"no\ steam"} \times 100$	105.4	121.1	115.7	119.7	121.7	122.6	122.1	120.9	117.0	113.1	109.3	105.1	100.5	95.8	91.4

Table 30: (a and b) – Conversion of the thirty cycle experiments performed with and without steam with Purbeck

a)

PURBECK	1	2	3	4	5	6	7	8	9	10	11	12	13	14	15
STEAM	51	38	33	29	26	24	23	22	22	20	19	19	18	18	17
NO STEAM	61	46	38	33	30	27	25	23	22	21	20	19	18	18	17
$\frac{"steam" - "no\ steam"}{"no\ steam"} \times 100$	-17.1	-16.5	-14.7	-13.8	-13.1	-11.6	-9.2	-7.4	1.0	-5.0	-3.6	-2.6	-1.1	0.2	0.9

b)

PURBECK	16	17	18	19	20	21	22	23	24	25	26	27	28	29	30
STEAM	17	17	16	16	16	16	15	15	15	15	15	15	15	14	14
NO STEAM	17	16	16	15	15	15	14	14	14	14	14	13	13	13	13
$\frac{"steam" - "no\ steam"}{"no\ steam"} \times 100$	1.7	2.8	3.8	4.5	5.4	6.1	7.1	7.4	8.0	8.4	9.3	9.7	10.7	11.1	11.9

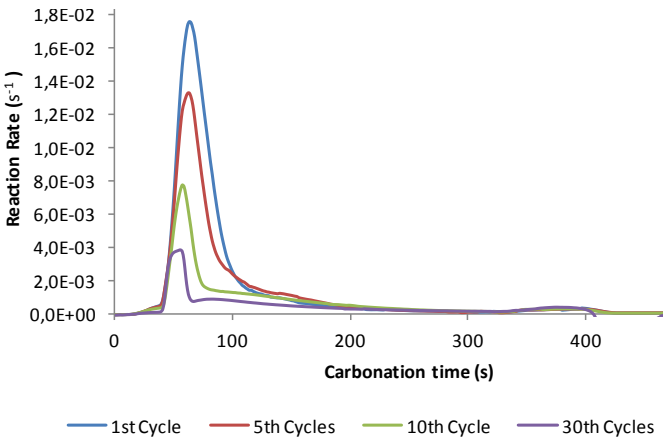

Figure 49: Reaction rate obtained in the steam experiments with Havelock